UNIVERSITÀ DEGLI STUDI DI MILANO

Scuola di Dottorato in Scienze Biologiche e Molecolari

XXVIII Ciclo

The role of parkin in modulating MT system in gene-based experimental models of Parkinson's disease

Carmelita De Gregorio

PhD Thesis

Scientific tutor: Prof.ssa Graziella Cappelletti

Academic year: 2015-2016

SSD: BIO/06

Thesis performed at the Department of Biosciences,
Università degli Studi di Milano

Cover:

Nigrostriatal fibers of *PARK2*-Q311X mice
immunostained for tyrosinated tubulin (blu), acetylated tubulin (red) and tyrosine hydroxylase (green)

Index

PART III

Manuscript in preparation: (De Gregorio et al.,)
"Parkin deficiency impacts on axonal transport in primary midbrain neurons by regulating microtubule dynamics"

SIDE RESEARCHES:

Published review: (Cappelletti et al., *Biochem Soc Trans*. 2015)
"Linking microtubules to Parkinson's disease: the case of parkin"

Published paper: (Cartelli et al., *Sci Rep* 2016)
"α-Synuclein is a novel microtubule dynamase"

Abbreviations

+TIP	Plus end-tracking protein
AR-JP	Autosomal recessive juvenile parkinsonism
ATP	Adenosine triphosphate
CCP	carboxipeptidase
DA	Dopamine
DAT	Dopamine transporter
DRP1	Dynamin-related protein 1
EB	End Binding protein
GDP	Guanosine diphosphate
GTP	Guanosine triphosphate
HDAC6	Histone deacetylase 6
IBR	In between ring
KIF	Kinesin superfamily motor proteins
KO	Knockout
LB	Lewy body
LRRK2	Leucine-rich repeat kinase 2, also called dardarin
MAP	Microtubule associated protein
MFN	Mitofusin
MPP^+	1-methyl-4-phenylpyridinium
MPTP	1-methyl-4-phenyl-1,2,3,6-tetrahydropyridine
MT	Microtubule
MTOC	Microtubule-organizing center
PARK2	Gene coding for parkin protein
$PARK2^{+/-}$	Heterozygous condition for *PARK2* gene
$PARK2^{-/-}$	Knockout condition for *PARK2* gene
PD	Parkinson's disease
PINK1	PTEN-induced putative kinase 1
PTM	Post-translational modification
REP	Repressor element of parkin
RING	Really interesting new gene
α-syn	α-synuclein
SN	*Substantia nigra*

ST	*Corpus striatum*
α-Tub	α-tubulin
β-Tub	β-tubulin
γ-Tub	γ-tubulin
Δ2 Tub	Δ2 tubulin
Ac Tub	Acetylated tubulin
deTyr Tub	detyrosinated tubulin
Tyr Tub	Tyrosinated tubulin
TH	Tyrosine hydroxylase
TAT	Acetyl transferase enzyme
TTL	Tubulin tyrosine ligase
TTLL	TTL-like proteins
UBL	Ubiquitin-like domain

Abstract

The molecular mechanisms underlying the dopaminergic neuronal death in Parkinson's disease (PD) result still unclear and thus proven strategy to prevent the disease also remains unknown and an unmet priority. Several pathogenic pathways have been implicated in PD pathogenesis and, among them, microtubule (MT) dysfunction is emerging as a contributing factor of the disease. MT cytoskeleton is a complex network essential for neuronal morphogenesis and its proper regulation is crucial for neuronal survival and functions including axonal transport. MTs are common targets for several PD-inducing toxins and PD-linked proteins including parkin that, beyond its E3 ubiquitin ligase activity, plays a role in regulating mitochondrial homeostasis and trafficking. Some data, derived from murine and human cell cultures, provide evidences that parkin mutations, which are responsible for both familial and sporadic forms of PD, affect MT system. In this scenario, we analyzed in detail the interplay between parkin, MT system and mitochondrial axonal transport using gene-based murine models of the disease.

First, we investigated MT dysfunction in *PARK2*-Q311X transgenic mice, a model that resembles the hallmark characteristic of the disease in age-dependent way. Our initial analyses showed that mice at 6 and 16 weeks of age did not show deficits in striatal innervations and depletion of tyrosine hydroxylases (TH), indicating that they could be suitable to study the early pathogenic phases that precede neuronal death. Thus, we studied the impact of parkin Q311X mutation on MT stability and mitochondrial homeostasis in 6 and 16 weeks old mice with the aim to pinpoint the involvement of their dysfunction as early event in neurodegeneration. We found that Q311X point mutation leads to the unbalance of post-translationally modified tubulins

(PTMs), which are associated with differences in MT stability, inside dopaminergic neurons. On the contrary, none alteration was observed for mitochondrial dynamics and distribution in nigrostriatal fibers at these very early time points. Notably, we also reported that the unbalance of tubulin PTMs occurs in *PARK2* knockout (KO) model during aging (2, 7 and 24 months of age) and precedes the block of mitochondrial transport within dopaminergic fibers. Collectively, our results from *PARK2* mouse models support the concept that early α-tubulin PTMs alterations might play an important role in PD etiopathogenesis.

Next, we moved to primary neuronal cultures obtained from midbrain of mouse embryos as experimental model for investigating in detail the effect of parkin in modulating MT dynamics and mitochondria motility. Morphometric analyses, performed on primary neurons isolated from *PARK2*KO and heterozygous mice showed that parkin deficiency affects axonal outgrowth. To test whether the impact of parkin deficiency on morphology is linked to MT dysfunction, we firstly investigated MT dynamics. Beyond the enrichment in the level of Tyr tubulin (marker of dynamic MTs), we observed that parkin deficiency increases MT dynamics by live cell imaging. Moreover, we assessed MT-based axonal transport and our results confirmed that loss of parkin affects mitochondria movement. We showed that this alteration depends on MT destabilization as it is rescued by MT stabilizer paclitaxel in primary neurons and also in *PARK2*-silenced PC12 cells.

Overall, these data pinpoint parkin as a regulator of tubulin PTMs and MT dynamics in neurons and reinforce the idea that MT dysfunction may be crucial and represent an early step in the chain of events leading to dopaminergic neuron death.

PART I

State of the Art

1.1 Microtubules

The cytoskeleton is a complex network of intracellular filaments and regulatory proteins that extends throughout the cytosol and provides support for cell shape and internal organization. In addition, cytoskeleton is involved in different functions, such as motility, chromosome segregation and intracellular transport. Many different components work together to form the cytoskeleton of eukaryotic cells that consists of three major classes of elements: actin filaments, intermediate filaments and microtubules (MTs).

Here we focus on MTs, which are non-covalent cytoskeletal polymers involved in many cellular processes including mitosis, cell motility, intracellular transport, secretion and morphogenesis. MTs are polarized and dynamic structures built up by α/β tubulin heterodimers, two highly similar proteins conserved among all eukaryotic species. Tubulin structure can be divided into three domains: the N-terminal part contains the nucleotide binding domain, the middle structure is involved in monomers contact and taxol binding, and, finally, the C-terminal domain that is implicated in protein interactions (Nogales et al. 1998). After the cloning of the first α- and β-tubulin genes, (Cleveland et al. 1978), the existence of different genes coding for α- and β-tubulin, at least 10 in mammals, was revealed. The tubulin isoforms are differently expressed during development and are specifically localized in certain type of cells and tissues. For instance, neuronal MTs are known to depend on some β-tubulin isotypes, whereas most of the other MT functions are independent on their composition (Janke and Bulinski 2011).

As shown in figure 1, tubulin dimers associate in a head-to-tail fashion to create linear protofilaments, which subsequently assemble laterally to form MT, a 25 nm wide hollow tube. A single MT is formed of 10–15 protofilaments, usually 13 in mammalian cells (Desai and Mitchison 1997). The head-to-tail association of the α/β heterodimers makes MTs polar structures with two distinct ends characterized by different polymerization rates: "plus end" and "minus end" exposing β and α monomer, respectively.

The intrinsic MT polarity is due to the different ability of α- and β-tubulin to hydrolyze the energy carrier guanosine-5'-triphosphate (GTP). Both α- and β-tubulin bind the GTP, but the site on α -tubulin is entrapped at the interface between the two monomers, avoiding the exchange between GTP and guanosine 5' diposphate (GDP) (non-exchangeable site N-site). On the contrary, the GTP binding domain on the β-tubulin monomer is exposed and this allows the GTP hydrolysis (exchangeable site E-site). The differences in GTP hydrolysis result in a fast-growing plus end and slow-growing minus end (Carlier et al. 1987). MTs switch between phases of rapid growth and shrinkage, process known as dynamic instability. Conversion from growth to shrinkage is termed "catastrophe" whereas the switch from shrinkage to growth is called "rescue" (Mitchison and Kirschner 1984). The dynamic instability depends on the equilibrium between the polymerization velocity and GTP hydrolysis on the E-site of β-monomer. After the GTP-tubulin is incorporated into MT, it is hydrolyzed into GDP and the energy stored in the subunits is released. Furthermore, it is believed that some of this energy goes to deform the tubulin subunit, being GDP-tubulin most stable in a curved state, and so MT rapidly shrinks (Burbank and Mitchison 2006). If the addition of free subunits is faster than the hydrolysis of GTP on incorporated subunits, the formation of GTP cap occurs and stabilizes MT. Once the GTP cap is lost, the protofilaments

splay apart resulting in a rapid MT depolymerization (catastrophe) (Conde and Cáceres 2009). The dynamic instability is described by 5 parameters: polymerization rate, shrinkage rate, catastrophe (transition from polymerizing to depolymerizing phase) frequency, rescue (transition from depolymerizing to polymerizing phase), and pause (time spent neither polymerizing nor depolymerizing). The polymerization rate of α/β heterodimers into MTs is proportional to the concentration of free tubulin and is regulated by temperature (37^0C), presence of Ca^{2+} at intracellular level (Keith et al. 1986), other than by the presence of GTP.

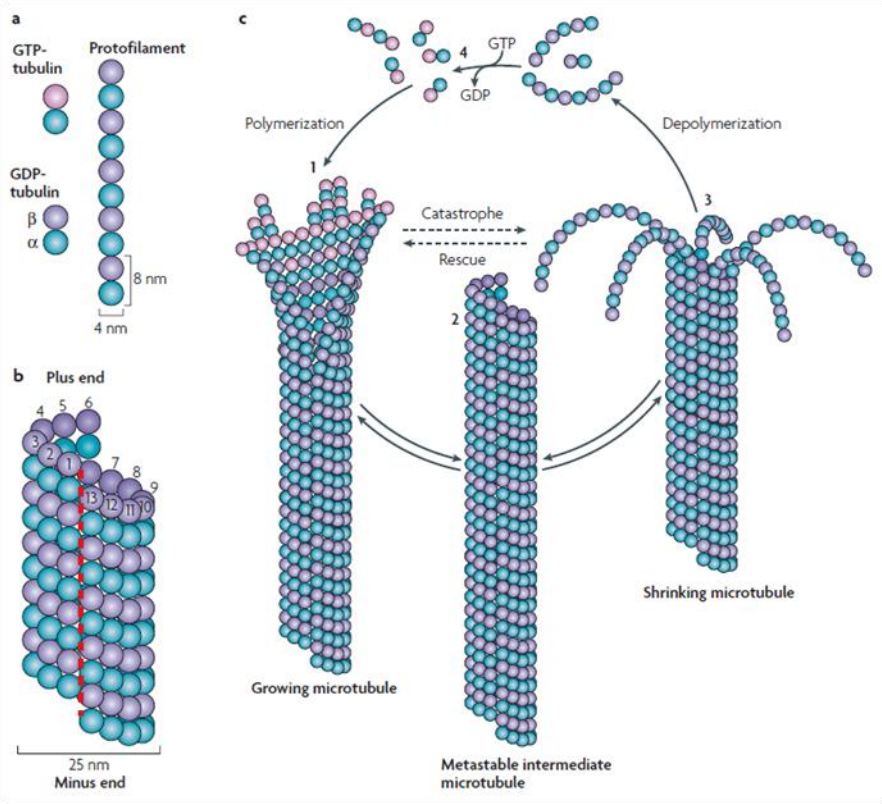

Figure 1. Representation of dynamic instability of microtubules.
(a) Structure of a protofilament and (b) MT. (c) Representative scheme of typical dynamic instability of MTs. (Conde and Cáceres 2009).

The dynamic instability allows the cell to adapt quickly to environmental changes and to respond to cellular needs, through reorganization of MTs. For instance, cells rapidly reorganize cytoskeleton throughout mitosis transition or during the extension of growth cones from neurons (Burbank and Mitchison 2006). The proper control of MT dynamic probably results from the sum of multiple proteins and post-translational modifications (PTMs) of α- and β-tubulins associated to MTs (Dubey et al. 2015). MTs interact with different proteins within cells, such as motor and non-motor MT-associated proteins (MAPs). Motor proteins, which include the family of kinesins (KIFs) and dyneins, are able to generate force using the adenosine 5'-triphosphate (ATP) hydrolisis and, upon interaction with MTs, are involved in different intracellular functions, most obviously intracellular transport (Janke and Bulinski 2011). Due to the viscous nature of the cytosol, the movement of cargo and organelles requires active transport along MT cytoskeleton by molecular motors inside the cells (Luby-Phelps 2000). KIFs are essentially responsible for anterograde transport, while the retrograde one is mediated by cytoplasmic dyneins. The heterogeneous group of non-motor MAPs includes many proteins that can both stabilize or destabilize, by changing the frequencies of transition between growing and shrinkage state. The structural MAPs are known to bind and stabilize MTs and, among them, tau, MAP1 and MAP2, are found specifically in neuronal cells, and MAP4 is expressed in others cell type (Conde and Cáceres 2009). One of the mechanisms involved in MAP regulation is the phosphorylation, which promotes their detachment from MTs and impairs their stabilizing function (Trinczek et al. 1995).

In addition, a group of intensively studied MAPs is formed by plus end tracking proteins (+ TIPs) that specifically accumulate at the plus end of growing MTs. The + TIPs control different aspects of cellular architecture through the

regulation of MT dynamics, the interaction of cellular structures and signaling molecules (Akhmanova and Steinmetz 2008). Some kinesins (e.g. kinesin 13 MCAK), which belong to that family, regulate MT dynamics and depolymerize MTs thus promoting spindle assembly and chromosome segregation (KlineSmith and Walczak, 2004). By contrast, EBs (end-binding) proteins, crucial among the +TIPs family, usually promote MT polymerization and inhibit catastrophe events, increasing MT rescue frequencies and decreasing the depolymerization rate (Lansbergen and Akhmanova, 2006). EBs form a comet-like accumulation on the distal part of MT and, in particular EB3, conjugated to fluorescent protein (e.g. EB3-mCherry), is amply used as a tool in live cell imaging approach to follow MT growth (Akhmanova and Steinmetz 2008). Moreover, a further class of MAP includes MT severing enzymes, such as spastin and katanin, which are able to destabilize the MT lattice. In particular, these enzymes generate internal break in a MT and are implicated in the regulation of neurite outgrowth as well as branching formation (Roll-Mecak and McNally 2010).

Tubulin is prone to a number of post-translational modifications (PTMs), which are intrinsic regulators of MT dynamics. The well-studied PTMs include tyrosination/deTyrosination, Δ2 and Δ3-tubulin, acetylation, polyglutamylation, polyglycilation, polyamilation, and phosphorylation (Figure 2). The generation of a specific pattern of PTMs, together with the incorporation of diverse isoforms of tubulin, confers a MTs identity namely "tubulin code". These modifications, which are differently distributed inside the cell, have the potential to generate complex molecular signals on MTs that can be read by others proteins. Most of these modifications interest α-tubulin, whereas fewer of them are associated with the C-terminal of β-tubulin. The enzymes, which catalyze such modifications, can act on tubulin dimers but most of them work

preferentially on tubulin already incorporated in MT (Conde and Cáceres 2009). Across different species, most α-tubulin genes encode the C-terminal tyrosine residue. Furthermore, α-tubulin is tyrosinated (Tyr) in its nascent state, with the cyclic addition and removal of tyrosine residue. Thus, the tyrosination/deTyrosination cycle starts with the removal of Tyr residue at the C-terminal of α-tubulin, which leads to the exposure of penultimate glutamate (named Glu residue) (deTyrosination); the subsequent re-addition of the Tyr residue serves to recover the nascent form of tubulin (Tyrosination).

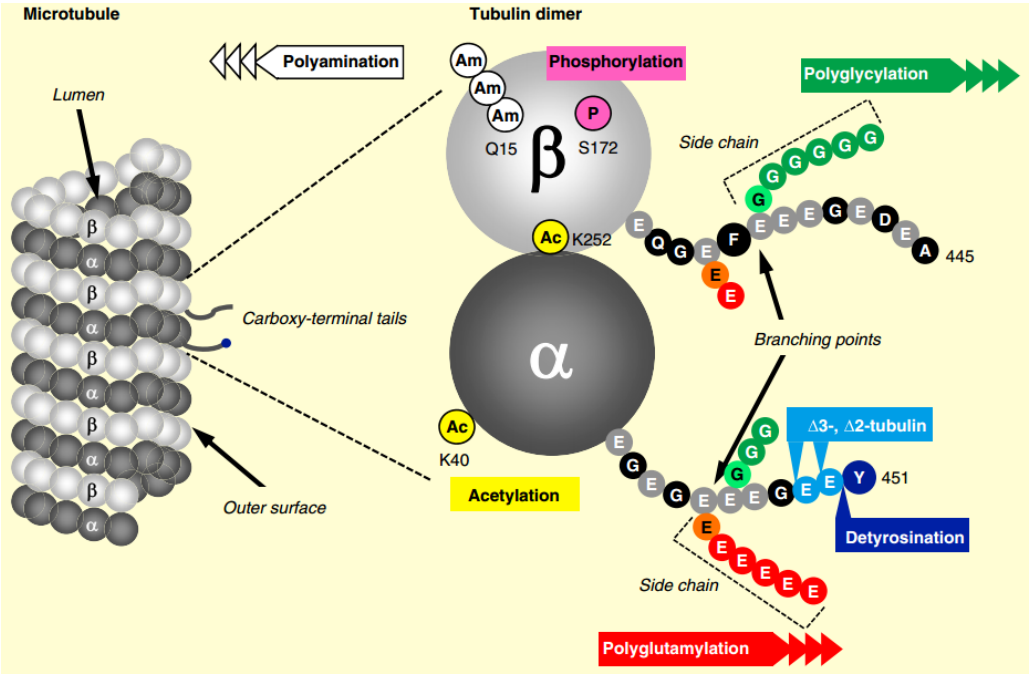

Figure 2. Tubulin post-translational modifications (PTMs).

Representation of different tubulin PTMs distribution on the α/β-tubulin dimer with respect to their position in the MT lattice (from Janke, 2014).

The tubulin tyrosine ligase (TTL) was the first enzyme, known to be involved in PTMs, to be purified (Schroder et al. 1985) and cloned (Ersfeld et al. 1993). The cytosolic enzyme carboxipeptidase (CCP), which removes the Tyr group, is still unknown. TTL enzyme acts exclusively on soluble tubulin dimers, whereas CCP favors the tubulin polymerized into MT and thus, the newly assembled MTs are almost formed of Tyr tubulin (Janke and Bulinski 2011). The removal of the Glu residue leads to a Δ2 tubulin modification, an irreversible PTM catalyzed by deglutamylase enzyme and, the subsequently proteolysis of the C-terminal tail generates Δ3 tubulin. While tyrosination is associated to dynamic MTs, deTyrosination and Δ3 tubulin are linked to MT stability. This latter tubulin PTM renders MT less susceptible to depolymerizing action of KIF 13, which binds preferentially tyrosinated plus end. Moreover, MT deTyrosination increases the affinity for KIF-1, involved in intracellular transport in neurons, without affecting its velocity. The second tubulin PTM to be discovered was the acetylation of Lys40 (K40) on α-tubulin (L'Hernault and Rosenbaum 1985). Recently, has been described also another acetylation event on Lys 252 (K252) of β-tubulin (Chu et al. 2011). The first modification was reported to take place on MT polymer (Maruta et al. 1986), whereas the second one preferentially on non-polymerized tubulin (Chu et al. 2011). Acetylation is enriched on stable MTs and, specifically, the K40 modification occurs in the inner face of MTs and affects the binding and the traffic of different proteins, such as kinesin (Dompierre et al. 2007). The enzyme involved in K40 acetylation is the acetyl transferase α-TAT1, whereas the removal of acetyl group is catalyzed by HDAC6 (histone deacetylase 6) and Sirt2 (sirtuin type 2) enzymes. How the enzyme gains access to K40 site is not clear, but recent studies propose that TAT scans MTs bi-directionally within the lumen using surfacing diffusion (Song and Brady 2015). Polyglutamylation is the addition of glutamate residues

variable in length which occurs on several glutamates sites of α and β tubulin in the C terminal domain. This modification was first discovered in the brain as well as on axonemal tubulin. The deglutamylase enzyme, involved in glutamate side chains removing, belongs to the CCP family. Tubulin polyglicylation or glycilation, like polyglutamylation generates side chains of glycine within the C terminal tails of α and β tubulin. Differently, in most organism analyzed so far, this modification occurs exclusively on cilia and flagella. The enzymes involved in glycilation reaction belong to TTL family and, in mammals, some of them can initiate or elongate the side chain. The role of that modification in MT function regulation is still unknown (Magiera and Janke 2014). Tubulin polyamilation is a recently discovered PTM and consist in the addition of amines to glutamine residues of α and β tubulin and, among several glutamine residues that can be polyaminated, glutamine 15 (Q15) on β tubulin is the primary modification site. The enzyme involved in the reaction is the transglutaminase that can act both on free tubulin and MTs and, most likely, this modification is associated to MT stabilization (Song et al. 2013). Phosphorylation of the serine residue S172 of β-tubulin, catalyzed by cyclin-dependent kinase 1, has been shown to regulate MT dynamic during cell division. It has also been identified another phosphorylation event on the C terminal of α tubulin, catalyzed by the tyrosine kinase Syk, that may affect MAP binding.

1.1.1 Microtubules in the neuron: a glance at physiological and pathological conditions

Neurons are highly polarized cells with a peculiar morphology that generally consists of cell body (soma), from which several shorter dendrites emerge, and a long axon. A critical aspect of neuronal function depends on establishing the

neuronal polarity between the somatodendritic and axonal compartments (Craig and Banker, 1994). Dendrites and axons differ in both morphology and function thanks to the diverse patterns of proteins expression and organelles associated. The dendrites are specialized to receive signal whereas the axon, transmits it to other neurons or muscles, through structures known as synapses. The MT organization mainly contributes to the establishment of cell polarization and in fact, in the early stages of neuronal differentiation, it navigates the growth cone and axon elongation. Furthermore, MTs are essential throughout the life of the neuron because they constitute both the architectural strut and the railway, required for the support of their peculiar morphology and for shape changes during neuroplasticity and intracellular transport, respectively. Neurons have different MTs organization between the two compartments: the axonal MTs are characterized by uniform orientation, with the plus end facing the axon tip, whereas dendritic MTs have mixed orientation, with their plus end facing either the cell body or the dendritic tips (Baas et al. 1988). The plus end is crucial site for tubulin polymerization, whereas minus end is often anchored to a MT-organizing center (MTOC) that constitutes the major center of MT nucleation. The most important MTOC in the animals is the centrosome, typically composed of two centrioles and periocentriolar materials. The nucleating structures is called γ-tubulin ring complex (γ-TuRC), where γ-tubulin binds specifically β-tubulin to establish the polarity orientation of MT polymerized from the complex. Some MTs remains attached to their nucleating structure while others MT may be released and transported away from the centrosome through the molecular motors (Baas et al. 2005).

The intrinsic polarity of MT allows the selective trafficking of cargo inside the neurons to establish the differences that distinguish the two compartments. Disorganization of MT polarity can result in the incorrect localization of cargo

(Dubey et al. 2015). For instance, most of neuronal proteins are synthesized in the cell body and anterograde axonal transport allows them to reach the distal part of the axon. The retrograde axonal transport, enhanced by dynein, conveys proteins from axon to the cell body for degradation and recycling.

Another key feature that contribute to the delivery of different cargo and distinguish the neuronal compartment is the different stability of MTs (Baas et al. 1991) generated by the expression of tubulin isotypes, MT associated proteins and tubulin PTMs (tubulin code) (Janke 2014). The pattern of expression of PTMs varies throughout neuron compartments and changes during neuronal differentiation (Figure 3). Older MTs are most stable because tubulin PTMs accumulate over time, due to the specific enzymes that act preferentially on assembled MT; by contrast, newly synthesized one is more dynamic. For instance, in developing neurons, where the dendrites and synapses are not yet differentiated and the axon is extending, the levels of deTyrosination, Δ2 tubulin, glutamylation and polyamilation are relatively low in the perikaryon. Acetylation, glutamylation and deTyrosination are high in the growing axon and reduced in the growth cone that is conversely enriched in tyrosinated tubulin, meaning that MTs are more dynamic for normal pathfinding. The minor neurites have a low amount of acetylated MTs but high level of deTyrosinated glutamylated/polyglutamileted MTs. In mature neurons, where the dendrites and synaptic specializations are formed, the enrichment of tubulin PTMs associated to stable MTs occurs. Polyamination of axonal MTs increases respect to young neurons and deTyrosinated and Δ2 tubulin remain relatively high. Acetylated MTs increase not only in both axon and dendrites but also in synaptic region, where dynamic MTs are reduced to form stable connections (Song and Brady 2015).

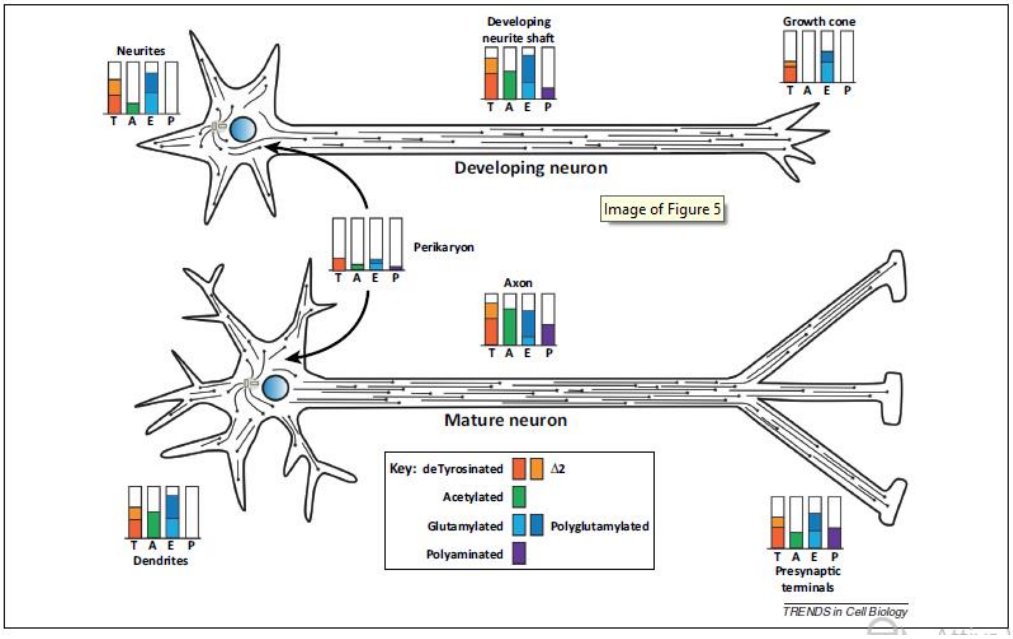

Figure 3. Post-translational modifications of tubulin vary in different regions of a neuron and change during neuronal differentiation. (from Song and Brady 2015)

In addition, the localization of MAPs differs as well: MAP2 is found exclusively in dendrites, where it decorates stable MT, and tau, found in both compartment, is mainly enriched in the distal axons (Kapitein and Hoogenraad 2011).

The proper functioning and regulation of MT dynamics and assortment of regulatory proteins are essential for the health of nervous system. Mounting evidence suggests that the alteration of neuronal MT organization constitutes a key insult in neurodegenerative disorders pathogenesis. Tubulin PTMs are involved, in some way, in regulating most of the processes based on MT function, and, interestingly, aberrations in the normal pattern of tubulin PTMs could directly or indirectly lead to disease (Janke and Bulinski 2011).

The generation of *TTL*- null mice reveals the importance of tyrosinated tubulin during brain development. These mice show a deleterious neuronal abnormalities and die after birth, meaning that TTL enzyme have a vital role for the nervous system. Cultured *TTL*-null neurons show anomalies in the morphogenesis such as an erratic time course of neurite outgrowth (Erck et al. 2005). However, these neurons display a mislocalization of CLIP70, a +TIP protein that accumulates to the plus end of growing MTs and regulates MT dynamics. Konishi et al. (2009) showed that the inhibition of TTL via siRNA knockdown in rat hippocampal neurons resulted in a decrease of tyrosinated tubulin and the subsequent mislocalization of kinesin-1. Moreover, also mutations in tubulin genes have been found to cause neuronal diseases. Specifically, mutations in βIII-tubulin, a neuron specific isoform, result in severe neurological symptoms, such as peripheral neuropathy and loss of axons in many kinds of brain neurons. Some of these mutations affect the binding on MTs and the function of a broad range of KIFs in neurons (Niwa et al. 2013).

Alteration of MT system was shown to be an early event in neurodegenerative disorders associated with axonal transport impairment. The proximal cause of cell death could be due to the accumulation and mislocalization of different organelles within neuron due to the axonal transport damage. For instance, a proper intracellular distribution of mitochondria is crucial for neuronal survival to fulfill the ATP demand to areas of need. Indeed, defects in mitochondrial transport that lead to energy deprivation, have been associated to several disease models (Vos et al. 2008).

Many major human neurodegenerative diseases, including amyotrophic lateral sclerosis (ALS), Huntington's disease (HD), Alzheimer's disease (AD) and Parkinson's disease (PD) have been shown to display an axonal transport impairment.

Reduced tubulin acetylation and altered MT-dependent axonal transport have been observed in HD model; enhanced MT acetylation leads to the recruitment of both molecular motors, kinesin and dynein, to MTs, with subsequent restore of brain-derived neurotrophic factor (BDNF) release in HD neurons (Dompierre et al. 2007). Misregulation of MAPs, such as the changes in tau expression and localization seen in AD, has the potential to alter the steady-state distribution of organelles (Perlson et al. 2010). Fanara et al. (2007) reported an increase of MT dynamics at very early stages before the axonal transport alteration in a mouse model of ALS. The treatment with MT stabilizing agent restores the transport, suggesting that the observed defect was due to the increase in MT dynamics. Next, striking data showed that MT alteration occurs very early in a toxic model of parkinsonism preceding the axonal transport impairment and that the treatment with a MT-stabilizer agent, epothilone D, exerts a neuroprotective effect (Cartelli et al. 2013).

Thus, the right balance between stable and dynamic MTs, the correct level of tubulin PTMs, and the proper function of motor and non-motor MAPs are the prerequisite for neuronal survival, neuronal development and also axonal transport.

1.2 Parkinson's disease

Parkinson's disease (PD) is the second most common neurodegenerative movement disorder affecting 1% of population who are over 65 years old and up to 5% of population by the age of 85 (Forman et al. 2004). More commonly, patients develop late-onset PD but some cases are characterized by early-onset that occurs before the age of 50 (Pellegrini et al. 2016). Clinically, PD is characterized by motor deficits including resting tremor, bradykinesia (slowness in movements), postural instability and rigidity. Motor impairment is often accompanied by non-motor symptoms and signs including mood, sleep and cognitive disturbances (Dauer and Przedborski 2003).

Although the pathological changes occur in different areas of the brain, the principle pathological hallmark of the disease, which underlies the characteristic motor phenotypes, is the loss of dopaminergic neurons that project from the midbrain *Substantia nigra pars compacta* (SNpc) to the *Corpus striatum* (ST) (Figure 4). Neurons whose cell bodies are located in the ventrolateral tier and project to the dorsolateral putamen are specifically affected. The loss of midbrain dopaminergic neurons results in striatal neurotrasmettitor dopamine (DA) deficiency. Thus, the nigrostriatal system, which allows an individual to execute proper and coordinated movements, is compromised in PD. A much more modest cell loss occurs in the mesolimbic dopaminergic neurons, where the cell bodies in the ventral tegmental area (VTA) project their terminals to the caudate. The PD symptoms become evident when the loss of dopaminergic neurons in the SNpc reaches the 60% and when DA is depleted about 80% (Dauer and Przedborski 2003). The nigral damage is always accompanied by extensive extra-nigral pathology, involving different neuronal populations in others brain regions such as cortex, thalamus and subthalamic nuclei (Braak et al. 2003). Another histopathological hallmark of

PD is the presence of fibrillar aggregates referred to as Lewy bodies (LBs), intraneuronal proteinacious cytoplasmic inclusions where α-synuclein (α-syn) is the major constituent (Spillantini et al. 1997). LBs are also found in the neuronal cell processes called intraneuritic LBs or Lewy neurites. LBs affect not only the surviving neurons in the SNpc but accumulate in several neuronal type in the brain such as, components of the autonomic, limbic and somatomotor systems. According to the Braak staging, during presymptomatic stages (1-2) LBs are confined to the medulla oblongata, pontine tegmentum and olfactory bulb. As disease evolves, the SN and nuclear greys of the midbrain and forebrain become to be affected (stages 3-4), and thus the patients start the pathological changes and probably have symptomatic phase of the illness. In advanced stages (5-6) the inclusion body pathology can be found in the limbic structures and neocortex (Braak et al. 2003).

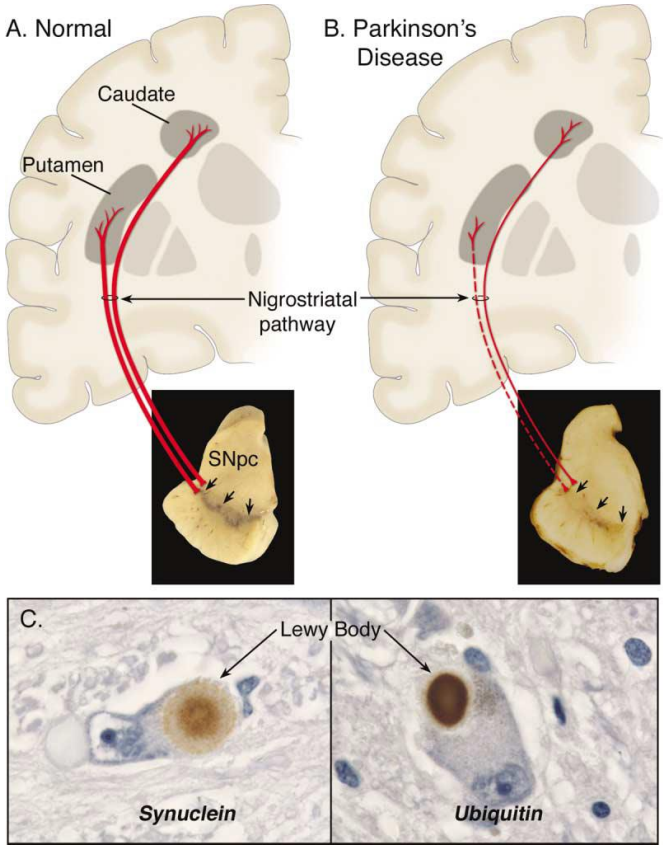

Figure 4. Neuropathology of Parkinson's disease.
(A) Schematic representation of the normal nigrostriatal pathway (in red). Cell bodies of dopaminergic neurons are located in the *Substantia nigra pars compacta* (SNpc). These neurons project to the basal ganglia and synapse in the *Corpus striatum*. Dopaminergic neurons are characterized by the pigmentation produced by neuromelanin. (B) Schematic representation of the diseased nigrostriatal pathway (in red). It is characterized by the loss of dopaminergic neurons that project to the putamen (dashed line) and a much more modest loss of those neurons projecting to the caudate (thin red solid line). It is observed depigmentation (decrease of pigment neuromelanin; arrows) of the SNpc due to the marked loss of dopaminergic neurons. (C) Immunohistochemical labeling of Lewy Body intraneuronal inclusions in a SNpc neuron containing α-synuclein and ubiquitin (from Dauer and Przedborski 2003).

The etiology of PD has yet to be established but the combination of both environmental components and genetic predisposition contributes to the incidence of the disease, even though ageing is considered the main risk factor.
Environmental toxins were long thought to be the predominant cause of PD; chronic or limited exposure to neurotoxins such as chemical compounds, herbicides, pesticides and hydrocarbon solvents promotes the progressive dopaminergic neurodegeneration. One of the best studied toxins is the 1-methyl- 4-phenyl-1,2,3,6-tetrahydropyridine (MPTP) that was associated to PD. In 1982, young drug users, during the illicit synthesis heroin developed a progressive parkinsonian syndrome (Langston et al. 1983). In humans, in monkeys and in rodents the administration of MPTP leads to a severe parkinsonian syndrome displaying all the features that characterize PD. The pre-toxin MPTP is converted to the active toxic molecule MPPP by oxidation in the glial cells. This is released by an unknown mechanism in the extracellular space and than is selectively up-taken by dopaminergic neurons through the dopamine transporter (DAT) rendering these neurons particularly vulnerable (Dauer and Przedborski 2003). Other compounds such as rotenone and paraquat, respectively pesticide and herbicide, are PD-neurotoxins and, among the hydrocarbon solvents, 2,5- hexanedione (2,5-HD), the toxic metabolite of n-hexane, has been shown to induce parkinsonism in animals and humans (Spencer and Schaumburg 1985; Pezzoli et al. 1990; Pezzoli et al. 2000).
Most of the environmental toxins have been demonstrated to be mitochondrial poisons that interfere with mitochondrial respiratory chain inhibiting the complex I. Thus, mitochondrial dysfunction and the consequent oxidative stress was considered the principal culprit in neuron death (Malkus et al. 2009) and may also act in part by causing the accumulation of misfolded proteins. Proteins aggregation could directly damaged the cells interfering with intracellular

trafficking, a MT-dependent process (Dauer and Przedborski 2003). Interestingly, some of the PD-toxins, mentioned above, have been shown to affect MT cytoskeleton and MT dynamics *in vitro* and *in vivo* models (Cappelletti et al. 1999; Cappelletti et al. 2005; Ren et al. 2005; Cartelli et al. 2010; Cartelli et al. 2013).

On the other hand, significant progress has been made on the understanding of PD pathogenesis through the discovery of several monogenic forms of the disease and genetic risk factors associated, respectively, with familial and apparently sporadic PD. Familial PD is characterized by early-onset with autosomal dominant or recessive pattern inheritance and to date, a growing number of mutations associated with PD have been discovered; nineteen loci that segregate with familial forms of the disease have been reported (Table 1).

Genetic studies, centered on idiopathic cases, have successfully identified genetic risk of the disorder, as well as polymorphisms that enhance disease susceptibility (Kumaran and Cookson 2005). Among the different genes associated to the disease, *SNCA (PARK1;* encoding α-synuclein) and LRRK2 (PARK8; encoding dardarin) are causative of autosomal dominant PD, whereas mutations in *PINK1 (PARK6*-PTEN-induced kinase 1), *DJ1 (PARK7), Parkin (PARK2),* and *ATP13A2 (PARK9)* cause the autosomal recessive forms of the disease. These related PD proteins, such as α-syn, parkin, and PINK1, are identified to participate in different process (Figure 5) including mitochondrial homeostasis, ubiquitin proteosome pathway and, interestingly, also in the regulation of MT system.

Since PD-related neurotoxins and PD-linked proteins are involved in a complex network of interrelated molecular events, an important open issue remains the identification of the upstream pathway that leads to dopaminergic-specific neuronal cell death.

Table 1. PARK loci and identified genes that segregate with familial forms of PD

PARK loci	Gene	Confirmed/putative	Inheritance	Function
PARK1/4	SNCA	Confirmed	AD	Protein aggregation/prion-like-transmission/synaptic function
PARK2	PARKIN	Confirmed	AR	Mitochondrial maintenance/mitophagy/ubiquitin-proteasome
PARK3	Unknown	Putative	AD	Unknown
PARK5	UCH-L1	Putative	AD	Ubiquitin hydrolase
PARK6	PINK1	Confirmed	AR	Mitochondrial function/mitophagy
PARK7	DJ-1	Confirmed	AR	Mitochondrial function/cell stress response
PARK8	LRRK2	Confirmed	AD	Protein and membrane trafficking/neurite structure/lysosomal autophagy/ synaptic function
PARK9	ATP13A2	Confirmed	AR	Lysosomal autophagy/mitochondrial function
PARK10	Unknown	Confirmed	Risk factor	Unknown
PARK11	GIGYF2	Putative	AD	Tyrosine kinase receptor signaling/insulin like growth factor pathway
PARK12	Unknown	Confirmed	Risk factor	Unknown
PARK13	HTRA2	Putative	AD	Mitochondrial function
PARK14	PLA2G6	Confirmed	AR	Mitochondrial function
PARK15	FBX07	Confirmed	AR	Mitochondrial maintenance/mitophagy/ubiquitin-proteasome
PARK16	RAB7L1	Confirmed	Risk factor	Protein and membrane trafficking/lysosomal autophagy
PARK17	VPS35	Confirmed	AD	Lysosomal autophagy/endocytosis
PARK18	EIF4G1	Putative	AD	Protein translation
PARK19	DNAJC6	Confirmed	AR	Synaptic function/endocytosis
PARK20	SYNJ1	Confirmed	AR	Synaptic function/endocytosis

Table 1. *PARK* loci and identified genes that segregate with familial forms of PD (from Kumaran and Cookson, 2015).

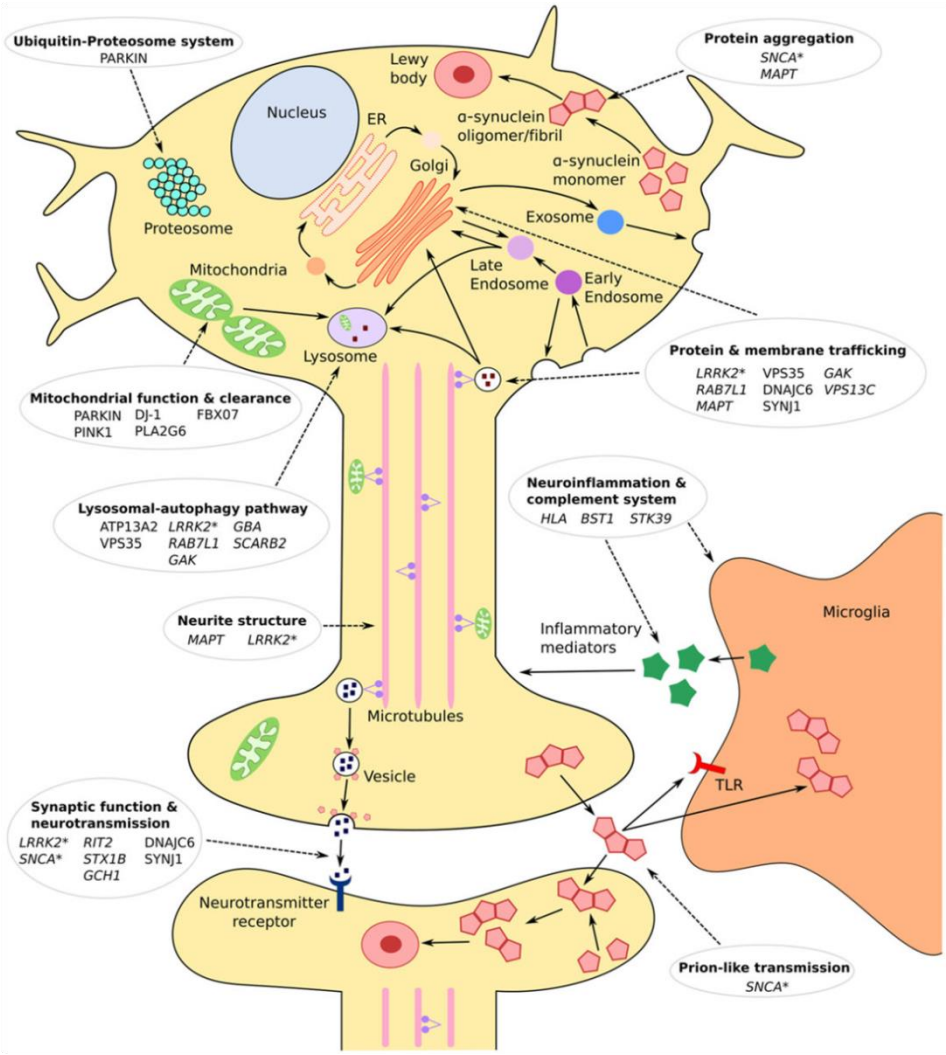

Figure 5. **Molecular processes involved in PD pathogenesis as highlighted by genetic findings.** Using genes recently nominated as risk factors for idiopathic PD along with those responsible for familial PD, it is possible to extrapolate a number of cellular processes that may underlie disease development. Genes listed in italics represent nominated risk factors for idiopathic PD, whereas those in normal font are associated with familial PD. An asterisk denotes that the gene is linked to both forms of the disorder. Some genes like SNCA and LRRK2 are associated with multiple processes. While the majority of cellular pathways contribute to both familial and sporadic forms of the disease, neuroinflammation likely plays a more prominent role the latter. Conversely, mitochondrial dysfunction shows a greater association with familial PD (from Kumaran and Cookson 2015).

1.2.1 Microtubules and Parkinson's disease

The molecular mechanism underlying neuronal death in PD results still unknown and current therapies offer just the management of symptoms rather than prevention of neuron death and the reversion or block of disease progression. Several pathogenic pathways, correlated each others, have been implicated in dopaminergic neurons degeneration such as, oxidative stress, mitochondrial dysfunctions, accumulation of misfolded proteins due the ubiquitin-proteasome system (UPS) and autophagic machinery impairment and local inflammation (Kumaran and Cookson 2015). Understanding which mechanism might be the primary insult leading to PD is a major challenge to deal. Interestingly, the early MT dysfunction is becoming established as a key insult in PD pathogenesis.

Within the context of studies based on PD-neurotoxins, appealing results have been shown for MPTP and rotenone. MPP^+, the toxic metabolite of MPTP, affects MT dynamics *in vitro*, acting as catastrophe promoter, increasing the frequency of transition from MT growth to shrinkage (Cappelletti et al. 2005). In addition, alterations of MT stability have been shown to precede mitochondria transport defect and neurite degeneration in MPP^+-exposed PC12 cells (Cartelli et al. 2010). The systemic injection of MPTP to mice induces MT alteration very early, before TH depletion, neuron degeneration and axonal transport impairment suggesting an important role of MT dysfunction in triggering neurodegeneration (Cartelli et al. 2013). MPP^+ has also been proved to decrease anterograde and increase retrograde axonal transport of membranous vesicles in squid axoplasm (Morfini 2007). Moreover, rotenone depolymerizes purified MTs *in vitro*, as well as MTs in the cell (Marshall 1978) (Ren et al. 2005). Depolymerization of MTs, induced by rotenone, disrupts vesicular transport in dopaminergic neurons. When MT alteration occurs, the

trafficking of vesicles collapses and their subsequent accumulation becomes evident in the cytoplasm. The leakage of DA from the vesicles leads to the generation of oxidative stress induced by DA oxidation, and, consequently, to neuronal death (Yong Ren, Wenhua Liu, Houbo Jiang 2005) (Choi et al. 2011).
Several PD-linked proteins, such as α-syn, LRRK2, parkin and DJ1, interact and affect MT system. The interaction of α-syn with tubulin promotes its aggregation in fibrils *in vitro* (Alim et al. 2002). Its cytotoxicity is attributed to oligomers formation, whose overexpression in cells elicits MT disruption (Prots et al. 2013). Recently, it has been proposed α-syn as a novel, foldable, MT-dynamase, which changes its conformation when binds to $\alpha_2\beta_2$ tetramers and regulates MT nucleation and dynamics *in vitro* and in cell. Furthermore, PD-related α-syn mutants are much less sensitive than WT-α syn to tubulin-induced folding and mainly promote tubulin aggregation. This could leads to an impairment of the correct MT organization on the neuronal processes (Cartelli et al. 2016). LRRK2 has been shown to interact and phosphorylate β-tubulin isoforms in the brain and to modulate MT stability (Law et al. 2014). Fibroblasts obtained from PD patients, carrying LRKK2 mutations, showed an altered MT stability (Cartelli et al. 2012). Finally, it has been reported also a novel role for DJ-1 in MT dynamics regulation (Sheng et al., 2013) and also the interplay between parkin and MTs and its involvement in PD pathogenesis has been investigated (as discussed in detail in the next paragraph).

1.3 Parkin

Parkin (*PARK2*) is the first gene associated with the autosomal recessive juvenile parkinsonism (AR-JP) (Kitada et al. 1998), one of the monogenic forms of PD. It is the second largest human gene (1.3 Mb) with 12 exons and maps to chromosome 6q25.2-q27. The high sequence conservation of *PARK2* gene across the species, not only in vertebrates (human, rat, mouse) but also in invertebrates (*Caenorhabditis elegans* and *Drosophila melanogaster*) (Kahle et al., 2000), suggests that parkin plays a common and evolutionary conserved role. Mutations in *PARK2* gene are responsible for about 50% of familial cases and about 70% of sporadic cases with an early onset (age < 20). Across the entire gene including all the 12 exons, a large number of *PARK2* mutations have been identified. Up to now, more than 170 different mutations, including missense/nonsense substitutions, exon deletions, multiplications, and point mutations, have been reported in AR-JP (Corti et al. 2011). *PARK2*-linked PD is characterized by a recessive inheritance. In recessively inherited disorders, two mutations—either the same mutation (homozygous) or two different changes in the two alleles (compound heterozygous)—are needed to cause the disease phenotype (Klein et al. 2007). Otherwise, the heterozygous subject, carrying a single mutation, should be unaffected. Nevertheless, several studies identified both diverse cases of late-onset PD with a single mutated allele (West et al. 2002) or heterozygous asymptomatic individuals with some nigrostriatal abnormalities. These evidences suggest that *PARK2* haploinsufficiency might be a risk of factor for PD progression (Khan et al., 2005). Moreover, genetic studies have revealed the existence of polymorphisms that enhance disease susceptibility rather than mutations that cause the disease.

PARK2 gene encodes for a cytosolic protein of 465 aminoacids (52 kDA), that is expressed in most of the tissues including heart, testis and skeletal muscles.

Moreover, it is abundantly expressed in the brain and especially in the SN (Kitada et al. 1998; Huynh et al. 2001).

In 2000, Shimura and colleagues showed that parkin is a member of E3 ubiquitin ligase and is responsible for the transfer of activated ubiquitin to protein substrates (Shimura et al. 2000). The ubiquitylation process occurs through the covalent attachment of monoubiquitin or polyubiquitin chains to lysine residues (most frequently K63, K48, K11 and K6 linkages) of the substrate (Hershko and Ciechanover 1998). E3 ligase enzyme, involved in the last step of ubiquitination pathway, plays an important role in targeting damaged or misfolded proteins that are degraded via the ubiquitin proteasome system (UPS). Ubiquitination pathway is carried out by the action of three enzymes: E1 ubiquitin activating enzymes, E2 ubiquitin conjugating enzymes and E3 ubiquitin ligase. The E1 enzyme uses ATP to activate ubiquitin, forming thioester between its catalytic cysteine and the C terminal carboxyl group of the ubiquitin. The ubiquitin is then transferred to cysteine active site of E2 by transthioestherification. Then, E2-ubiquitin interacts with E3 ligase, which mediates the transfer of ubiquitin to substrate protein.

Parkin belongs to the RBR (RING between RING) class of E3 ubiquitin ligases, which combine the structure similarity of RING and the chemistry of HECT ligase to transfer the ubiquitin to the substrate (Wenzel et al. 2012; Lazarou et al. 2013). Structurally, parkin protein consists of an ubiquitin-like (UBL) domain at the N-terminal region and the RBR (Ring-Between-Ring) domain at the C-terminal region (Figure 6 A). The UBL is involved in different processes, such as proteosome association, substrate recognition and the regulation of parkin level and activity. The RBRs comprises a C3CHC4-type RING (really interesting new gene) domain RING1, which binds the E2 enzymes but it is not involved directly in catalysis and RING2 domain, which contains the catalytic

cysteine (cys 431), receives the ubiquitin from the E2. The two RING domains are separated by two Cysteine/Histidine (Cys/His)-rich Zn-binding domains in-between-RING (IBR). Different studies showed the existence of the His 433 and Glu444 in the proximity of Cys 431, suggesting the presence of catalytic dyad or triad (Wauer and Komander 2013; Trempe et al. 2013). Parkin contains also two flexible linker domains: the first one (following the UBL domain) is poorly conserved with an unknown function and, the second one, located between the IBR and RING2 domain is named repressor element of parkin (REP), because it is involved in parkin activity regulation. RING0, also known as unique parkin domain (UPD) domain, is an atypical RING located at the N-terminal of RBR domain.

The activity of parkin within the cell is tightly regulated by multiple mechanisms of auto-inhibition (Figure 6 B). Cytosolic parkin exists in the auto-inhibited conformation and the high resolution crystal structures of RING0-RBR domains, which lack the UBL domain, revealed multiple interactions that regulate parkin activity (Kumar et al. 2015). The catalytic domain in RING2 is buried by the hydrofobic interaction with RING0 (Wauer and Komander 2013; Trempe et al. 2013); REP domain forms two-turn helix which bounds to RING1 and, thereby, prevents the interaction between RING1 and ubiquitin charged E2 (Trempe et al. 2013). The N-terminal UBL uses hydrophobic interaction, centered around Ile44, to bind and occlude the RING1 domain.

Different studies have made progress in understanding the molecular mechanisms underlying parkin activation. PINK1, the mitochondrial Ser/Thr kinase, is required for parkin activation. These two proteins are involved in common pathways that regulate mitophagy of damaged mitochondria (Narendra et al. 2012).

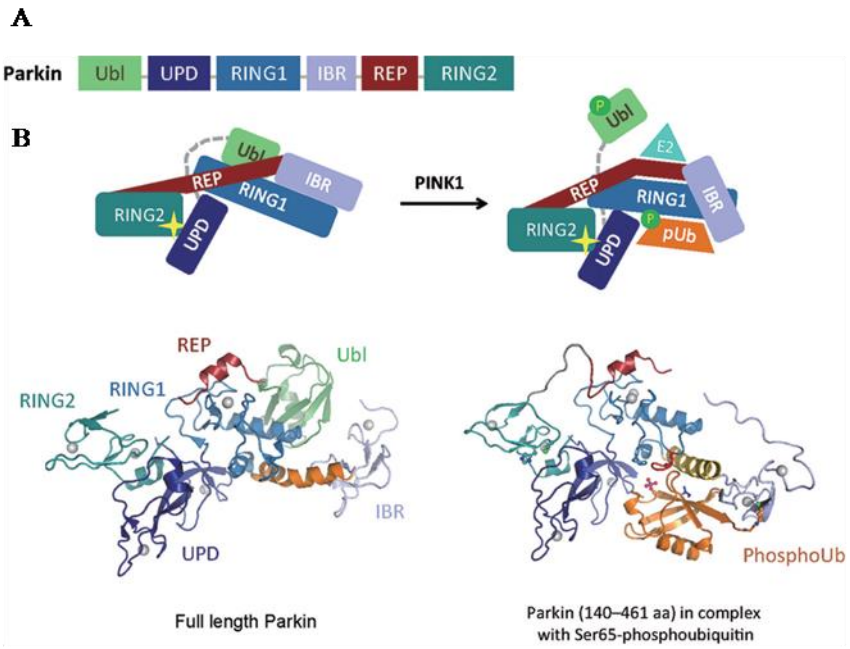

Figure 6. (A) Schematic structure of parkin shows the different domains of the protein and (B) representation of parkin-phosphoubiquitin (phosphoUb) complex. The yellow star mark represents the catalytic cysteine in the RING2 domain (from Zheng and Hunter 2015).

Studies derived from mammalian cell lines and human fibroblasts showed that the carbonyl cyanide *m*-chlorophenyl hydrazone (CCC) treatment, which causes a mitochondrial depolarization, promotes the recruitment of parkin on mitochondria in a PINK1-dependent manner. This leads to a reduction of mitochondrial mass and the colocalization of mitochondrial proteins with autophagosomal e lysosomal markers (Narendra et al. 2008).

PINK1 activates parkin through two events of phosphorylation, one occurs on Ser 65 of UBL domain and the other one on the equivalent residue in ubiquitin molecule (Figure 6 B) (Pickrell and Youle 2015). In 2015, Kumar and colleagues have demonstrated that UBL phosphorylation optimizes parkin for

phosphoubiquitin recruitment at the interface between RING0 and RING1 domains, a binding that promotes the displacement of the UBL domain (Kumar et al. 2015). Recent studies demonstrate that phosphoubiquitin binding is necessary for the translocation of parkin to mitochondria. Wauer and colleagues (2015) showed that phosphoubiquitin binding induces a straightening of the helix in the RING1 domain, which promotes conformational changes. This leads to destabilization of inhibitory interaction between REP and RING2 and to the release of UBL from RBR domain. Moreover, the release of UBL enhances its phosphorylation by PINK1, leading to open conformational changes, which activate parkin. This phosphorylation enables parkin to ubiquitinate different substrates within the cells, from cytosolic to outer mitochondrial membrane proteins and target them for mitophagy (Pickrell and Youle 2015; Chan et al. 2011).

Parkin, together with PINK1, is involved in the "mitochondrial quality control", a term used to describe the coordination of mitochondrial dynamics, mitophagy and biogenesis in order to maintain a mitochondrial healthy pool in cell (Scarffe et al. 2014). Thus, parkin/PINK1 pathway might control the distribution of mitochondria within the cells through the axonal transport regulation. PINK1, when is exposed on the surface of dysfunctional mitochondria, phosphorylates miro. Miro is a Ca^{2+} binding GTPase at the outer mitochondrial membrane (OMM) necessary for anterograde transport regulation. Its phosphorylation mediated by PINK1, in turn, promotes the ubiquitination by parkin and the subsequent degradation by proteosome. This process leads to the dissociation of kinesin motors from mitochondria. Therefore, PINK1/parkin may stop the movement of impaired mitochondria into neurites to quarantine the mitophagy (Itho et al. 2013). Mitochondrial dynamics is a term associated to fusion and fission events, which are crucial inside cells for mitochondrial number, shape

and transport. The fusion event of two mitochondria enables the exchange of contents to acquire components from healthy mitochondria. Conversely, fission process allows the mitochondrial division into smaller pieces, promoting the degradation of damaged components. This process is necessary both to produce one functional mitochondria (Youle et al. 2012) and to facilitate mitochondrial transport. Parkin deficient *Drosophila*, which results in reduced lifespan, male sterility and severe defect in flight and climbing abilities, show mitochondrial alterations (Greene et al. 2003) and flight muscle degeneration. Whitworth and colleagues (2005) has observed a mild dopaminergic neuronal loss in parkin mutants flies. Loss of parkin or PINK1 promotes in both flight muscle and dopaminergic neuron the formation of swollen mitochondria, supporting the idea that parkin promotes mitochondrial fission or inhibits mitochondrial fusion. These defects are suppressed by increasing the expression of dynamin-related GTPase (DRP1), or by downregulation of the fusion-promoting GTPases, Mitofusin (MFN) and OPA1. In *Drosophila* parkin induces MFN2 ubiquitination and its subsequent proteosomal degradation (Ziviani et al. 2010). Different studies performed on mammalian cells have complicated this point of view because some of the studies demonstrates that PINK1/parkin promotes fusion, (Lutz et al. 2009), even though not all are in agreement with each others. MFN a protein involved in fusion events, it has been demonstrated to be a substrate of both PINK1 and parkin (Ziviani et al. 2010). Interestingly, MFN2 interacts also with Miro, independently of its role in fusion events (Misko et al. 2010). DRP1 is a regulator of mitochondrial fission and it is also has been proposed to be substrate of parkin (Wang et al. 2011).

The proper control of mitochondrial dynamics is crucial for neurons to fulfill the needs in the different compartments and to reorganize working pieces into well functioning machinery (Scarffe et al. 2014). When the organelles is

completely damaged, they are removed by the proteosomal degradation and mitophagy, and the replenish of new functional mitochondria or the increase in cellular demands requires the mitochondrial biogenesis. Parkin plays also a functional role in mitochondrial biogenesis by regulating the level of PARIS, a zinc finger protein, which mediates repression of a master regulator of mitochondrial biogenesisis, the peroxixome proliferator-activated receptor gamma (*PPARγ*) coactivator-1α (PGC1α) (Scarffe et al. 2014).

Parkin has several others substrates, such as CDC-rel1 (a synaptic vesicles associated GTPase), cyclin E, p38 transfer RNA, Paelr1 (parkin associated endothelin receptor like receptor), O-glycosylated form of α-syn (named αSp22) and synphilin-1 (an α-syn interacting protein), synaptotagmin XI, α- and β-tubulin and many others. Moreover, pakin is autoubiquitinated and so it can be considered a self-substrate. Pathogenic mutations associated to PD occur throughout the domains of parkin protein; these mutations lead to different consequences: they could compromise the structural integrity of the protein (e.g. C212Y, C289G and C441R affect zinc coordination, while R42P, K211N and T351P disrupt protein folding or stability), interfere with substrates binding (e.g. R42P, K161N and T2403) or directly affect the enzyme activity (e.g. T415N, G430D, C431F, M434K, C418R and C441R). Only these latter mutations, that affect RING2 domain, abolish parkin E3 enzymatic activity meaning that the RING2 finger motif is the catalytic core of parkin.

Different studies highlighted the neuroprotective capacity of parkin against several insults, preventing cell death under various stress conditions: mitochondrial and endoplasmic reticulum (ER), accumulation of toxic and misfolded protein, such as α-syn (Feany et al. 2003) and MT destabilization.

1.3.1 Parkin and Microtubules

In 2003, Ren et al. reported the discovery of parkin as a novel tubulin-binding protein, as well as a MT-associated protein.

In rat brain lysates or transfected human embryonic kidney (HEK) 293 cells, α- and β-tubulin strongly co-immunoprecipitated with parkin after the treatment with colchicine and the incubation at 4°C, conditions that ensure MT depolymerization. They showed that parkin tightly binds to MT in taxol-mediated MT coassembly assays and that it is localized in a puncta manner along MTs. The treatment with colchicine, a MT-destabilizing drug, leads parkin to be more diffuse on the cytoplasm. Moreover, they also showed that the expression of wild-type parkin in cells significantly increased the ubiquitination and facilitated the degradation of α- and β-tubulin through its E3 ligase activity, whereas the parkin AR-JP-linked mutants (K161N, T240R, C431F) abolished the activity of parkin towards tubulins and others substrates. Next, it has been demonstrated that parkin is able to bind tubulin and MTs through three independent domains: Linker, RING1 and RING2. The expression of these domains in cells reduced the ability of colchicine to depolymerize MTs, suggesting a role of parkin in MT stabilization. PD-linked mutations (K161N in the Linker, T240R in RING1, C431F in RING2) did not disrupt the binding between parkin and tubulin or MTs as well as its ability to attenuate MT depolymerization induced by colchicine, meaning that the ability to bind tubulin and stabilize MTs is independent of E3 ligase activity (Yang et al. 2005) Therefore, the interaction of parkin with MTs may facilitate its E3 ligase activity (Feng 2006). The expression of wild-type parkin has been demonstrated to protect dopaminergic neurons against MT-depolymerizing PD-toxins, such as colchicine and rotenone, through MAP kinase pathway activation. In contrast the protective effect of parkin was abrogated by its PD-

linked mutant, that produces a truncated protein lacking any three MT-binding domains (Ren et al. 2009). This demonstrated that the integrity of MT network is essential for the survival of midbrain neurons (Feng 2006). Midbrain dopaminergic neurons are particularly vulnerable to MT depolymerization because of their peculiar morphology and neurochemistry. Dopaminergic neurons characterized by long and elaborate axon, rely on MTs to transport vesicles containing DA (Feng 2006). Recently, it has been demonstrated that parkin maintains morphological complexity of human midbrain derived-iPSc neurons by its MT-stabilizing effect (Ren et al. 2015). Parkin PD-linked mutants reduce the complexity of neuronal process and promote MT destabilization; the overexpression of wild-type parkin significantly increases MT stability and rescues the morphological defects, the same effect obtained by treating the cells with MT-stabilizing taxol.

Noteworthy, Cartelli et al. (2012) demonstrated that MT stability is compromised in human fibroblasts carrying *PARK2* mutation. In particular, they showed morphological alteration, reduced MT mass, and changes in molecular pathways implicated in MT stability. Moreover, *PARK2* fibroblasts display an enrichment of Tyr tubulin, suggesting that MT system becomes more dynamic when parkin is mutated. The pharmacological MT stabilization and the transfection of wild type parkin rescue fibroblast phenotype and restore MT stability.

Aim of the Project

The tightly control of MT system is crucial for neuron survival and many evidences support the concept that MT dysfunction could contribute to PD pathogenesis. Mutations in *PARK2* gene, responsible for the majority of AR-JP, cause MT destabilization and reduce the complexity of neuronal process in both murine and human dopaminergic neurons (Ren et al., 2009; Ren et al., 2015). Moreover, striking data derived from our laboratory showed that PD-patient skin fibroblasts, bearing *PARK2* mutations, display reduced MT mass and morphological defects (Cartelli et al. 2012). Interestingly, besides the well-known ligase activity, parkin regulates other cellular functions such as mitochondria homeostasis, including mitochondrial dynamics and transport (Scarffe et al. 2014), and MT stability (Yang et al. 2005).

To gain more insight into the intracellular roles of parkin, our aim was to investigate its influence on MT stability and MT-based neuronal function, namely axonal transport, in gene-based models of the pathology and, in particular, we wondered whether MT dysfunction could be an early event triggering neurodegeneration.

The first task we faced was to characterize MT system *in vivo*. We used*PARK2*-Q311X transgenic mice expressing the C-terminal truncated human parkin associated with Turkish early-onset PD (Lu et al. 2009) which resembles the hallmarks characteristic of the disease in an age-dependent way. We aimed to investigate if the point mutation Q311X affects MT and mitochondrial system in the nigrostriatal pathway through the analysis of tubulin PTMs, crucial controller of MT stability, and of proteins involved in mitochondrial dynamics and transport, respectively. To pinpoint the timetable of events in triggering neurodegeneration, we performed our experiments in young and adult mice (6

and 16 weeks old) before the onset of the previously described defects and neuronal loss (Lu et al. 2009). Furthermore, we studied the impact of parkin absence on MT and mitochondrial system in *PARK2* KO mice (Goldberg et al. 2003) at different ages, ranging from young adult to old mice (2-24 months). Since *PARK2* KO mice do not show the pathological hallmarks of the pathology, except for some nigrostriatal abnormalities, we used this model both to elucidate the physiological role of parkin and to unravel the early events in PD pathogenesis.

Then we moved to cultured neuronal cells. MT stability and mitochondrial transport were assessed in *PARK2*-silenced PC12 cells, extensively studied as a model of dopaminergic neurons in culture, and in primary midbrain cultures obtained from *PARK2* KO and heterozygous mice. In order to verify the hypothesis that parkin modulates MT dynamics directly and to investigate in detail the interplay between MT system and mitochondrial transport we used a live cell imaging approach.

Main Results

Our understanding of the mechanisms underlying the initiation and the progression of PD began with the study of *PARK2*-Q311X transgenic mice at different ages (6 and 16 weeks old) in the attempt to disclose the time course of MT dysfunction and to compare these defects with changes in mitochondrial dynamics and transport. The quantification of dopaminergic terminals in the *Corpus striatum* ruled out the occurrence of neurodegeneration in these young and adult mice, whereas a modest but significant increase of TH levels within the cell body of dopaminergic neurons in the *Substantia nigra* of *PARK2*-Q311X mice, at both 6 and 16 weeks of age, was observed. The characterization of MT system has been carried by analysing tubulin PTMs that are associated to MTs with different stability. The results showed an unbalance in the levels of tubulin PTMs in the early phases of the disease, namely before neurodegeneration occurs. Biochemical analysis, performed on total protein extract, showed a significant decrease of deTyr tubulin, associated with stable MTs, on ventral mesencephalon of 16 weeks old mice. On the contrary, we observed an increase of acetylated tubulin, associated with stable MTs, in the *Corpus striatum* at the same time point. Confocal analysis showed that α-tubulin PTMs changes occur specifically inside dopaminergic cell soma of the *Substantia nigra* and becomes evident already in 6 weeks old mice. In particular, the quantification of fluorescence intensity within single TH positive-cells in *Substantia nigra* showed a significant reduction of Tyr tubulin, marker of dynamics MTs; the observed changes of Tyr tubulin in 6 weeks old mice seems to be transient as older mice do not show any significant alteration with respect to controls. Furthermore, our analyses also revealed a concomitant enrichment of deTyr tubulin in the *Substantia nigra* followed by a significant

decrease in older mice (16 weeks). On the contrary, western blot analyses of proteins involved in mitochondrial fusion and fission (MFN2 and DRP1, respectively) did not show any significant alteration in their levels in ventral mesencephalon and in *Corpus striatum*of both 6 and 16 weeks old *PARK2*-Q311X mice. The distribution of mitochondria along dopaminergic fibers was investigated as it is a useful, even if indirect, approach to assess axonal transport but we did not observe any impairment at the same time points (De Gregorio et al., to be submitted, PART II).

The early unbalance of tubulin PTMs was also reported for *PARK2* knockout mice that showed an increase in dynamic MTs followed by the accumulation of stable MT pools, both in the *Substantia nigra* and *Corpus striatum*, which precedes the block of mitochondrial transport without affecting the levels of protein involved in mitochondrial dynamics (Cartelli et al., to be submitted, PART II). Collectively, our data coming from two different mouse disease models support the relevance of parkin in modulating tubulin PTMs *in vivo*.

In the second part of the project, we evaluated the impact of parkin deficiency on MT system and on the interplay between MT and mitochondrial transport in cultured cells. Live cell imaging analyses carried out in *PARK2*-silenced PC12 cells clearly showed that the absence of parkin significantly accelerates MT-growth, causing MT destabilization. At the same time, parkin-silencing speeds up specifically the anterograde transport velocity, with no effects on the retrograde one; noteworthy, silenced cells display a higher fraction of mitochondria moving towards the soma, meaning that parkin absence causes a disorientated mitochondrial trafficking. These axonal transport defects were restored by the MT-stabilizing agent paclitaxel, confirming the importance of modulation of parkin on MT stability (Cartelli et al., to be submitted, PART II).

Next, we moved to primary mesencephalic neuronal cultures obtained from

PARK2 KO and *PARK2* heterozygous mice. Neurons isolated from *PARK2* KO showed the defective axonal outgrowth at 1 and 2 day *in vitro* (DIV) of differentiation with a concomitantly increase of neuronal sprouting only at 1 DIV, that to say in cells that are actively involved in neurite emission. In agreement with the data obtained in *PARK2*-silenced PC12 cells, parkin deficiency causes MT destabilization, that consequently leads to altered mitochondria axonal transport. In primary neurons the absence of parkin significantly accelerates MT growth and at the same time slightly speeds up the total velocity of mitochondrial axonal transport, with a mild but not significant increase in anterograde or retrograde transport specifically. Instead, parkin absence did not affect mitochondrial trafficking direction in primary neurons. The treatment with paclitaxel decreased mitochondrial velocity compared also to the control cells. Probably, the effect could be due to the high concentration of paclitaxel that we have used for our experiments. Finally, the effect of parkin on MT stability was assessed also by immunofluorescence analysisof tubulin PTMs that revealed an enrichment of Tyr tubulin in primary neurons derived from *PARK2* KOmice respect to *PARK2* heterozygous and control mice (De Gregorio et al, Manuscript in preparation, PART III).

In conclusion, these results strongly indicate that parkin is a regulator of MT stability in cultured neurons and *in vivo* and, together with all the striking data coming from other gene- and toxins-based models of the disease, reinforce the idea that MT dysfunction may be crucial in PD pathogenesis (Pellegrini et al. 2015; Cappelletti et al. 2015; Cartelli and Cappelletti, 2016).

Conclusions and Future Perspectives

Here, we have demonstrated the impact of parkin on the regulation of tubulin PTMs and MT dynamics in neurons and in murine gene-based experimental models of the disease. Importantly, our data strongly suggest that alterations of MT stability accounts for very early event underlying PD pathogenesis and likely triggers defects in axonal transport.

We showed that the absence of parkin, according to its proposed MT-stabilizing effect (Yang et al. 2005), alters the equilibrium between stable and dynamic pools of MTs making this cytoskeletal system destabilized with respect to the controls, in both neuronal cultures and *in vivo* (Cartelli et al., to be submitted, PART II; De Gregorio et al., manuscript in preparation, PART III). Interestingly, the early enrichment of dynamic MT pool is followed by the accumulation of PTMs associated with stable MTs in late stages and precedes the block of mitochondrial axonal transport in *PARK2* KO mice (Cartelli et al., to be submitted, PART II).

Furthermore, we showed that the rare pathogenic mutation *PARK2*-Q311X induces the very early unbalance of tubulin PTMs *in vivo* and becomes noticeable before that TH depletion and dopaminergic neuron loss occurs (De Gregorio et al., to be submitted, PART II). In detail, Q311X mutation results in the early enrichment of tubulin PTMs associated to stable pool. Most likely, the over-stabilization effect may be due to a dominant gain of a toxic novel function of the mutant protein. This could be view as an attempt of dopaminergic neurons to balance or counteract the depolymerizing insult, through the accumulation of tubulin PTMs that protect them from the collapsing MT system (Cartelli and Cappelletti, 2016).

Since the transgenic mouse models have their specificities and limitations, the

future perspectives of this project involve the analysis of MT stability in the context of human neuronal cells taking advantage of iPSC-derived dopaminergic neurons obtained from the PD patients bearing different *PARK2* mutations. This allows investigating whether the decrease of MT mass described by Ren et al. (2015), due to the effect of parkin mutations, correlates with the unbalance of tubulin PTMs.

An expected consequence of the alteration of MT stability is the dysregulation of axonal transport. Indeed, our data demonstrate that parkin regulates mitochondrial trafficking in a MT-dependent manner by showing that the impairment of mitochondrial transport along axons is rescued by MT stabilizer agent paclitaxel. The concept that the stabilization of MT could be an efficient strategy for neuroprotection is supported by data coming from others experimental models of PD (Ren et al. 2009; Cartelli et al. 2012). Importantly, Epothilone D, drug acting as aMT stabilizer agent, exerts neuroprotective effects in a toxin-based murine model of PD (Cartelli et al. 2013). Thus, MT system could represent a reliable therapeutic target for management of the disease (Brunden et al. 2014). These findings will open the way to deeply investigate how to control MT stability using different strategies, including the modulation of enzymes that specifically regulate PTMs of tubulin, crucial controller of MT dynamics and mitochondrial transport.

Finally, a side research of the lab demonstrated that the PD-related pre-synaptic protein α-syn is a novel, foldable, MT-dynamase, which changes its conformation when binds to $\alpha_2\beta_2$tetramers and regulates MT nucleation and dynamics, enhancing MT growth rate and catastrophe frequency, *in vitro* and in cell. Furthermore, we confirmed interaction of α-syn with β-III tubulin and we observed its co-localization with the most dynamic MTs pool (tyrosinated tubulin), at pre-synapse of PC12 cells and human neurons. Furthermore, PD-

related α-syn mutants are much less sensitive than WT α-syn to fold upon tubulin binding and cause tubulin aggregation rather than polymerization. This could potentially lead to impairment of the proper MT organization in the neuronal processes at the pre-synapse. Therefore, these results obtained from PD-linked α-syn mutants provide hints for the pathogenesis in PD, which could involve MT-dependent processes, such as axonal transport (Cartelli et al. 2016). Future work will be necessary to better understand the link between axonal transport impairment, α-syn/MT in the context of PD.

Overall, the data arising from the present work reinforce the idea that MT dysfunction may play a crucial role in the chain of events leading to neurodegenerative processes underlying PD pathogenesis. Indeed, MT system represents a point of converge in the action of neurotoxins and different proteins related to PD, including parkin and α-syn, whose mutations we reported to cause defects in MT dynamics and/or stability. Furthermore, alterations of MT dynamics that become noticeable before any other signs of neurodegeneration (Cartelli et al. 2013; Cartelli et al. to be submitted; II parte; De Gregorio et al., to be submitted) might result in the failure of the axonal transport that is a common defect of many neurodegenerative diseases, including PD. Indeed, the morphology of dopaminergic neurons, which have a complex neurite arborization, makes them particularly sensitive to axonal transport failure. According to this, the primary step in the PD pathogenesis is the degeneration of striatal dopaminergic terminals that, in turn, triggers the neuron death, the so called "dying back" process (Coleman et al. 2005). This could be likely due to axonal transport failure or MTs alteration.

Importantly, all these evidences make the study of MT dysfunction a challenge for a better comprehension of PD pathogenesis and, notably, supply the rationale for the development of novel MT-target based therapeutic strategies to

treat PD and other disorders of central nervous system (Cartelli and Cappelletti 2016).

References

Akhmanova, A. and Steinmetz, M.O., 2008. Tracking the ends: a dynamic protein network controls the fate of microtubule tips. *Nat Rev Mol Cell Biol*, **9**, 309–322.

Alim, M.A. et al., 2002. Tubulin Seeds α -Synuclein Fibril Formation . *J Biol Chem*, **277**, 2112–2117.

Baas, P.W., Slaughter, T., Brown, A., Black, M.M. 1991. Microtubule dynamics in axons and dendrites. *J Neurosci Res*, **30**, 134-53.

Baas, P.W., Deitch, J.S., Black, M.M., Banker, G. 1988. Polarity orientation of microtubules in hippocampal neurons: uniformity in the axon and non uniformity in the dendrite. *Proc Natl Acad Sci U S A*, **85**, 8335–8339.

Baas, P.W., Karabay, A., Qiang, L. 2005. Microtubules cut and run. *Trends Cell Biol*, **15**, 518-24.

Braak, H. et al.,. 2003. Staging of brain pathology related to sporadic Parkinson' s disease. *Neurobiol Aging*, **24**, 197–211.

Brunden, K.R. et al., 2014. Microtubule-stabilizing agents as potential therapeutics for neurodegenerative disease. *Bioorg Med Chem*, **22**, 5040–5049.

Burbank, K.S. & Mitchison, T.J., 2006. Microtubule dynamic instability. *Curr Biol*, **16**, R516–517.

Cannon, J.R., Greenamyre, J.T. 2013. Gene-environment interactions in Parkinson's disease: specific evidence in humans and mammalian models. *Neurobiol Dis*, **57**, 38–46.

Cappelletti, G., Maggioni, M.G. and Maci, R., 1999. Influence of MPP+ on the State of Tubulin Polymerisation in NGF-Differentiated. *J Neurosci Res*. **55**, 28–35.

Cappelletti, G., Surrey, T. and Maci, R., 2005. The parkinsonism producing neurotoxin MPP + affects microtubule dynamics by acting as a destabilising factor. FEBS Lett, **579**, 4781–4786.

Cappelletti, G. et al., 2015. Linking microtubules to Parkinson's disease: the case of parkin. *Biochem Soci Trans*, **43**, 292–6.

Carlier M.F., Didry D., Pantaloni D. 1987. Microtubule elongation and guanosine 5'-triphosphate hydrolysis. Role of guanine nucleotides in microtubule dynamics. *Biochemistry*. **26**, 4428-37.

Cartelli, D. et al., 2010. Microtubule dysfunction precedes transport impairment and mitochondria damage in MPP+-induced neurodegeneration. *J Neurochem*, **115**, 247–258.

Cartelli, D. et al., 2012. Microtubule Destabilization Is Shared by Genetic and Idiopathic Parkinson's Disease Patient Fibroblasts. *PLoS* ONE, **7**,1–12.

Cartelli, D. et al., 2013. Microtubule Alterations Occur Early in Experimental Parkinsonism and The Microtubule Stabilizer Epothilone D Is Neuroprotective. *SciRep*, **3**:1837.

Cartelli, D. et al., 2016. α -Synuclein is a Novel Microtubule Dynamase. *Sci Rep*, **6**:33289.

Cartelli, D. and Cappelletti, G., 2016. Microtubule Destabilization Paves the Way to Parkinson's Disease. *Mol Neurobiol*. Epub doi: 10.1007/s12035-016-0188-5

Chan, N.C. et al., 2011. Broad activation of the ubiquitin–proteasome system by Parkin is critical for mitophagy. *Hum Mol Genet*, **120**, 1726–1737.

Choi, W., Palmiter, R.D. and Xia, Z., 2011. Loss of mitochondrial complex I activity potentiates dopamine neuron death induced by microtubule dysfunction in a Parkinson's disease model. *J Cell Biol.* **192**, 873-82.

Chu, C. et al., 2011. A novel acetylation of β -tubulin by San modulates microtubule polymerization via down-regulating tubulin incorporation. *Mol Biol Cell*, **22,** 448-56.

Cleveland, D.W., Kirschner M.W., Cowan N.J. 1978. Isolation of separate mRNAs for alpha- and β- tubulin and characterization of the corresponding in vitro translation products. *Cell*, 15, 1021-31.

Conde, C. and Cáceres, A., 2009. Microtubule assembly , organization and dynamics in axons and dendrites. *Nat Rev Neurosci*, 10, 319-32.

Coleman, M. (2005). Axon degeneration mechanisms: commonality amid diversity. N*at Rev Neurosci* 6; 889–98.

Corti, O., Lesage, S. and Brice, A., 2011. What genetics tells us about the causes and mechanisms of Parkinson's disease. *Physiol Rev*, 91, 1161–1218.

Craig, A.M., Banker, G. 1994. Neuronal polarity. *Annu Rev Neurosc*i, **17**, 267-310.

Dauer, W. and Przedborski, S., 2003. Parkinson ' s Disease: Mechanisms and Models. *Neuron*, **39**, 889–909.

Desai, A. and Mitchison, T.J., 1997. Microtubule Polymerization Dynamic. *Annu Rev Cell Dev Biol.* **13**, 83–117.

Dompierre, J.P. et al., 2007. Histone Deacetylase 6 Inhibition Compensates for the Transport Deficit in Huntington' s Disease by Increasing Tubulin Acetylation. *J Neurosci*, **27**, 3571–3583.

Dubey, J. et al., 2015. Neurodegeneration and microtubule dynamics : death by a thousand cuts. *Front Cell Neuroscin*, **9**, 10-26.

Erck, C. et al., 2005. A vital role of tubulin-tyrosine-ligase for neuronal organization. *Proc Natl Acad Sci U S A*,**102**, 7853-8.

Ersfeld, K. et al., 1993. Characterization of the Tubulin-Tyrosine Ligase. *J Cell Biol*, **120**, 725–732.

Fanara, P. et al., 2007. Stabilization of Hyperdynamic Microtubules Is Neuroprotective in Amyotrophic Lateral Sclerosis. *J. Biol Chem*, **282**, 23465–23472.

Feany, M.B., Pallanck, L.J. and Avenue, L., 2003. Parkin: A Multipurpose Neuroprotective Agent ? *Neuron*, **38**,13–16.

Feng, J., 2006. Microtubule : A Common Target for Parkin and Parkinson ' s Disease Toxins. *Neuroscientist*, **12**, 469–476.

Forman, M.S., Trojanowski, J.Q. and Lee, V.M., 2004. Neurodegenerative diseases: a decade of discoveries paves the way for therapeutic breakthroughs. *Nat Med*, **10,** 1055–1063.

Greenamyre, J.T., Betarbet, R., Sherer, T.B. 2003. The rotenone model of Parkinson's disease: genes, environment and mitochondria. *Parkinsonism Relat Disord*, **9**, 59–64.

Greene, J.C. et al., 2003. Mitochondrial pathology and apoptotic muscle degeneration in Drosophila parkin mutants. *Proc Natl Acad Sci U S A,***100**, 4078-83

Hershko A., Ciechanover A. 1998. The ubiquitin system. *Annu Rev Biochem*, **67,** 425-79.

Hernandez, D.G**.**, Reed, X**.**, Singleton, A.B. 2016. Genetics in Parkinson disease: Mendelian versus non-Mendelian inheritance. *J Neurochem*, **1**, 59-74.

Huynh, D.P. et al., 2001. Differential expression and tissue distribution of parkin isoforms during mouse development. *Brain Res Dev Brain Res.* **130**, 173–81.

Itoh K., Nakamura K., Iijima M., and H.S., 2013. Mitochondrial Dynamics in Neurodegeneration. *Trends in Cell Biology*, **23**, 64–71

Janke, C. and Bulinski, J.C., 2011. Post-translational regulation of the microtubule cytoskeleton: mechanisms and functions. *Nat Rev Mol Cell Bio,***12**, 773-86

Janke, C., 2014. The tubulin code : Molecular components , readout mechanisms , and functions. *J Cell Biol* **206**, 461–472.Kahle P.J., Leimer U., Haass C. 2000. Does failure of parkin-mediated ubiquitination cause juvenile parkinsonism? *Trends Biochem Sci*, **25**, 524-7.

Kapitein, L.C. and Hoogenraad, C.C., 2011. Which way to go ? Cytoskeletal organization and polarized transport in neurons. *Mol Cell Neurosci*, **46**, 9–20.

Keith,, C.H., Bajer, A.S., Ratan, R., Maxfield, F.R., Shelanski, M.L. 1986. Calcium and calmodulin in the regulation of the microtubular cytoskeleton. *Ann N Y Acad Sci*, **466**, 375-91.

Khan, N.L. et al., 2005 dysfunction in unrelated, asymptomatic carriers of a single parkin. *Neurology*, **64**,134–136.

Kitada, T. et al., 1998. Mutations in the parkin gene cause autosomal recessive juvenile parkinsonism. *Nature*, **392**, 605–608.

Konishi, Y. and Setou, M., 2009. Tubulin tyrosination navigates the kinesin-1 motor domain to axons. *Nat Neurosci*, **12**, 559–567.

Kumar, K. R., Djarmati-Westenberger, A. and Grunewald, A. 2011. Genetics of Parkinson's disease. *Semin. Neurol*. **31**, 433–440.

Kumar, A. et al., 2015. Disruption of the autoinhibited state primes the E 3 ligase parkin for activation and catalysis. *EMBO J*, **34**, 2506–2521.

Kumaran, R. and Cookson, M.R., 2015. Pathways to Parkinsonism Redux : convergent pathobiological mechanisms in genetics of Parkinson' s disease. *Hum Mol Genet*, **24**, R32-44.

L'Hernault SW, Rosenbaum JL. 1985. Chlamydomonas alpha-tubulin is posttranslationally modified by acetylation on the epsilon-amino group of a lysine. . *Biochemistry* ; **24**,473-8.

Langston J.W., Ballard P., and Irwin I., 1983. Chronic parkinsonism in humans due to a product of meperidine-analog synthesis. *Science,* **219**, 979-980

Lansbergen, G. and Akhmanova, A., 2006. Microtubule Plus End: A Hub of Cellular Activities *Traffic*, **7**, 499–507.

Law, B.M.H. et al., 2014. A Direct Interaction between Leucine-rich Repeat Kinase 2 and Specific β -Tubulin Isoforms Regulates Tubulin. *J Biol Chem*, **289**, 895–908.

Lazarou, M. et al., 2013. PINK1 drives Parkin self-association and HECT-like E3 activity upstream of mitochondrial binding. *J Cell Biol*, **200**, 163-72.

Luby-Phelps, K. 2000. Cytoarchitecture and physical properties of cytoplasm: volume, viscosity, diffusion, intracellular surface area. *Int Rev Cytol.* **192,** 189-221.

Lu, X. et al., 2009. Bacterial Artificial Chromosome Transgenic Mice Expressing a Truncated Mutant Parkin Exhibit Age-Dependent Hypokinetic Motor Deficits , Dopaminergic Neuron Degeneration, and Accumulation of Proteinase K-Resistant α -Synuclein. *J Neurosc*i, **29**,1962–1976.

Lutz, A.K. et al., 2009. Loss of Parkin or PINK1 Function Increases Drp1-dependent. *J Biol Chem*,. **284**, 22938-51.

Magiera, M.M. and Janke, C., 2014. Post-translational modifications of tubulin. *Curr Biol*, **24**, R351–R354.

Malkus, K.A., Tsika, E. and Ischiropoulos, H., 2009. protein degradation in Parkinson ' s disease : how neurons are lost in the Bermuda triangle. *Mol Neurodegener*, **5**, 4,24.

Mitchison, T. and Kirschner M. 1984. Dynamic instability of microtubule growth. *Nature,* **312,** 237-42.

Marsden, C.D. 1983. Neuromelanin and Parkinson's disease. *J. Neural Transm. Suppl*. **19**, 121–141.

Marshall, L.E. and Himes, R.H., 1978. Rotenone inhibition of tubulina self-assembly. *Biochim Biophys Acta,* **543**, 590-594.

Maruta, H., Greer K., Rosenbaum, J.L. 1986. The acetylation of α-tubulin and its relationship to the assembly and disassembly of microtubules. *J Cell Biol.* **103**, 571-9.

Mitchison, T., Kirschner, M. 1984. Dynamic instability of microtubule growth. *Nature*, **312**, 237-42

Misko, A., Jiang, S., Wegorzewska, I., Milbrandt, J., and and Baloh, R.H., 2010. Mitofusin 2 is necessary for transport of axonal mitochondria and interacts with the Miro/Milton complex. *J Neurosci*, **30**, 4232–4240.

Nalls, M.A., McLean, C.Y., Rick J., Eberly, S., Hutten, S.J., Gwinn, K., et al., 2015. Diagnosis of Parkinson's disease on the basis of clinical and genetic classification: a population-based modelling study, *Lancet Neurol,* **14**, 1002-9.

Narendra, D. et al., 2008. Parkin is recruited selectively to impaired mitochondria and promotes their autophagy. *J Cell Biol*, **183**, 795–803.

Narendra, D., Walker, J.E. and Youle, R., 2012. Mitochondrial Quality Control Mediated by PINK1 and Parkin : Links to Parkinsonism, *Cold Spring Harb Perspect Biol,* 1;4.

Niwa, S., Takahashi, H. and Hirokawa, N., 2013. β -Tubulin mutations that cause severe neuropathies disrupt axonal transport. *EMBO J*, **68**, 610–638

Nogales, E., Wolf, S.G. and Downing, K.H., 1998. Structure of the αβ Tubulin Dimer by Electron Crystallography. *Nature*, **391**, 199–204.

Pellegrini, L., Wetzel,, A., Grannó S., Heaton, G., Harvey, K. 2016. Back to the tubule: microtubule dynamics in Parkinson's disease. Cell Mol Life Sci 1-26

Perlson, E. et al., 2010. Retrograde axonal transport : pathways to cell death ? *Trends Neurosci,* **33**, 335–344.

Pezzoli G., Ricciardi S., Masotto C., et al 1990. N-Hexane Induces Parkinsonism in Rodents. *Brain Res,* **531**, 355–7.

Pezzoli G., Canesi M., Antonini A., et al. 2000. Hydrocarbon exposure and Parkinson's disease. *Neurology*, **55**, 667–673.

Pickrell, A.M. and Youle, R.J., 2015. The Roles of PINK1, Parkin, and Mitochondrial Fidelity in Parkinson' s Disease. *Neuron*, **85**, 257–273.

Prots, I. et al., 2013. α-Synuclein Oligomers Impair Neuronal Microtubule-Kinesin. *J Biol Chem*, **288**, 21742–21754.

Ren, Y., Zhao, J. and Feng, J., 2003. Parkin Binds to α/ β Tubulin and Increases their Ubiquitination and Degradation. *J Neurosci*, 23, 3316-24

Ren, Y., Liu W., Jiang H., Jiang Q., Feng J. 2005. Selective vulnerability of dopaminergic neurons to microtubule depolymerization. *J Biol Chem*, **280**, 34105–34112.

Ren, Y. et al., 2009. Parkin protects dopaminergic neurons against microtubule-depolymerizing toxins by attenuating microtubule-associated protein kinase activation. *J Biol Chem*, **284,** 4009–4017.

Ren, Y. et al., 2015. Parkin Mutations Reduce the Complexity of Neuronal Processes in IPSC-Derived Human. *Stem Cells*, **33**, 68-78.

Roll-Mecak, A. and McNally, F.J., 2010. Microtubule-severing enzymes. *Curr Opin Cell Biol*, **22**, 96–103.

Scarffe, L.A. et al., 2014. Parkin and PINK1: much more than mitophagy. *Trends Neurosci*, **37**, 315–324.

Sheng, C., Heng, X., Zhang, G., Xiong, R., Li, H., Zheng, S. and Chen, S. 2013, DJ-1 deficiency perturbs microtubule dynamics and impairs striatal neurite outgrowth. *Neurobiol Aging,* **34**, 489–498

Schroder, H., Wehland, J. and Weber, K., 1985. Purification of Brain Tubulin-Tyrosine Ligase by Biochemical and Immunological Methods. *J Cell Biol*,**100**, 276-81

Shimura, H. et al., 2000. Familial Parkinson disease gene product , parkin , is a ubiquitin-protein ligase. *Nat Genet* ,**25**,302-5.

Song, Y. et al., 2013. Article Transglutaminase and Polyamination of Tubulin : Posttranslational Modification for Stabilizing Axonal Microtubules. *Neuron*, **78**,109–123.

Song, Y. and Brady, S.T., 2015. Post-translational modifications of tubulin : pathways to functional diversity of microtubules. *Trends in Cell Biology*, **25**,125–136.

Spencer, P.S., Schaumburg, H-H. 1985. Organic solvent neurotoxicity: Facts and research needs. *Scand J Work Environ Heal*, **11**, 53–60.

Spillantini M.G., Schmidt M.L., Lee VM-Y., et al 1997. Alpha-Synuclein in Lewy bodies. *Nature*, **388**, 839–840

Trempe, J. et al., 2013. Structure of Parkin Reveals Mechanism for Ubiquitin Ligase Activation. *Science*, **340**, 1451-5.

Trinczek, B. et al., 1995. Domains of Tau Protein , Differential Phosphorylation , and Dynamic Instability of Microtubules. *Mol Biol Cell*, **6**, 1887-902.

Vance J.M., Ali S., Bradley W.G., et al. 2010. Gene-environment interactions in Parkinson's disease and other forms of parkinsonism. *Neurotoxicology*, **31**, 598–602.

Vos, K.J. De et al., 2008. Role of Axonal Transport in Neurodegenerative Diseases . *Annu Rev Neurosci*, **31**, 151-73

Wang, H. et al., 2011. Parkin Ubiquitinates Drp1 for Proteasome-dependent Degradation. *J Biol Chem*, **286**, 11649–11658.

Wauer, T. and Komander, D., 2013. Structure of the human Parkin ligase domain in an autoinhibited state. *The EMBO Journal*, **32**, 2099–2112.

Wenzel, D.M. et al., 2012. UBCH7 reactivity profile reveals parkin and HHARI to be RING/HECT hybrids. *Nature*, **474**, 105–108.

West, A.B. et al., 2002. Functional association of the parkin gene promoter with idiopathic Parkinson ' s disease. *Hum Mol Genet*, **11**, 2787–2792.

Whitworth A.J., et al, 2005 . Increased glutathione S-transferase activity rescues dopaminergic neuron loss in a Drosophila model of Parkinson's disease. *Proc Natl Acad Sci U S A.* **102**, 8024-9.

Yang, F. et al., 2005. Parkin Stabilizes Microtubules through Strong Binding Mediated by Three Independent Domains Parkin. *J BiolChem*, **280**, 17154–17162.

Youle, R.J. et al., 2012. Mitochondrial Fission, Fusion, and Stress. *Science*, **337,** 1062-5.

Zheng, X. and Hunter, T., 2015. How phosphoubiquitin activates Parkin. *Cell Res*, **25**, 1087–1088.

Ziviani, E., Tao, R.N. and Whitworth, A.J., 2010. Drosophila Parkin requires PINK1 for mitochondrial translocation and ubiquitinates Mitofusin. *Proc Natl Acad Sci U S A*, **107**, 5018-5023

Acknowledgements

I would like to thank all the people that supported me during these important years, making this PhD thesis possible.

I am grateful to my supervisor Prof.ssa Graziella Cappelletti who gave me the opportunity to work in her lab discovering the exciting world of the research. Thanks to her experience and guide I enriched my scientific knowledge.

I also thank all the members of my Thesis Committee, Prof.ssa Graziella Messina and Prof.ssa Paola Riva for their remarkable advices throughout the annual progress reports.

Special thanks to all the friends of the Cappelletti's Lab; in particular a huge thank to the " SENIOR" Alessandra, Francesca Casagrande, Daniele, Francesca Cantele, Samanta, Jacopo. I will always be grateful because they were my shoulder supporting me by a theoretical and methodological point of view. I shared with them concerns and frustrations but also ideas and satisfactions.

I thank all the thesis students and especially those I have followed: Marta Valerio, Ludovica, Anna and Silvia, that in turn have taught and given me so much.

I am grateful to all the people who contributed to this work: Dott.ssa Alida Amadeo, for the technical and scientific support in mice neuroanatomy; Dott.ssa Jenny Sassone for transgenic mice management; Dott.ssa Ginetta Collo for gave me the opportunity to acquire the skill to work with dopaminercic primary coltures; Dott.ssa Miriam Ascagni for her help and advices about confocal microscopy.

Last but not the least, a huge thank to my family, which was always present and always supported me in any situation, encouraging to overcome the difficulties. Without them I probably would not be able to reach this aim.

PART II

Contents

Manuscript 1

De Gregorio C,.Casagrande F.V.M., Calogero A.M., Cartelli D., Mazzetti S., Ferretti M., Beltramone S., Amadeo A., Sassone J., Pezzoli G. and Cappelletti G. "*PARK2*-Q311X mutation induces the early unbalance of post-translationally modified tubulin *in vivo"*
To be submitted.

Manuscript 2

Cartelli D., Amadeo A., Casagrande F.V.M., **De Gregorio C**., Calogero A.M., Gioria M., Kuzumaki N.,Costa I., Sassone J., Ciammola A., Hattori N., Okano H., Goldwurm S., Roybon L., Pezzoli G. and Cappelletti G.
"Parkin modulates microtubule dynamics and balances tubulin post translational modifications"
To be submitted.

PARK2-Q311X MUTATION INDUCES THE EARLY UNBALANCE OF POST-TRANSLATIONALLY MODIFIED TUBULINS *IN VIVO*

Carmelita De Gregorio[1], Francesca V.M. Casagrande[1], Alessandra M. Calogero[1], Daniele Cartelli[1], Samanta Mazzetti[1], Marta Ferretti[1], Silvia Beltramone[1], Alida Amadeo[1], Jenny Sassone[2], Gianni Pezzoli[3], and Graziella Cappelletti[1,4*].

[1]Department of Biosciences, Università degli Studi di Milano, Milano, Italy

[2]Department of Neurology and Laboratory of Neuroscience, IRCCS Istituto Auxologico Italiano, Cusano Milanino (MI), 20095, Italy

[3]Parkinson Institute, ASST G. Pini-CTO, ex ICP, Milano, Italy.

[4]Center of Excellence on Neurodegenerative Diseases, Università degli Studi di Milano, Milano, Italy

***Corresponding Author:**
Graziella Cappelletti
Department of Biosciences
Università degli studi di Milano
Via Celoria, 26
20133 Milano
Italy
Tel:0039 02 50314752
Fax:0039 02 50314801
E-mail: graziella.cappelletti@unimi.it

ABSTRACT

Parkinson's disease (PD) is a movement disorder due to the progressive loss of dopaminergic neurons whose pathogenesis remains still unclear. So far, neurodegeneration in PD is likely caused by a combination of multifactorial events and involves different pathogenic pathways. Among them, the dysfunction of microtubules is emerging as novel contributing factor of the disease, and this evidence is supported by several studies on toxin-based experimental models of PD. Our goal is to further investigate the role of microtubule dysfunction in PD neurodegeneration using a gene-based model of the disease, namely *PARK2*-Q311X transgenic mice which that show age-dependent loss of dopaminergic neurons, and we investigated whether this point mutation Q311X of parkin affects microtubule system in the nigrostriatal pathway. In particular, we analyzed microtubule stability and mitochondrial system in young mice (6-16 weeks old), before the onset of the previously described defects and neuronal loss, with the aim to discover the timetable of events in triggering neurodegeneration. In order to reveal the possible alterations in microtubule and/or mitochondrial system, respectively, we performed different analysis of post-translational modifications of tubulin and of proteins involved in mitochondrial fusion and fission. Throughout biochemical and confocal analyses, our results highlighted an early microtubule dysfunction associated with the unbalance of different α-tubulin post-translational modifications within dopaminergic neurons in young *PARK2*-Q311X transgenic mice. On the contrary, none alteration was observed in mitochondrial dynamics and distribution in nigrostriatal fibers, at least at the time points we investigated. Finally, the quantification of dopaminergic terminals in the *Corpus striatum* ruled out the occurrence of neurodegeneration in these young mice. Taken together, our results suggest that the observed

alterations in microtubule stability could be attributable to a very early event underlying neurodegeneration in *PARK2*-Q311X mice.

INTRODUCTION

Parkinson's disease (PD) is a progressive and multifactorial neurodegenerative disorder characterized by the selective degeneration of dopaminergic neurons projecting from the *Substantia nigra pars compacta* (SN) to the *Corpus striatum* (ST). This leads to a severe striatal dopamine deficiency and, consequently, to the typical movement disorders of parkinsonism (Dauer & Przedborski 2003). The molecular mechanisms underlying the neuronal loss are still unclear, but several pathogenic pathways have been reported causing dopaminergic neurons degeneration including oxidative stress, mitochondrial dysfunctions, proteolytic stress due the ubiquitin-proteasome system (UPS) impairment and local inflammation (Kumaran & Cookson 2015). Recently, the microtubule (MT) dysfunction is becoming established as a promising hypothesis in PD pathogenesis. *PARK2* gene, whose mutations result in both familial and sporadic forms of PD (Shimura et al. 2000), encodes for parkin which is a RING-between-RING E3 ligase that catalyses the attachment of ubiquitin to specific substrates and, in addition, it has been implicated in many other cellular functions, such as mitochondrial homeostasis and MT cytoskeleton stabilization. Indeed, a large body of evidence showed the ability of parkin to modulate mitochondrial dynamics (fusion and fission), mitophagy and transport (Scarffe et al. 2014), but also its capacity to bind α- and β-tubulin heterodimers promoting their degradation (Ren et al. 2003) and to stabilize MTs through the redundant interaction of three domains (Yang et al. 2005). Further

work performed both on murine and human induced pluripotent stem cells (iPSC)-derived dopaminergic midbrain neurons showed that parkin protects neurons against depolymerizing agents, such as rotenone and colchicine (Ren et al. 2009; Ren et al. 2015). Striking data coming from our laboratory showed that human fibroblasts, obtained from PD patients carrying *PARK2* mutations, exhibit an altered MT stability, and the pharmacological MT stabilization and the transfection of wild type parkin restores MT stability (Cartelli et al. 2012). These evidences strongly support the concept that the interplay between parkin and MTs could have a crucial role in PD context.

Nevertheless, the impact of parkin on MTs *in vivo* has been poorly investigated to date. Mouse transgenic models that are actually available have their own specificities but also limitations. The parkin knockout mice developed until now do not exhibits dopaminergic neurons loss or motor impairment, except for nigrostriatal abnormalities (Goldberg et al. 2003), *Locus coeruleus* alterations (Von Coelln et al. 2004), features of mitochondrial dysfunction and oxidative damage (Palacino et al. 2004). On the other hand, transgenic mouse model selectively overexpressing a truncated human mutant parkin (Parkin-Q311X) in dopaminergic neurons, display age-related neuropathologies of PD (Lu et al. 2009). Thus, *PARK2*-Q311X transgenic mouse is a good gene-based experimental model of the disease, because it shows dopaminergic neurons degeneration in the *Substantia nigra* at 16 months of age that is preceded by a significant loss of their terminals in the *Corpus striatum*, progressive motor deficits, α-synuclein pathology and the reduction of the striatal dopamine levels (Lu et al. 2009). Recently, it has also been demonstrated that *PARK2*-Q311X mice display an impairment of the autophagic pathway at the level of lysosomal function which, in turn, coincides with defects in mitochondrial quality control and increased neurodegenerative and behavioural phenotypes (Siddiqui et al.

2015). Thus, this genetic model seems to be appropriate for investigating whether the point mutation Q311X affects MT system in the nigrostriatal pathway in a context of the neurodegenerative process.

In this work, we used *PARK2*-Q311X mice at different ages in the attempt to disclose the time course of MT dysfunction and to compare these defects with changes in mitochondrial dynamics. A cohort of young *PARK2*-Q311X and wild type control littermate mice were tested at 6 and 16 weeks of age. For this purpose, we used different approaches to examine α-tubulin post-translational modifications (PTMs), associated to MTs with different stability, and mitochondrial dynamics and distribution in nigrostriatal fibers. Our data revealed early alterations in MT dynamics in two regions of interest, the *Substantia nigra* and the *Corpus striatum*, that occur already in 6 weeks old transgenic mice. On the other hand, none alteration was observed for mitochondrial dynamics and transport. Thus, we suggest that the observed changes in MT stability could be attributable to a very early event in a gene-based model of the disease.

RESULTS

PARK2-Q311X mutation does not cause the loss of dopaminergic fibers in the *Corpus striatum* of young mice.

To evaluate the impact of Q311X mutation on MT and mitochondrial systems focusing on early events, we analyzed young mice (6 and 16 weeks old). The first approach was the quantitative analysis of tyrosine hydroxylase in *Substantia nigra* and *Corpus striatum* to point out whether signs of dopaminergic neurons loss were detectable in the nigrostriatal pathway of mice at this young age.

For this purpose, we first performed immunostaining with anti-TH antibodies on coronal sections prepared from *Corpus striatum* of 16 weeks old mice and analyzed the dopaminergic terminals both in the whole region (Figure 1A) and in four sub-regions, namely dorsal, dorso-medial, dorso-lateral and ventral *Corpus striatum* (Figure 1B). We found that *PARK2*-Q311X transgenic mice at 16 weeks of age did not show any significant difference in the optical density of TH-positive fibers when compared to wild type, although a mild but not significant decrease was observed in the ventral *Corpus striatum* (Figure 1C). Then we moved to a biochemical approach and we performed western blot and densitometric analyses on lysates obtained from ventral mesencephalon, that contains the *Substantia nigra*, and we found no apparent differences between *PARK2*-Q311X and wild type littermate mice (Figure 2A). In addition, the analysis of lysates obtained from *striatum* revealed a modest decrease of TH level at 6 weeks while a mild increase was observed in 16 weeks old transgenic mice (Figure 2B). Finally, we further confirmed our results by immunofluorescence staining with anti-TH antibodies in sagittal sections obtained from differently aged *PARK2*-Q311X mice. Sagittal sections offer the advantage to allow analyzing the entire nigrostriatal pathway, from dopaminergic cell bodies in *Substantia nigra* to fibers and, in the end, terminals in *Corpus striatum*. We quantified TH immunofluorescence in these three neuronal compartments (Figure 3A). We observed a modest but significant increase of TH level within the cell body of dopaminergic neurons in the *Substantia nigra* of *PARK2*-Q311X mice at both 6 and 16 weeks of age compared to the wild type mice (Figure 3 B-C), whereas no differences were observed for the others compartments.

Taken together, these results did not reveal any loss of dopaminergic terminals in the *striatum* of *PARK2*-Q311X mice, thus suggesting that neuronal

degeneration usually associated to PD is not detectable in young mice, at least until 16 weeks of age, and that this could be a reliable time point for investigating early events in this PD model. The functional role of the increase in TH level we observed in cell bodies of neurons located in the *Substantia nigra* remains to be deeply investigated.

PARK2-Q311X mutation impacts on the level of post-translationally modified α-tubulin.

Parkin is involved in different cellular functions and, interestingly, it has also been shown to interact with MTs and, in particular, is involved in their stabilization (Yang et al. 2005) other than in the ubiquitination of misfolded α/β tubulin heterodimers, thus promoting their degradation via UPS (Ren et al. 2003). Up to now, proof of the association of parkin with tubulin comes from cell-based assays whereas their interplay *in vivo* has been poorly investigated. Here, we hypothesized that the MT system could be affected in the early-stage of neurodegeneration *in vivo*. To verify this hypothesis, we looked at α-tubulin PTMs in *Substantia nigra* and *striatum* of young wild type and *PARK2*-Q311X mice (6 and 16 weeks old). α-Tubulin PTMs are related to MTs with different stability, being tyrosinated (Tyr) the most dynamic pool and deTyrosinated (deTyr), delta2 (Δ2), acetylated (Ac) the more stable ones (Janke & Kneussel 2010). Biochemical analysis, performed on total protein extract, showed a significant decrease of deTyr tubulin on ventral mesencephalon of 16 weeks old mice (Figure 4A) whereas an increase of acetylated tubulin occurs, in the *striatum* at the same time point (Figure 4B).

Next, to uncover whether the observed changes of α-tubulin PTMs might be attributed specifically to dopaminergic neurons or to other cell types resident in these brain areas, we moved to confocal microscopy. For this purpose, each

sagittal section was concurrently immunostained with anti-TH antibody, to identify the dopaminergic neurons, and α-tubulin PTMs antibodies. Confocal analysis showed that α-tubulin PTMs changes occur within dopaminergic cell soma and becomes evident already in 6 weeks old mice (Figure 5A, 6A). Surprisingly, the quantification of fluorescence intensity within single TH positive-cells in *Substantia nigra* showed a significant reduction of Tyr tubulin (Figure 5B); the observed changes of Tyr tubulin in 6 weeks old mice seems to be transient as older mice do not show any significant alteration with respect to controls (Figure 5C). The slight but not significant reduction of Tyr tubulin levels observed by biochemical analyses of ventral mesencephalon lysates is probably due to the contribution of other cell types, such as glia or non-dopaminergic neurons. Furthermore, our analyses also revealed a concomitant enrichment of deTyr tubulinin *Substantia nigra* (Figure 6B) followed by a significant decrease in older one (16 weeks) (Figure 6C), suggesting that an unbalance of tubulin PTMs occurs very early in dopaminergic neurons of *PARK2*-Q311X mice with respect to controls.

On the other hand, looking a further modified tubulin associated to stable MTs, Ac tubulin, any apparent alteration was found in the three brain regions in *PARK2*-Q311X mice versus wild type mice both at 6 and 16 weeks old of age (Figure S1).

The analysis of fluorescence intensity of Tyr, deTyr and Ac tubulin performed in TH-positive fibers of the nigrostriatal pathway and terminalsin the *striatum* did not reveal any significant alteration in *PARK2*-Q311X mice compared to wild type mice for both time points.The increase of Ac tubulin levels observed by western blotting in *Corpus striatum* of 16 weeks old *PARK2*-Q311X mice was not confirmed by immunohistochemical analyses. This result could be probably due to an alteration occurring in other cell types resident inside the

striatum area. Our data revealed that the unbalance of α-tubulin PTMs which becomes evident in 6 weeks old *PARK2*-Q311X mice is likely an early event associated with dopaminergic neurons.

***PARK2*-Q311X mutation does not compromise mitochondrial dynamics.**

Accumulating evidence demonstrates that mutations in *PARK2* gene act via the formation of insoluble parkin protein and subsequent loss of its E3 ligase activity, which, in turn, could result in the inability to govern the "mitochondrial quality control" within the cell. Mitochondrial dynamics, which consists of fission and fusion events important for the isolation and clearance of unhealthy mitochondria (Detmer & Chan 2007), is one of the pathway where parkin and (PTEN)-induced Putative Kinase-1 (PINK1) work together to control mitochondrial health (Scarffe et al. 2014). The alteration of fusion and fission equilibrium has been found in PD (Santos & Cardoso 2012). Thus, to assess the status of mitochondria dynamics in *PARK2*-Q311X mice, we performed biochemical analyses on brain lysates and checked for two crucial proteins involved in the process. We analyzed the levels of mitofusin-2 (MFN2) and dynamin-related protein-1 (DRP1), that are involved in mitochondria fusion and fission processes, respectively.The level of MFN2 and DRP1 were normalized on voltage-dependent anion channel (VDAC)/porin, a structural protein of the mitochondrial pore. Western blot and densitometric analysis did not show any significant alteration in the levels of the two proteins in ventral mesencephalon (Figure 7A) and in *Corpus striatum* (Figure 7B) of both 6 and 16 weeks old *PARK2*-Q311X mice.

Therefore, we hypothesized that execution of mitochondrial fusion and fission processes is not impaired by Q311X mutation in parkin *in vivo*, at least in young mice.

Mitochondria distribution is not altered in the nigrostriatal pathway of *PARK2*-Q311X mice.

Axonal transport impairment is involved in many neurodegenerative disease and it has been shown that axon degeneration could depend mainly on this defect (Burke & O'Malley 2013). Moreover, studies performed on hippocampal neurons demonstrated that PINK1/parkin pathway arrests the movement of damage mitochondria (Wang et al. 2011). On the ground that axonal transport is a MT-dependent process, we wondered if the defects in MT system we observed in young *PARK2*-Q311X mice could be related to any impairment of axonal transport.

To assess the status of axonal transport, we evaluated the distribution of mitochondria along fibers as it is a useful, even if indirect, approach. For this purpose, we performed a double immunostaining of TH and VDAC/porin in sagittal sections including the nigrostriatal pathway from 16 weeks old *PARK2*-Q311X and control mice.We observed dopaminergic fibers with a homogeneous distribution and fibers with scattered mitochondria, being the last a typical feature of transport impairment (Figure 8A). We scored the two different fibers in the nigrostriatal pathway and we did not found any difference in mitochondria distribution in *PARK2*-Q311X (Figure 8B). In addition, fluorescence intensity analysis of VDAC inside the *Substantia nigra* cell bodies and *Corpus striatum* terminals did not reveal mitochondrial accumulation within the two cellular compartments (Figure 8C).

DISCUSSION

The concept that neuronal cytoskeletal dysfunction is involved in several disorders of the central nervous system is emerging and, nowadays, it is unclear whether this alteration could be crucial, even the primary cause, in the neurodegenerative process. In particular, MT alteration has been reported in many gene and toxic-based experimental model of parkinsonisms (Cappelletti et al. 2015; Cartelli & Cappelletti 2016; Pellegrini et al. 2016). Here, we investigated whether MT dysfunction could be considered a culprit in triggering neurodegeneration in a transgenic mouse genetic model of PD, *PARK2*-Q311X mice, which resembles the characteristic hallmarks of the disease in age-dependent way. We demonstrated, that the over-expression of truncated Q311X mutant parkin, a rare mutation found in Turkish early-onset PD patient (Hattori et al. 1998), impacts on the MT system in mice and becomes noticeable at 6 weeks of age before that TH depletion and dopaminergic neuron loss occurs (16 months of age). Importantly, no alterations were observed in the mitochondria dynamics and mitochondria transport in the nigrostriatal fibers at the same time points. Thus, we speculate that the observed changes in MT stability could be attributable to a very early event in neurodegeneration, at least in this genetic model of PD.

Up to now, several pathogenic pathways correlated each other, have been implicated in PD pathogenesis. Understanding which mechanism might be the primary insult leading to dopaminergic neuron degeneration is a major challenge to deal for uncovering suitable therapeutic targets of the disease. In order to reveal whether MT dysfunction could be a key event involved PD progression, we had to investigate MT system in the early phases of the disease, before that neurodegeneration occurs. Since the primary target of the degenerative process in PD is the striatal dopaminergic terminals (the so called

"dying back" process) (Dauer & Przedborski 2003) and asymptomatic heterozygous mice bearing *PARK2* mutation display a pre-synaptic dopaminergic dysfunction in the *Corpus striatum* (Binkofski et al. 2007), we analyzed the possible dopaminergic terminal deficit in the *Corpus striatum* of *PARK2*-Q311X transgenic mice. Thus, the analysis of dopaminergic axonal innervations and the quantification of fluorescence intensity of TH in the nigrostriatal pathway, confirmed that young *PARK2*-Q311X transgenic mice did not show striatal denervation and TH depletion. This result fits with the late-onset of dopaminergic neurodegeneration,16 months of age, as reported by Lu et al. (Lu et al. 2009). Therefore, young *PARK2*-Q311X mice we employed in the present work, namely 6 and 16 weeks old mice, might be considered a suitable model to study the early pathogenic phases that precede neuronal death. Tubulin PTMs have been linked to neurodegenerative processes (Rogowski et al. 2010) and in particular, their alteration has been reported in the gene and toxic-based model of PD (Cartelli et al. 2012; Cartelli et al. 2013). We characterized the impact of mutant parkin on MT cytoskeleton in the nigrostriatal system and, from our results the occurrence of α-tubulin PTMs unbalance emerges. Biochemical analysis showed the specific unbalance of modified forms of α-tubulin in the ventral mesencephalon and on *Corpus striatum* of 16 weeks old *PARK2*-Q311X mice; on the other hand, immunofluorescence microscopy of α-tubulin PTMs, performed selectively within dopaminergic neurons, revealed earlier alteration on MT system (6weeks). Probably, we do not observe the reduction of Tyr tubulin by Western blotting because of the presence of other cell type in ventral mesencephalon region. Consistent with these results, we can speculate that dopaminergic neurons, involved in the neurodegeneration process, are likely earlier altered and more sensitive to MT alteration in respect to other cell type. The proper

control of MT system is crucial for neuronal survival and function and in particular, dopaminergic neurons appear to be highly vulnerable to any insults that could damage MT cytoskeleton because of their peculiar morphology characterized by long axons that project from the *Substantia nigra* to *Corpus striatum* which that made these complex neurons strongly dependent on intracellular trafficking (Feng et al. 2006; Hunn et al. 2015). According to the proposed MT-stabilizing effect of parkin (Yang et al. 2005), its mutations are expected to impact on MT system. Recently, it has been shown that MT destabilization and unbalance of the α-tubulin PTMs occur in human fibroblast derived from PD patients carrying *PARK2* mutations (Cartelli et al. 2012). Moreover, further evidence comes from a very recent work by Ren et al. (Ren et al. 2015) that has been performed in iPSC-derived dopaminergic neurons which were generated from *PARK2*-linked PD patients, and that reported the significant reduction in MT stability and neuronal processes complexity. The genetic manipulation via over-expression of wild type parkin or pharmacological treatment with taxol rescued the control phenotype in both human fibroblast and iPSC-derived dopaminergic neurons. This process seems to be mediated by MAP kinase signaling pathway (Ren et al. 2009) which, in turn regulates MT stability through the modulation of α-tubulin PTMs.

Here, we demonstrated that Q311X mutation induced an enrichment of deTyr tubulin and a concomitant decrease of Tyr tubulin, which are associated with stable and dynamic MTs pool, respectively, within dopaminergic neurons of 6 weeks old mice. Most likely, this over-stabilization effect could be due to a dominant gain of a toxic novel function of the mutant protein. An alternative explanation is that dopaminergic neurons attempt to balance or counteract the depolymerizing insult, through the accumulation of tubulin PTMs that protect

MTs from depolymerization, such as deTyrosination or acetylation (Cartelli & Cappelletti 2016).

Looking at the multiple cellular culprits involved in neurodegeneration, autophagy and mitochondria dysfunction are intensively investigated. In contrast to other *PARK2* mutations, recently, Q311X it has been recently reported to impact the autophagic pathway at the level of lysosomal function (Siddiqui et al. 2015). Several studies suggest that impaired mitochondria underpin PD pathology (Yao and Wood 2009; Malkus et al. 2009); parkin is linked to PINK1 and acts in the same pathway to remove damaged mitochondria, via mitophagy (Narendra et al. 2008). The same pathway is also implicated in mitochondrial dynamics that includes fusion and fission processes. Loss of parkin protein in *Drosophila* results in swollen mitochondria in flight muscles and dopaminergic neurons; this phenotype suggests that the balance of fission to fusion is pushed towards the fusion (Clark et al. 2006; Park et al. 2006). In contrast, in mammalian cells PINK1/parkin pathway results to be pro-fusion, even if its role is still controversial (Yu et al. 2011). Recently, it has been demonstrated also a functional interplay between parkin and DRP1 in mitochondrial fission and clearance (Buhlman et al. 2014). Because of these evidences, we checked for defect in mitochondrial dynamics in *PARK2*-Q311X mice. Biochemical analysis of protein involved in fusion and fission (MFN2 and DRP1) did not show any change. Our data suggest that Q311X mutation in parkin did not affect the correct execution of mitochondrial fusion and fission processes, at least in young mice.

It is commonly assumed that impairment in axonal transport is a key pathological event in neurodegeneration (Millecamps & Julien 2013). The accumulation of specific proteins, which characterizes many neurodegenerative diseases, impacts on axonal transport, but is still subject of debate whether such

accumulation could be the cause or a byproduct in the pathogenic pathways. Since axonal transport is a MT-dependent process, it is crucial to understand whether the dysfunction of MT system could drive the transport impairment in disease models. Among the neurodegenerative disorders, intracellular trafficking is altered in PD through the dysfunction of dopaminergic pathway (Hunn et al. 2015). PINK1/parkin pathway regulates mitochondria transport, promoting the degradation of Miro, a protein that allows mitochondria interaction with MT. Thus, this pathway leads to the dissociation of kinesin motors from mitochondria and the subsequently block of anterograde transport (Itoh, et al. 2013). Interestingly, the unbalance in α-tubulin PTMs precedes the impairment of the mitochondrial axonal transport in PC12 cells and in MPTP-treated mice (Cartelli et al. 2010; Cartelli et al. 2013). Based on these evidences, we supposed that a similar scenario could occur in *PARK2*-Q311X mice. Indeed, 16 weeks old *PARK2*-Q311X mice, which displayed the significant reduction in deTyr tubulin, did not show any impairment in the mitochondrial axonal transport. Indeed, we cannot exclude that older mice might display this phenotype before any sign of dopaminergic cell loss occurs. However, the earlier increase of TH (Figure 3) in the cell bodies observed in the *Substantia nigra*, could be due to the block of anterograde transport of TH-positive vesicles along the axons, other than to the increase of TH synthesis as a compensative mechanism of dopaminergic neurons implicated in neurodegeneration (16 months of age). Further work will be certainly needed to deeper investigate the axonal transport in *PARK2*-Q311X mice, looking, for example, at the motor protein kinesin-1, which is highly expressed in neuronal cells and whose recruitment to MTs sustains axonal transport and is regulated by tubulin PTMs (Reed et al. 2006; Konishi & Setou 2009).

Collectively, our results show that parkin modulates tubulin PTMs in rodent experimental model of PD and, interestingly, that MT dysfunction occurs very early thus suggesting the pivotal role of this cytoskeletal element in PD pathogenesis.

Future work will be focused on our understanding of signalling pathways involved in MT dysfunction in PD neurodegeneration, and also the molecular mechanisms underlying the interplay between parkin and MTs system.

MATERIALS AND METHODS

Animals

Female wild type and *PARK2*-Q311X (Lu et al. 2009) were kindly gifted by Dr. Fasano S. (Institute of Experimental Neurology, division of Neuroscience, IRCSS-San Raffaele Scientific Institute, Milano) and used for all experiments. Mice were generated by interbreeding Q311X mutant FVB with wild type C57 Black mice to obtain heterozygous offspring with respect to the *PARK2*-Q311X transgene and, non transgenic littermates were used as controls.

Their genotype was screened through PCR-based genotyping using the following primers: Transgene Forward 5'-ATG GAC TAC AAA GAC GAT GAC GAC AAG-3', Transgene Reverse 5'-ATT CTG CAC AGT CCA GTC ATT CCT C-3', Internal Positive Control Forward 5'- CTA GGC CAC AGA ATT GAA AGA TCT-3' and Internal Positive Control Reverse 5'- GTA GGT GGA AAT TCT AGC ATC ATC C-3'.Mice were host under environmentally controlled conditions (room temperature = 22°C, humidity = 40%) on a 12-h light/dark cycle with food and water *ad libitum* and in pathogen-free conditions. All procedures were conformed to Italian law (D. Lgs n° 2014/26, implementation of the 2010/63/UE) and approved by the Animal Welfare Body

of the University of Milan and by the Italian Minister of Health. All efforts were made to minimize suffering. Female mice, 6 and 16 weeks of age at the time of the experiment and were killed by decapitation or by transcardiac perfusion to perform biochemical or immunohistochemical analyses, respectively.

Western blot analysis

Western blot analyses were performed on protein extracts obtained from mouse brain tissues. To get protein samples, *Corpus striatum* and ventral mesencephalon were immediately dissected out on ice, mechanically homogenized and, subsequently, sonicated in SDS-PAGE sample buffer. Western blots were made as previously described (Cartelli et al. 2013) using the following antibodies: anti-Tyrosin hydroxylase (TH) rabbit IgG (ab152, Millipore, Darmstadt, Germany)1:600; anti-Actin rabbit IgG (A2066, Sigma-Aldrich, Saint Louis, MO) 1:200,anti-α-tubulin mouse IgG (clone B-5-1-2, Sigma-Aldrich) 1:2000; anti-Tyr tubulin rat IgG (clone YL 1/2, Abcam, Cambridge, UK) 1:5000; anti-deTyr tubulin rabbit IgG (ab 48389, Abcam) 1:1000; anti-Ac tubulin mouse IgG (clone 6-11B-1, Sigma-Aldrich) 1:10000; anti-Δ2-tubulina rabbit IgG (Millipore) 1:5000; anti-DRP1 rabbit IgG (clone D6C7, Cell Signaling, Danvers, MA,USA) 1:1000; anti-MFN2 rabbit IgG (clone D2D10, Cell Signaling) 1:2000; anti-porin rabbit IgG (VDAC1/porinab15895, Abcam) 1:2000.Membranes were washed for 30 min and incubated for 1 h at room temperature with the appropriate secondary antibodies: HRP donkey anti-mouse IgG (Pierce, Rockford, IL), HRP goat anti-rat IgG (Sigma-Aldrich), or HRP goat anti-rabbit IgG (Pierce).

To determine protein concentration of total brain lysate the bicinchinonic agent reagent assay (Micro BCA, Pierce) was used and compared with a standard curve of bovine serum albumine.

Immunostaining was revealed by enhanced chemiluminescence (Super-Signal West Pico Chemiluminescent, Pierce). Acquisition and quantification were performed by ChemiDoc and Image Lab software (Bio-Rad, Hercules,CA).

Immunohistochemistry and confocal analysis

A cohort of *PARK2*-Q311X and wild type controls littermates, were anesthetized with chloralium hydrate (320 mg/kg, i.p.) via intraperitoneal injection and transcardially perfused with 4% paraformaldheyde (PFA) in 0.1 M phosphate buffer, pH 7.4. Mouse brains were removed and post-fixed for 3 h in 4%PFA in agitation at room temperature. Brains were stored in 0.1 M PB plus sodium azide (NaN_3) at 4°C and were cut with a Vibratome (VT1000S, Leica). Sagittal sections (50 μm thick) were washed once in 0.1 M PB plus NaN_3 and incubated with 0.05 M NH_4Cl in 0.01 M PBS pH 7.4 (0.15 M NaCl, 2mM KH_2PO_4, 8mM Na2PO4) for 30 min at room temperature to block the aldehydic groups. After three 5 min washes in 0.01 M PBS, the sections were incubated with 1% bovine serum albumin, 0.2% Triton X-100 in 0.1 M PBS for 30 min. The sections were stained with the following antibodies previously used for immmunoblotting: anti-deTyr tubulin rabbit IgG (1:300); anti-Tyr tubulin rat IgG (1: 500); anti-Ac tubulin mouse IgG (1: 500); anti-VDAC1/porin rabbit IgG (1:300). Each sagittal section was concurrently immunostained with anti-TH antibody to identify the dopaminergic neurons. For staining of dopaminergic neurons, we used anti-TH mouseIgG (clone LNC1, Millipore, Darmstadt, Germany) 1:200 or anti-TH rabbits IgG1:200 (Millipore) antibodyas appropriate. As secondary antibodies we used

AlexaFluor™ 568 donkey anti-mouse IgG (1:200), Alexa Fluor™488 goat anti-rabbit IgG (1:200) and AlexaFluor™ 568 donkey anti-rat IgG (1:200) (abcam). Coverslips were mounted in Mowiol®-DABCO and examined with a confocal laser scan microscope imaging system (TCS SP5, Leica Microsystem, Heidelberg, Germany). Parameters were kept constant for all acquisitions to compare the fluorescence intensity between the two groups.

Quantification of the fluorescence intensity for TH, tubulin PTMs and VDAC staining was performed within cell body of the dopaminergic neurons in the *Substantia nigra*, within their terminals in the *Corpus striatum* and in the fibers, using the appropriate module of NIH ImageJ software.

Immunohistochemical analysis of tyrosine hydroxylase-positive terminals in the *Corpus striatum* with DAB.

For quantification of TH in the *Corpus striatum*, coronal brain sections were cut with a Vibratome (VT1000S, Leica) (50 μm thick) and stained with anti-TH rabbit IgG(Millipore). Sections were rinsed in 0.01 M PBS containing 0.05 M NH_4Cl and NaN_3 and incubated for 30 min at room temperature. After 15 min wash in 0.01 M PBS, sections were treated with 1% H_2O_2 for 10 min to block endogenous peroxidase activity. After three 10 min washes in 0.01 M PBS, the sections were incubated in 0.01 M PBS containing normal goat serum (NGS 1:20) and 0.2% Triton X-100 for 30 min at room temperature and, successively, incubated at 4^0C overnight with primary anti-TH antibody (1:200). After three 10 min washes in 0.01 M PBS, sections were incubated with a secondary antibody anti-rabbit (DAKO EnVision 1:2). After two 10 min washes in 0.01 M PBS and 5 min wash with 0.05 M Tris-HCl buffer, pH 7.2, the staining was visualized by incubation with 3,3' diaminobenzidinetetrahydrovhloride (DAB) and H_2O_2in 0.05 M Tris-HCl buffer, pH 7.2. Sections were rinsed in 0.05 M

Tris-HCl buffer, pH 7.2,for 5 min and washed twice with 0.01 M PBS for 10 min. Sections were subsequently dehydrated and mounted on slides.

The intensity of TH fibers (expressed in optical density) in the *striatum* was measured in four slices per animal using ImageJ software. Measurements were performed on the total *Corpus striatum* or on the following four areas: dorsal, dorso-lateral, dorso-medial and ventral *striatum* (Figure 1 B). To minimize background noise, the intensity of the *corpus callosum* was subtracted to the intensity of the TH of the region under investigation.

To evaluate the mitochondria distribution, the VDAC/porin signal was superimposed on dopaminergic fibers, using the mask tool of the Leica Confocal Software (Leica). We considered dopaminergic fibers any TH positive signal longer than 5 μm and as two distinct fibers signals separated by more than 10 μm.

Statistical analysis and data management

All data were expressed as mean ± S.E.M. (standard error of measurement). The statistical significance was assessed by Student's t-test between the two groups. χ^2 test was used to analyze qualitative variables.

REFERENCES

Binkofski, F. et al., 2007. Morphometric fingerprint of mutation carriers in the basal ganglia. *Neurology*, **69**, 842–850.

Buhlman, L. et al., 2014. Functional interplay between Parkin and Drp1 in mitochondrial fission and clearance. *Biochim Biophys Acta*, **1843**, 2012–2026.

Burke, R.E. & O'Malley, K., 2013. Axon degeneration in Parkinson's disease. *Exp Neurol*, 246, 72–83.

Cappelletti, G. et al., 2015. Linking microtubules to Parkinson's disease: the case of parkin. *Biochem Soc trans*, **43**,292–6.

Cartelli, D. et al., 2010. Microtubule dysfunction precedes transport impairment and mitochondria damage in MPP+-induced neurodegeneration. *J Neurochem*, **115**, 247–258.

Cartelli, D. et al., 2012. Microtubule Destabilization Is Shared by Genetic and Idiopathic Parkinson' s Disease Patient Fibroblasts. *PLoS ONE*, **7**:e37467.

Cartelli, D. et al., 2013. Microtubule Alterations Occur Early in Experimental Parkinsonism and The Microtubule Stabilizer Epothilone D Is Neuroprotective. *Scic Rep*, **3**, 1837.

Cartelli, D. & Cappelletti, G., 2016. Microtubule Destabilization Paves the Way to Parkinson's Disease. *Mol Neurobiol*. Epub. DOI: 10.1007/s12035-016-0188-5

Clark, I.E. et al., 2006. Drosophila pink1 is required for mitochondrial function and interacts genetically with parkin. *Nature*, **441**, 1162-6.

Dauer, W. & Przedborski, S., 2003. Parkinson' s Disease: Mechanisms and Models. *Neuron*, **39**, 889–909.

Detmer, S. a & Chan, D.C., 2007. Functions and dysfunctions of mitochondrial

dynamics. *Nat Rev Mol Cell Biol*, **8**, 870–879.

Feng, J., 2006 Microtubule: a common target for parkin and Parkinson's disease toxins. *Neuroscientist* 12:469–76.

Goldberg, M.S. et al., 2003. Parkin-deficient Mice Exhibit Nigrostriatal Deficits but not Loss of Dopaminergic Neurons. *J Biol Chem*, **278**, 43628–43635.

Kumaran, R. & Cookson, M.R., 2015. Pathways to Parkinsonism Redux : convergent pathobiological mechanisms in genetics of Parkinson' s disease. *Hum Mol Genet*, **24**(R1):R32-44.

Hattori, N. et al., 1998. Point mutations (Thr240Arg and Gln311Stop) [correction of Thr240Arg and Ala311Stop] in the Parkin gene. *Biochem Biophys Res Commun*, **249**, 754–8.

Hunn, B.H.M. et al., 2015. Impaired intracellular trafficking defines early Parkinson's disease. *Trends Neurosci*, **38**, 178–188.

Itoh K., Nakamura K., Iijima M., and H.S., 2013. Mitochondrial Dynamics in Neurodegeneration. *Trends Cell Biol*, **100,** 64–71.

Janke, C. & Kneussel, M., 2010. Tubulin post-translational modifications : encoding functions on the neuronal microtubule cytoskeleton. *Trends Neurosci*, **33**, 362–372.

Konishi, Y. & Setou, M., 2009. Tubulin tyrosination navigates the kinesin-1 motor domain to axons. *Nat Neurosci.*, **12**, 559–567.

Lu, X. et al., 2009. Bacterial Artificial Chromosome Transgenic Mice Expressing a Truncated Mutant Parkin Exhibit Age-Dependent Hypokinetic Motor Deficits, Dopaminergic Neuron Degeneration, and Accumulation of Proteinase K-Resistant α -Synuclein. *J Neurosci*, **29,** 1962–1976.

Malkus K., Tsika E., Ischiropoulos H. 2009. Oxidative modifications, mitochondrial dysfunction, and impaired protein degradation in

Parkinson's disease: how neurons are lost in the Bermuda triangle. *Mol Neurodegener*, **5**, 4-24.

Millecamps, S. & Julien, J.-P., 2013. Axonal transport deficits and neurodegenerative diseases. *Nat Rev Neurosci*, **14**, 161–76.

Narendra, D. et al., 2008. Parkin is recruited selectively to impaired mitochondria and promotes their autophagy. *J Cell Biol*, **183**,795–803.

Palacino, J.J. et al., 2004. Mitochondrial Dysfunction and Oxidative Damage in parkin -deficient Mice. *J Biol Chem*, **279,** 18614–18622.

Park, J. et al., 2006. Mitochondrial dysfunction in Drosophila PINK1 mutants is complemented by parkin. *Nature*, **441**, 1157–1161.

Pellegrini L., Wetzel A., Grannó S., Heaton G., Harvey K. 2016. Back to the tubule: microtubule dynamics in Parkinson's disease. *Cell Mol Life* Sci 1-26

Reed, N.A., Cai, D., Blasius, T.L., Jih, G.T., Meyhoferm, E., Gaertig, J. and Verhey, K.J. 2006. Microtubule acetylation promotes kinesin-1 binding and transport. *Curr. Biol*. **16**, 2166-2172.

Ren, Y. et al., 2009. Parkin Protects Dopaminergic Neurons against Microtubule-depolymerizing Toxins by Attenuating Microtubule-associated Protein Kinase Activation . *J. Biol. Chem*, **284**, 4009–4017.

Ren, Y., Zhao, J. & Feng, J., 2003. Parkin Binds to α / β Tubulin and Increases their Ubiquitination and Degradation. *J Neurosci*, **23**, 3316–3324.

Ren, Y. et al., 2015. Parkin Mutations Reduce the Complexity of Neuronal Processes in IPSC-Derived Human. *Stem Cells*, **33**, 68–78.

Rogowski, K. et al., 2010. A family of protein-deglutamylating enzymes associated with neurodegeneration. *Cell*, **143**, 564–578.

Santos, D. & Cardoso, S.M., 2012. Mitochondrial dynamics and neuronal fate in Parkinson's disease. *Mitochondrion*, 12, 428–437.

Scarffe, L.A. et al., 2014. Parkin and PINK1 : much more than mitophagy. *Trends Neurosci*, **37**, 315–324.

Shimura, H. et al., 2000. Familial Parkinson disease gene product , parkin , is a ubiquitin-protein ligase. *Nat Genet*, **25**, 302-305.

Siddiqui, A. et al., 2015. Mitochondrial Quality Control via the PGC1 α -TFEB Signaling Pathway Is Compromised by Parkin Q311X Mutation But Independently Restored by Rapamycin. *J Neurosci*, **35**, 12833–12844.

Von Coelln, R. et al., 2004. Loss of locus coeruleus neurons and reduced startle in parkin null mice. *Proc. Natl. Acad. Sci.*, **101**, 10744–10749.

Wang, X. et al., 2011. PINK1 and Parkin target miro for phosphorylation and degradation to arrest mitochondrial motility. *Cell*, **147**, 893–906.

Yang, F. et al., 2005. Parkin Stabilizes Microtubules through Strong Binding Mediated by Three Independent Domains Parkin. *J Biolog Chem*, **280**, 17154–17162.

Yao Z., Wood N.W., 2009. Cell Death Pathways in Parkinson ' s Disease : Role of Mitochondria. *Antioxid Redox Signal*, **11**,2135–2149.

Yu, W. et al., 2011. The PINK1/Parkin pathway regulates mitochondrial dynamics and function in mammalian hippocampal and dopaminergic neurons. *Hum Mol Genet*, **20**, 3227–3240.

LEGENDS

Figure 1. *PARK2*-Q311X mutation does not cause the loss of dopaminergic fibers in the *Corpus striatum*.

(A) Overview of representative micrographs of the *Corpus striatum* used for quantitative immunohistochemical analysis. The analysis was performed with ImageJ software in different regions of the *Corpus striatum* **(B)**. The yellow outlines define the area of the *Corpus striatum* analyzed: total (a,b,c), dorsal (a and b) dorso-lateral (a), dorso-medial (b) and ventral (c) *striatum*. **(C)** Densitometric analyses of TH-positive fibers in total, dorso-lateral, dorso-medial and ventral *Corpus striatum* of WT and *PARK2*-Q311X16weeks old mice. The number of mice in the experimental groups was the following: WT (n = 4), *PARK2*-Q311X (n=3). n= 4 sections for each animal. All the values are expressed as mean ± SEM. No significant differences were observed between the genotypes.

Figure 2. The levels of tyrosine hydroxylase do not change in ventral mesencephalon and in *Corpus striatum* of *PARK2*-Q311X mice.

Representative western blot and densitometric analysis of tyrosine hydroxylase (TH) and actin on ventral mesencephalon **(A)** and *Corpus striatum* **(B)** protein extracts of wild type (WT, grey bars) and *PARK2*-Q311X mice (black bars) of different ages (6 and 16 weeks). The level of TH was normalized on the level of actin, in the respective sample, and is expresses as fold change on WT level. All the values are expressed as mean ± SEM. The number of mice in the experimental groups was the following: WT (n=8) and *PARK2*-Q311X (n=6) for the 6 weeks old mice; WT (n=5) e *PARK2*-Q311X (n=5) for the 16 weeks

old mice. No significant differences were observed between the genotypes in both brain regions at the two different time points.

Figure 3. The levels of tyrosine hydroxylase increase within dopaminergic neurons in *PARK2*-Q311X mice.

(A) Representative confocal images of sagittal sections showing dopaminergic neurons in the *Substantia nigra, Corpus striatum* and nigrostriatal pathway of *PARK2*-Q311X and wild type (WT) littermates of different ages (6 and 16 weeks old). Immunostaining represents tyrosine hydroxylase (TH). Scale bar, 20 μm. Analysis of fluorescence intensity of TH staining in the *Substantia nigra* (SN), *Corpus striatum* (ST) and nigrostriatal pathway (NP) of 6 **(B)** and 16 weeks old mice **(C)**. The number of mice in the experimental groups was the following: WT (n=4) and *PARK2*-Q311X (n=4) for the 6 weeks old mice; WT (n=4) and *PARK2*-Q311X (n=3) for the 16 weeks old mice. n= 2 sections for each animals. *$p<0.05$ according to Student's t-Test. All the values are expressed as mean ± SEM.

Figure 4. *PARK2*-Q311X mutation affects the levels post-translational modifications of tubulin (PTMs) in ventral mesencephalon.

Representative western blot and densitometric analysis of Acetylated (Ac Tub), Tyrosinated (Tyr Tub), deTyrosinated (deTyr Tub) and delta 2 (Δ2 Tub) tubulin in ventral mesencephalon **(A)** and *Corpus striatum* **(B)** protein lysates of wild type (WT, grey bars) and *PARK2*-Q311X (black bars) at different ages (6 and 16 weeks). The levels of α-tubulin PTMs were normalized on the level of total α-tubulin (α Tub) in the respective sample. The number of mice in the experimental groups was the following: WT (n=8) and *PARK2*-Q311X (n=6) for the 6 weeks old mice; WT (n=5) e *PARK2*-Q311X (n=5) for the 16 weeks

old mice. *p<0.05 according to Student's t-Test. All the values are expressed as fold change on wild type level (mean ± SEM).

Figure 5. *PARK2*-Q311X mutation affects the level of Tyr tubulin in the dopaminergic neurons of *Substantia nigra.*

(A) Representative confocal images of sagittal sections showing dopaminergic neurons in the *Substantia nigra* (SN), *Corpus striatum* (ST) and nigrostriatal pathway (NP) of *PARK2*-Q311X and wild type (WT) littermates of different ages (6 and 16 weeks old). Green signal represents tyrosine hydroxylase (TH) immunostaining and the blue signal Tyr tubulin. Scale bar, 20 μm. Analysis of fluorescence intensity of Tyr tubulin staining inside dopaminergic neuron in all the brain areas of 6 **(B)** and 16 weeks old mice **(C)**. *p<0.05 according to Student's t-Test performed on rough data. All the values are expressed as mean ± SEM (n = 2 sections for each mouse from 3-4 mice per group).

Figure 6. *PARK2*-Q311X mutation affects the level of deTyr tubulin in the dopaminergic neurons of *Substantia nigra.*

(A) Representative confocal images of sagittal sections showing dopaminergic neurons in the *Substantia nigra* (SN) and *Corpus striatum* (ST) of *PARK2*-Q311X and wild type (WT) littermates of different ages (6 and 16 weeks old). Red signal represents tyrosine hydroxylase (TH) immunostaining and the green signal deTyr tubulin. Scale bar, 20 μm. Analysis of fluorescence intensity of deTyr tubulin staining inside dopaminergic neurons in all the brain areas of 6 **(B)** and 16 weeks old mice **(C)**. *p<0.05 according to Student's t-Test performed on rough data. All the values are expressed as mean ± SEM. (n = 2 sections for each mouse from 3-4 mice per group).

Figure 7. *PARK2*-Q311X mutation does not alter mitochondrial dynamics. Representative western blot and densitometric analysis of dynamin related protein 1 (DRP1) and mitofusin 2 (MFN2) on lysates of ventral mesencephalon (**A)** and *Corpus striatum* (**B**) of wild type (WT, grey bars) and *PARK2*-Q311X (black bars) mice of different ages (6 and 16 months). The level of total proteins was normalized on the level of voltage dependent anion channel (VDAC) in the respective sample. The number of mice in the experimental groups was the following: WT (n=8) and *PARK2*-Q311X (n=6) for 6 weeks old mice; WT (n=5) and *PARK2*-Q311X (n=5) for 16 weeks old mice. Data are expressed as fold change of wild type (mean ± SEM).

Figure 8. The axonal mitochondrial transport is not altered in *PARK2*-Q311X mice.

(A) Representative confocal images showing the different distribution of mitochondria (VDAC/porin, white signal) within dopaminergic fibers (TH, red signal). Arrowhead indicates a fibre with a homogeneous distribution of mitochondria (left image), whereas arrow indicates a fibre with a scattered distribution of mitochondria (right image). Scale bar, 5 µm. **(B)** Histogram representing the percentage of dopaminergic fibers displaying a homogeneous distribution of mitochondria or fibers with scattered distribution in wild type (WT, grey bars) and *PARK2*-Q311X (black bars) mice of 16 weeks of age. **(C)** Analysis of fluorescence intensity of VDAC/porin inside the *Substantia nigra* (SN) and *Corpus striatum* (ST) of wild type (WT) and *PARK2*-Q311X of 16 weeks of age (n = 2 sections for each mouse from 3-4 mice per group).

Figure S1. Ac tubulin is not altered in dopaminergic neurons of nigrostriatal pathway in *PARK2*-Q311X mice.

(A) Representative confocal images of sagittal sections showing dopaminergic neurons in the *Substantia nigra* (SN), *Corpus striatum* (ST) and nigrostriatal pathway (NP) of *PARK2*-Q311X and wild type (WT) littermates of different ages (6 and 16 weeks old). Green signal represents tyrosine hydroxylase (TH) immunostaining and the red signal Ac tubulin. Scale bar, 20 μm. Analysis of fluorescence intensity of TH staining in all the brain areas of 6 **(B)** and 16 weeks old mice **(C)**. *$p<0.05$ according to Student's t-Test. All the values are expressed as mean ± SEM (n = 2 sections for each mouse from 3-4 mice per group).

Figure 1

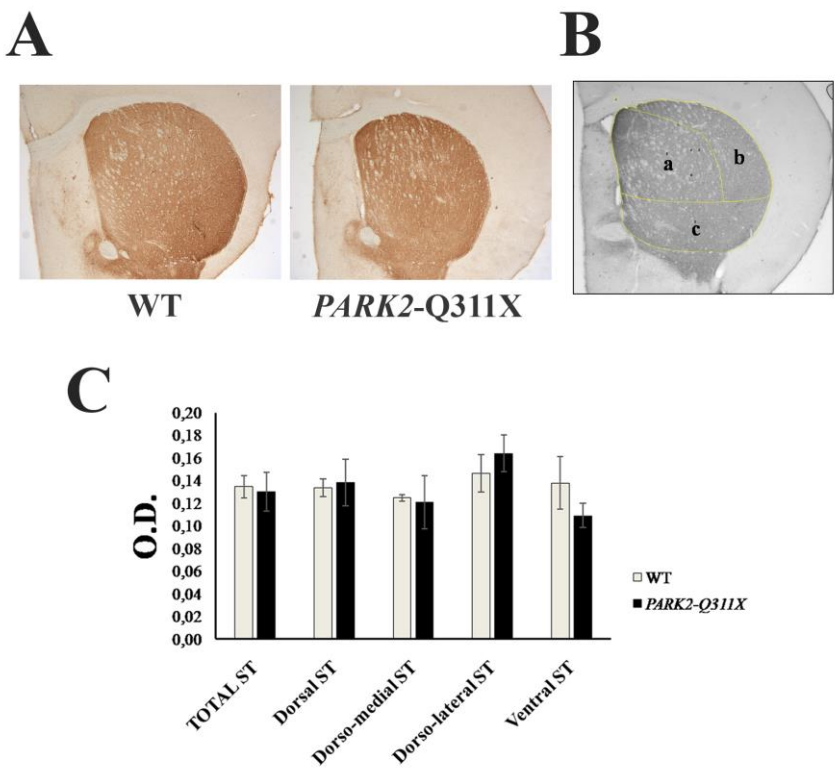
A
B
a
b
c
WT
PARK2-Q311X
C
O.D.
0,20
0,18
0,16
0,14
0,12
0,10
0,08
0,06
0,04
0,02
0,00
WT
PARK2-Q311X
TOTAL ST
Dorsal ST
Dorso-medial ST
Dorso-lateral ST
Ventral ST

Figure 2

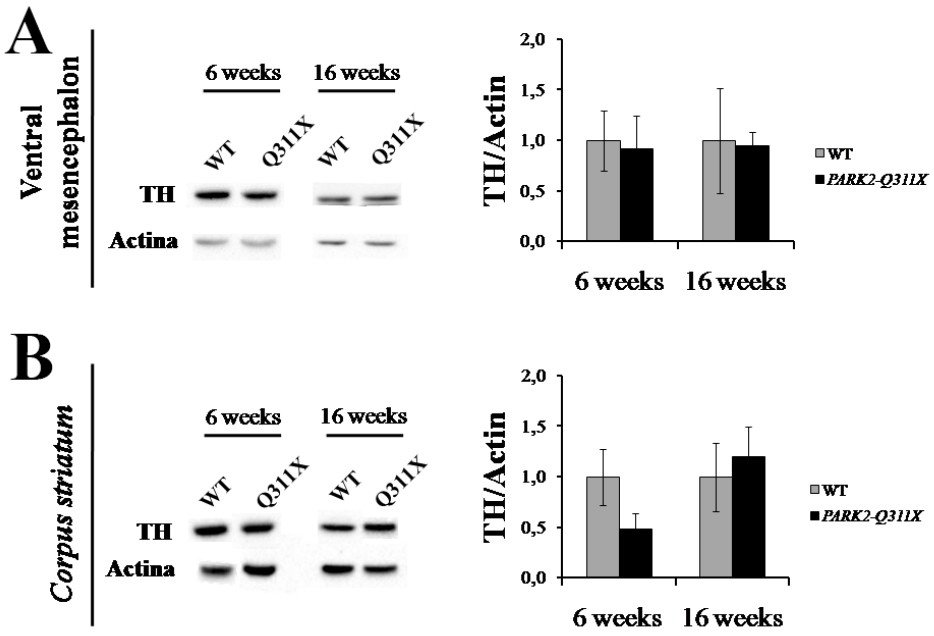
A
Ventral mesencephalon
6 weeks
16 weeks
WT
Q311X
WT
Q311X
TH
Actina
TH/Actin
2,0
1,5
1,0
0,5
0,0
6 weeks
16 weeks
WT
PARK2-Q311X
B
Corpus striatum
6 weeks
16 weeks
WT
Q311X
WT
Q311X
TH
Actina
TH/Actin
2,0
1,5
1,0
0,5
0,0
6 weeks
16 weeks
WT
PARK2-Q311X

Figure 3

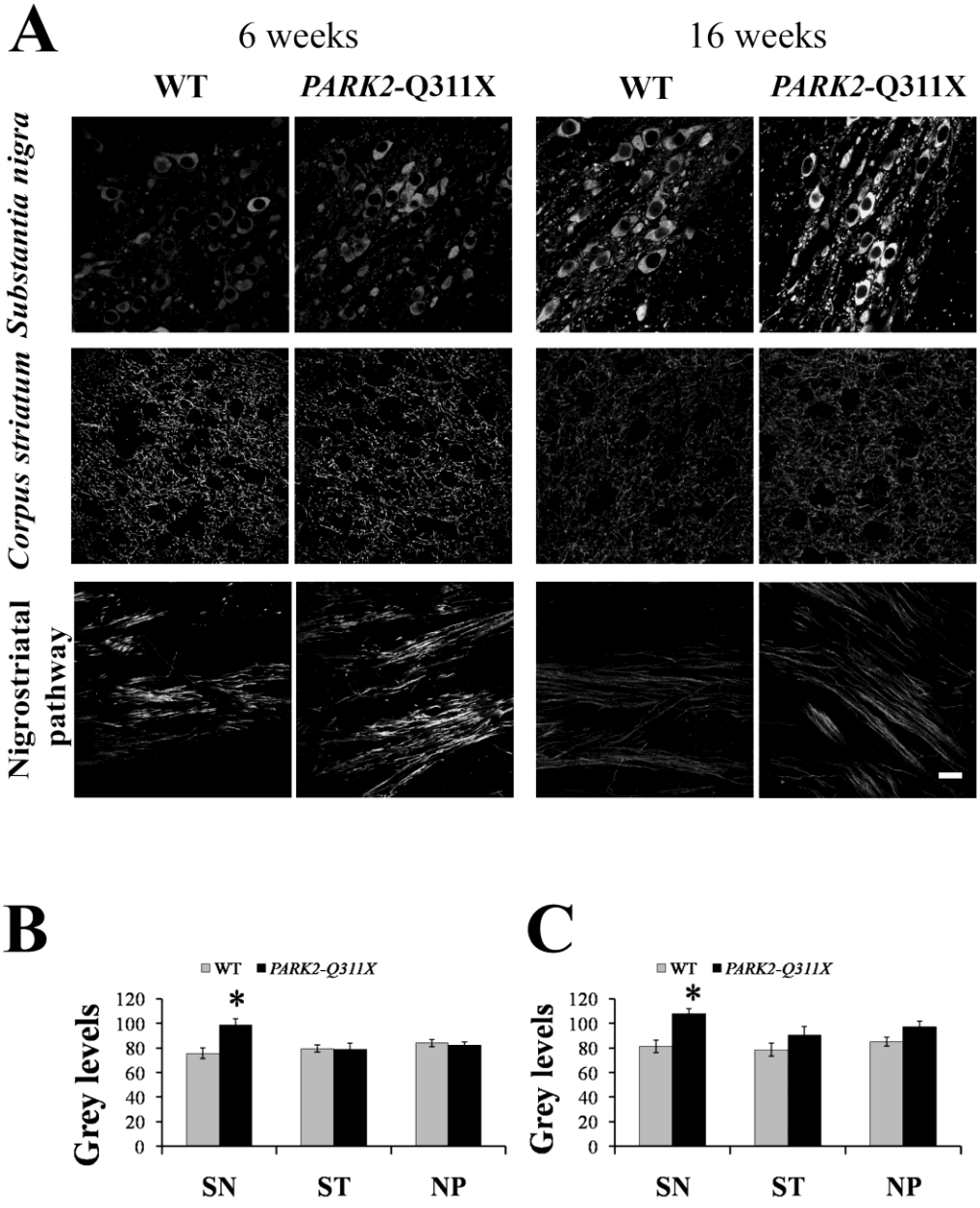
A
6 weeks
16 weeks
WT
PARK2-Q311X
WT
PARK2-Q311X
Substantia nigra
Corpus striatum
Nigrostriatal pathway
B
WT
PARK2-Q311X
Grey levels
120
100
80
60
40
20
0
*
SN
ST
NP
C
WT
PARK2-Q311X
Grey levels
120
100
80
60
40
20
0
*
SN
ST
NP

Figure 4

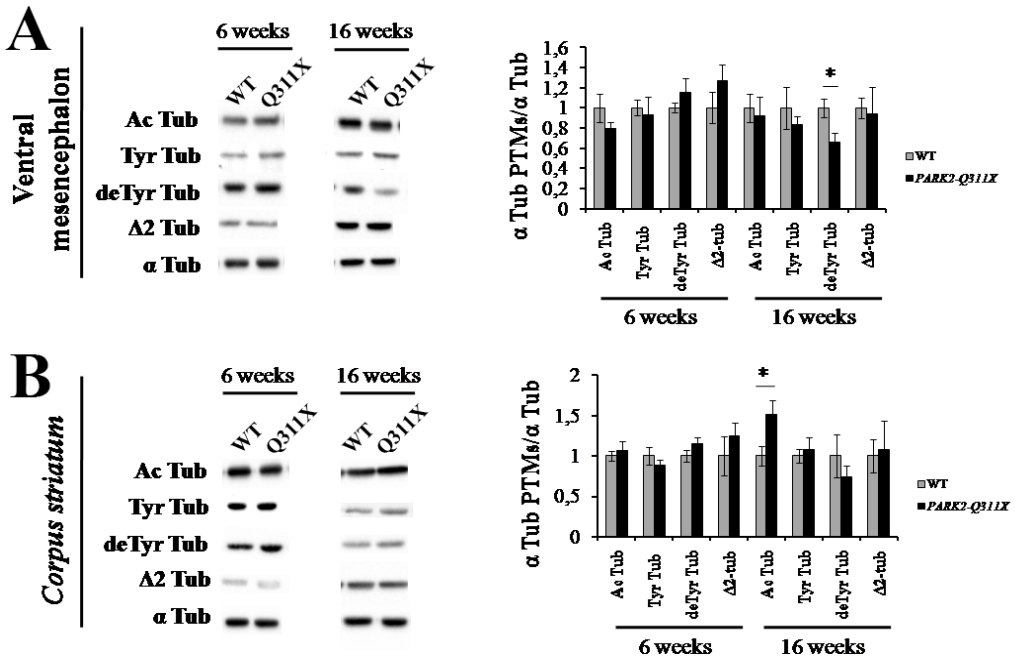
A
Ventral mesencephalon
6 weeks
16 weeks
WT
Q311X
Ac Tub
Tyr Tub
deTyr Tub
Δ2 Tub
α Tub
α Tub PTMs/α Tub
1,6
1,4
1,2
1
0,8
0,6
0,4
0,2
0
*
WT
PARK2-Q311X
Ac Tub
Tyr Tub
deTyr Tub
Δ2-tub
6 weeks
16 weeks
B
Corpus striatum
6 weeks
16 weeks
WT
Q311X
Ac Tub
Tyr Tub
deTyr Tub
Δ2 Tub
α Tub
α Tub PTMs/α Tub
2
1,5
1
0,5
0
*
WT
PARK2-Q311X
Ac Tub
Tyr Tub
deTyr Tub
Δ2-tub
6 weeks
16 weeks

Figure 5

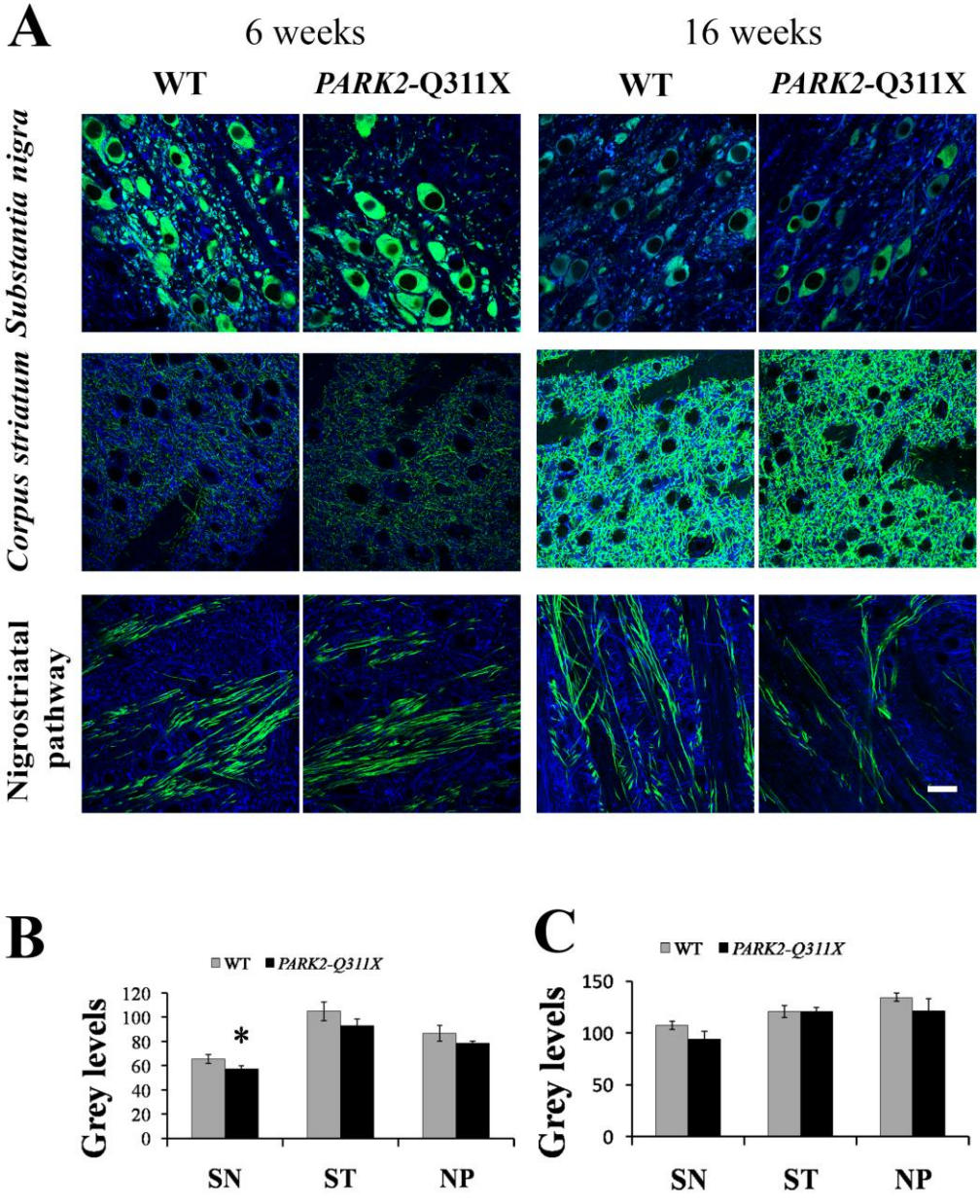
A
6 weeks
16 weeks
WT
PARK2-Q311X
WT
PARK2-Q311X
Substantia nigra
Corpus striatum
Nigrostriatal pathway
B
WT
PARK2-Q311X
Grey levels
120
100
80
60
40
20
0
*
SN
ST
NP
C
WT
PARK2-Q311X
Grey levels
150
100
50
0
SN
ST
NP

Figure 6

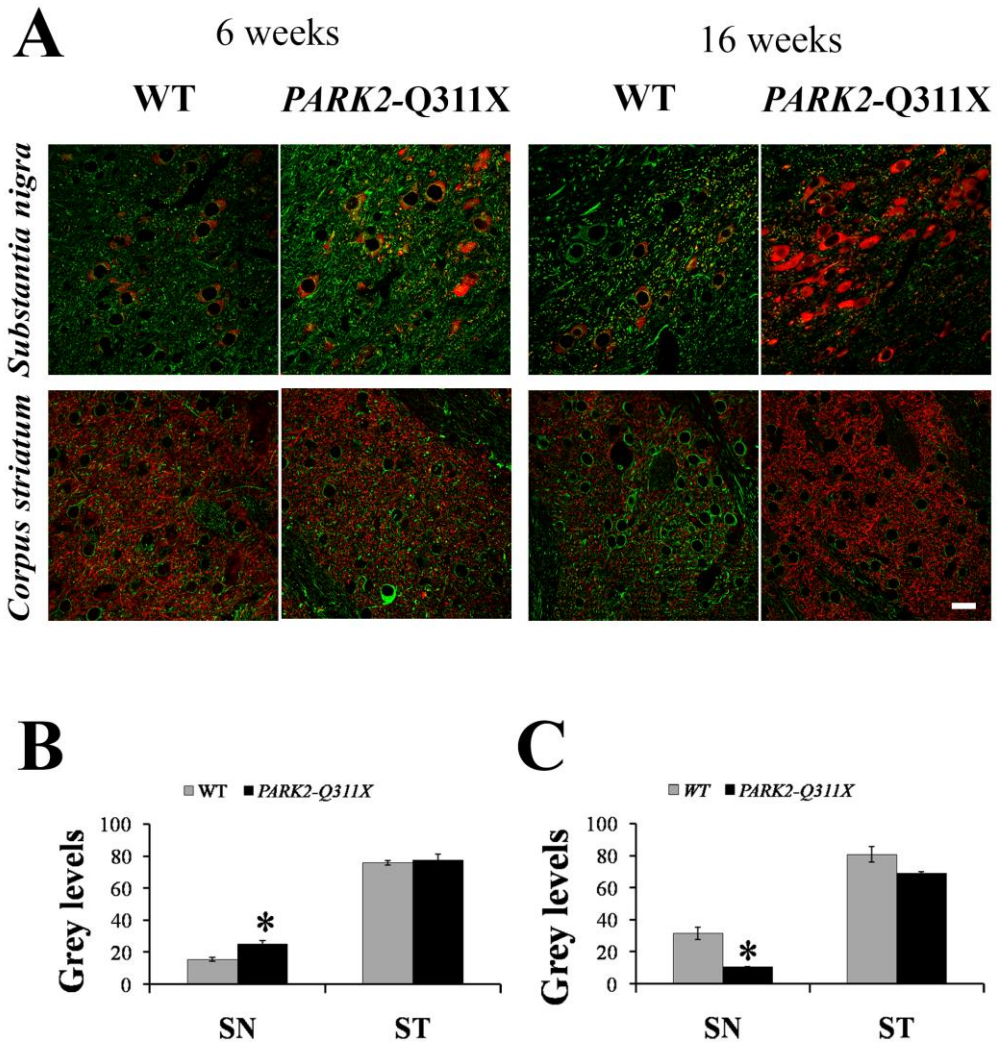
A
6 weeks
16 weeks
WT
PARK2-Q311X
WT
PARK2-Q311X
Substantia nigra
Corpus striatum
B
WT
PARK2-Q311X
Grey levels
100
80
60
40
20
0
*
SN
ST
C
WT
PARK2-Q311X
Grey levels
100
80
60
40
20
0
*
SN
ST

Figure 7

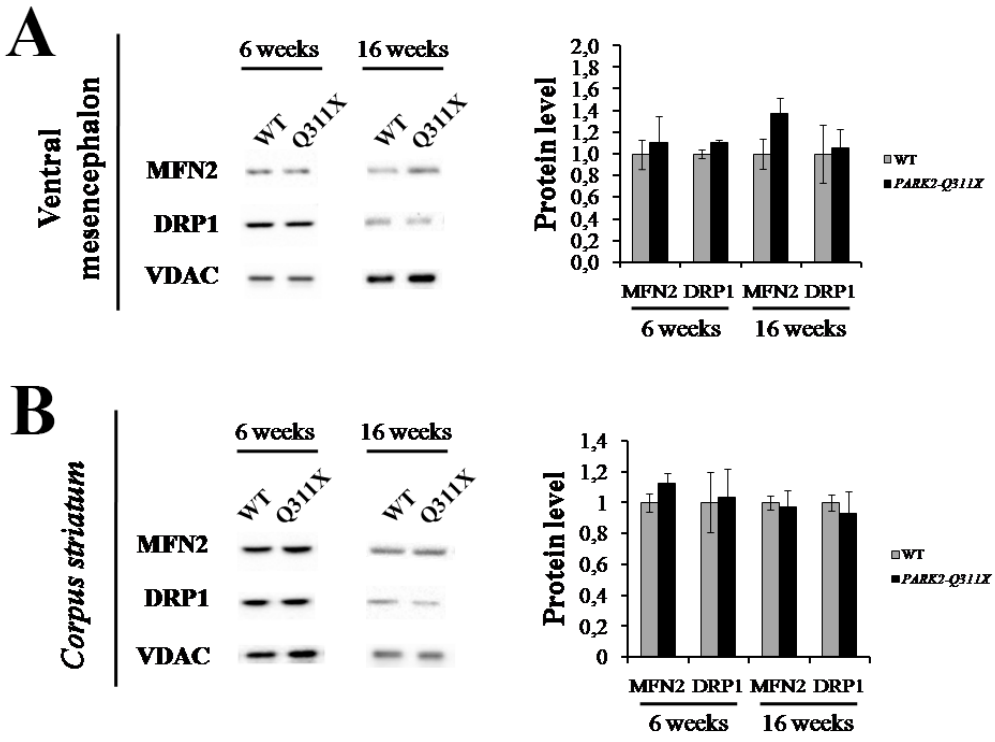
A
Ventral mesencephalon
6 weeks
16 weeks
WT
Q311X
WT
Q311X
MFN2
DRP1
VDAC
Protein level
2,0
1,8
1,6
1,4
1,2
1,0
0,8
0,6
0,4
0,2
0,0
WT
PARK2-Q311X
MFN2 DRP1 MFN2 DRP1
6 weeks
16 weeks
B
Corpus striatum
6 weeks
16 weeks
WT
Q311X
WT
Q311X
MFN2
DRP1
VDAC
Protein level
1,4
1,2
1
0,8
0,6
0,4
0,2
0
WT
PARK2-Q311X
MFN2 DRP1 MFN2 DRP1
6 weeks
16 weeks

Figure 8

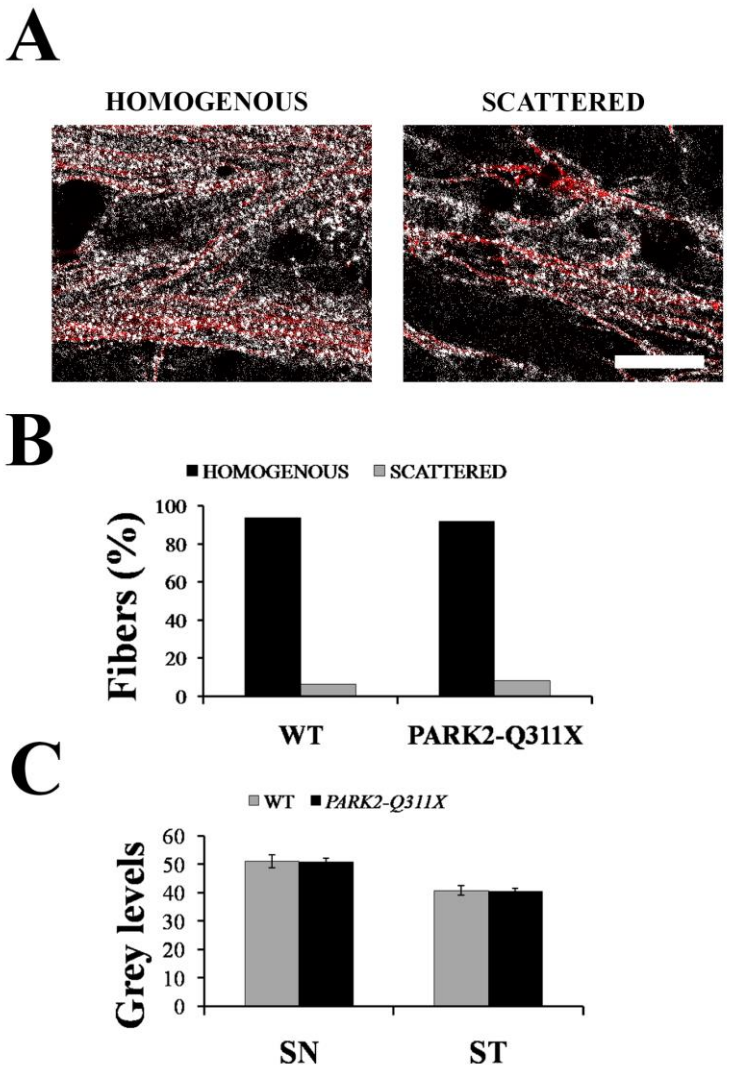
A
HOMOGENOUS
SCATTERED
B
HOMOGENOUS
SCATTERED
Fibers (%)
100
80
60
40
20
0
WT
PARK2-Q311X
C
WT
PARK2-Q311X
Grey levels
60
50
40
30
20
10
0
SN
ST

Figure S1

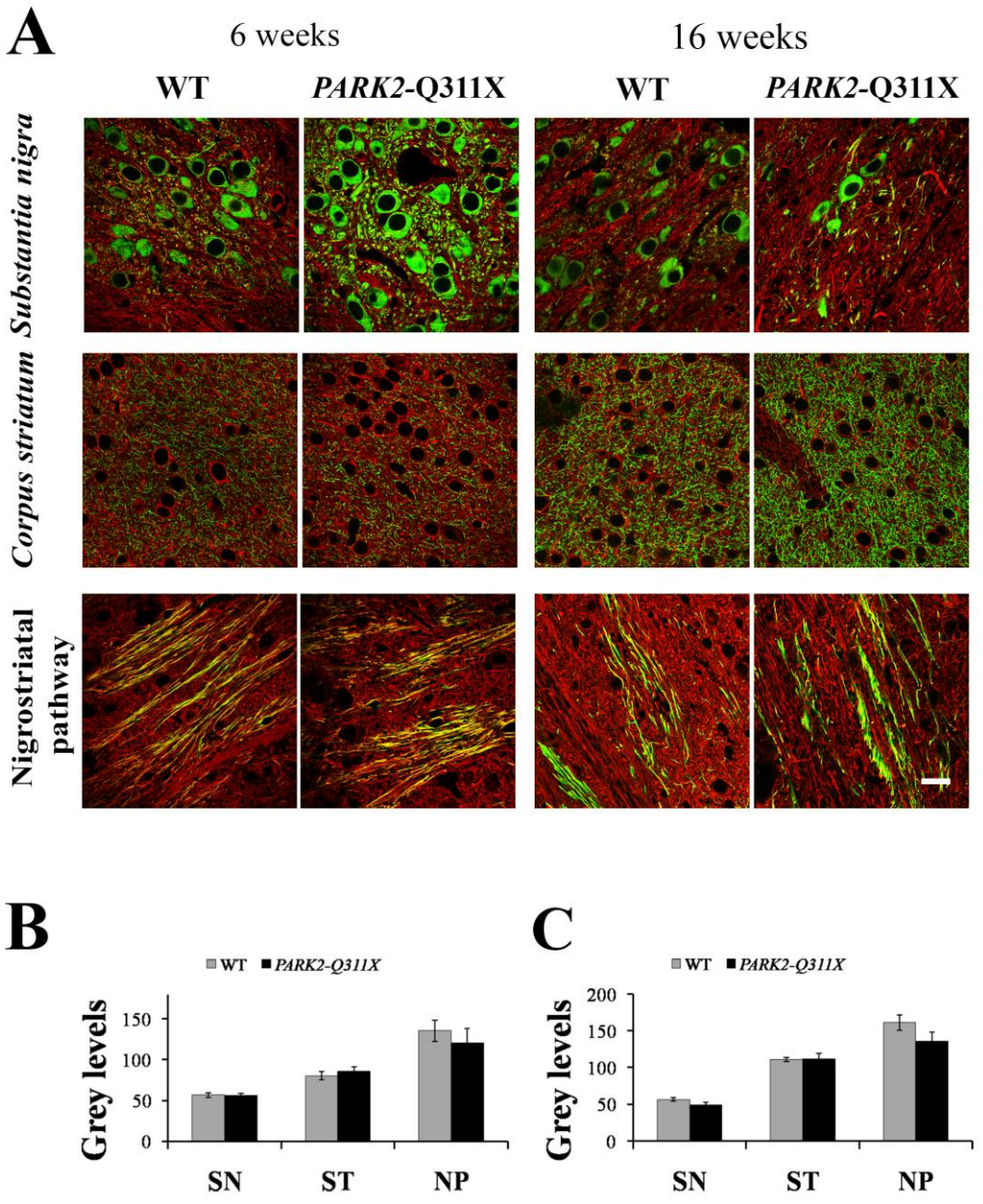
A
6 weeks
16 weeks
WT
PARK2-Q311X
WT
PARK2-Q311X
Substantia nigra
Corpus striatum
Nigrostriatal pathway
B
WT
PARK2-Q311X
Grey levels
150
100
50
0
SN
ST
NP
C
WT
PARK2-Q311X
Grey levels
200
150
100
50
0
SN
ST
NP

PARKIN MODULATES MICROTUBULE DYNAMICS AND BALANCES TUBULIN POST-TRANSLATIONAL MODIFICATIONS

Cartelli D.*, Department of Biosciences, Università degli Studi di Milano, Milano, 20133, Italy;
Amadeo A.*, Department of Biosciences, Università degli Studi di Milano, Milano, 20133, Italy;
Casagrande F.V.M., Department of Biosciences, Università degli Studi di Milano, Milano, 20133, Italy;
De Gregorio C., Department of Biosciences, Università degli Studi di Milano, Milano, 20133, Italy;
Calogero A.M., Department of Biosciences, Università degli Studi di Milano, Milano, 20133, Italy;
Gioria M.,Department of Biosciences, Università degli Studi di Milano, Milano, 20133, Italy;
Kuzumaki N.°, Department of Physiology, Keio University School of Medicine, Tokyo, 160-8582, Japan;
Costa I.,Department of Biosciences, Università degli Studi di Milano, Milano, 20133, Italy;
Sassone J.#, University of Ferrara, Department of Medical Sciences, Section of Pharmacology, Ferrara, 44121, Italy;
Ciammola A., Department of Neurology and Laboratory of Neuroscience, IRCCS IstitutoAuxologicoItaliano, Cusano Milanino (MI), 20095, Italy;
Hattori N., Department of Neurology, Juntendo University School of Medicine, Tokyo, 113-8421, Japan;
Okano H., Department of Physiology, Keio University School of Medicine, Tokyo, 160-8582, Japan;
Goldwurm S., Parkinson Institute, G. Pini-CTO, ex ICP, Milano, 20126, Italy
Roybon L., Stem Cell laboratory for CNS Disease Modeling, Wallenberg Neuroscience Center, Department of Experimental Medical Science, Lund University, BMC A10, 22184, Lund, Sweden; Strategic Research Area MultiPark and Lund Stem Cell Center, Lund University, 22184, Lund, Sweden;
Pezzoli G., Parkinson Institute,G. Pini-CTO, ex ICP, Milano, 20126, Italy
Cappelletti G.§,Department of Biosciences, Università degli Studi di Milano, Milano, 20133, Italy;

°present address: Department of Pharmacology, Hoshi University, Pharmacy and Pharmaceutical Sciences, Tokyo, 142-8501 Japan;
#present address: Neuroalgology and Headache Unit, IRCCS Foundation 'Carlo Besta' Neurological Institute, Milano, 20133, Italy.
*These authors contributed equally to the work
§ To whom correspondence should be addressed: Graziella Cappelletti, Department of Biosciences, UniversitàdegliStudi di Milano, Via Celoria 26, Milano, 20133, Italy.Tel: +39 0250314752; Fax: +30 0250315044; Email: graziella.cappelletti@unimi.it

ABSTRACT

Loss of function mutations in the parkin gene (*PARK2*) lead to familial forms of Parkinson's disease.Besides the well-known ligase activity, parkin seems to regulate other cellular functions including mitochondria homeostasis and microtubule stability, although the latter one has been largely neglected during the past years. We investigated here the role of parkin in modulating microtubule stabilityand mitochondria motility. We found that loss of parkin function leads to the imbalance of post-translationally modified tubulins, that are associated with differences in microtubule stability, during aging in *PARK2* knockout mice. In particular, acetylated tubulin accumulates over time both in dopaminergic neurons and fibers, which are localized in the *substantia nigra* and *corpus striatum*, respectively. These changes, *in vivo*, precede the alteration of mitochondria transport as assessed by mitochondria accumulation inside dopaminergic fibres. *In vitro* experiments confirmed that loss of parkin function affects mitochondria movement and showed that this abnormality depends on microtubule stability as it is rescued by paclitaxel, that is a well known microtubule stabilizer. Therefore, our work pinpoints parkin as a regulator of tubulin post-translational modifications and, thus, microtubule systemin neurons, reinforcing the hypothesis that microtubule dysfunction may be crucial in the pathogenesis of Parkinson's disease.

INTRODUCTION

Mutations in the parkin gene (*PARK2*) are tightly associated with neurodegeneration and lead tofamilial forms of Parkinson's disease (PD) known as Autosomal Recessive Juvenile Parkinsonism (ARJP, OMIM #600116; Lesage and Brice, 2009).Parkin is an ubiquitin E3-ligase involved in the maintenance of cellular health (Shimura et al., 2000): its enzymatic activity promotes the degradation of misfolded and damaged proteins through the ubiquitin-proteasome system (UPS). In addition to its ligase activity, parkin seems to participate in other cellular functions (Alves da Costa and Checler, 2012) and is able to interact with two targets involved in the pathogenesis of PD: mitochondria and microtubules (MTs).

The ability of parkin to regulate mitochondrial dynamics, through the modulation of fusion and fission processes (Scarffe et al., 2014), is largely accepted. The phosphatase and tensin homolog (PTEN)-induced putative kinase 1 (PINK1)/parkin pathway acts upstream of mitofusininducing mitochondrial fusion. The same pathway regulates the transport of mitochondria, promoting the docking of damaged ones prior to their degradation (Wang et al., 2011). Nevertheless, the direct involvement of PINK1/parkin in the regulation of mitophagy is somewhat controversial. Supportingobservations came mainly from cultured mammalian cells overexpressing parkin, but in induced-pluripotent stem cell (iPSC)-derived human neurons the endogenous parkin is not sufficient to initiate mitophagy (Rakovic et al., 2013). Therefore, it is unclear whether parkininvolvementin this process really is relevant in neurons orduring PD pathogenesis or not (Grenier et al., 2013).

Notably, parkin not only interacts with tubulin, the building block of MTs, promoting its ubiquitination and degradation via UPS (Ren et al., 2003), but it

is also able to directly bind and stabilize MTs (Yang et al., 2005). Therefore, it is not surprising that *PARK2* mutations or exons' deletion destabilize MTs and abolish the ability of parkin to counteract theMT depolymerization induced by rotenone and colchicine in both murine and human midbrain dopaminergic neurons (Ren et al., 2009 and 2015). This process seems to be mediated by the regulation of MAP kinase pathway (Ren et al., 2009) which, interestingly, has been suggested as a possible regulator of MT system,via the modulation of tubulin post-translational modifications (PTMs). In agreement with these observations, we recently reported that PD-patient skin fibroblasts bearing *PARK2* mutations display altered tubulin PTM patterns and reduced MT mass, and either MT-targeted pharmacological treatment or the overexpression of wild-type (WT) parkin rescues control phenotype (Cartelli et al., 2012).

In order to clarify the effects of parkin on the MT system and MT-dependent functions in neurons, we look at *PARK2* knock out (KO) mice and show that, in the absence of parkin,the equilibrium between stable and dynamic MTs is altered, a shift which preceeds mitochondria accumulaton, a well-accepted sign of axonal transport block. Afterward, using live cell imaging, we demonstrate that parkin-silencing accelerates MT growth and, consequently, impairs mitochondrial trafficking in a neuronal cell model.

MATERIALS & METHODS

Animals

Wild type and *PARK2* knock out (16) C57 Black mice (male and female)were purchased from Charles River (Calco, Italy) and used for all experiments. Mice were kept under environmentally controlled conditions (ambient temperature =

22°C, humidity = 40%) on a 12-h light/dark cycle with food and water *ad libitum*. Mice were kept in pathogen-free conditions and all procedures complied with Italian law (D. Lgs n° 2014/26, implementation of the 2010/63/EU) and were approved by the University of Milan Animal Welfare Body and by the Italian Minister of Health. All efforts were made to minimize suffering. Miceat different ages (2, 7 and 24 months) were sacrificed by decapitation or by transcardiac perfusion to perform biochemical or immunohistochemical analysis, respectively.

Western blot analysis

Western blot analysis was performed on protein extracts obtained from PC12 cells or mouse brain regions, accordingly to the previously reported protocols (Cartelli et al., 2010; Cartelli et al., 2013). Western blots were made as previously described using the following antibodies: α tubulin mouse IgG (clone B-5-1-2, Sigma-Aldrich,Saint Louis, MO); deTyrosinated(deTyr) tubulin rabbit IgG (Chemicon, Temecula, CA); Tyrosinated(Tyr) tubulin rat IgG (clone YL 1/2, Abcam, Cambridge, UK); Acetylated(Ac) tubulin mouse IgG (clone 6-11B-1, Sigma-Aldrich); mitofusin-2 (MFN2) rabbit IgG (clone D2D10, Cell Signaling Technology, Beverly, MA); dynamin-related protein-1 (DRP-1) rabbit IgG (clone D6C7, Cell Signaling Technology); phospho-DRP-1 (S616) rabbit IgG (clone D9A1, Cell Signaling Technology); VDAC1-porin rabbit IgG (Abcam). Membranes were washed for 30 min and incubated for 1 h at room temperature with HRP donkey anti-mouse IgG (Pierce, Rockford, IL), HRP goat anti-rat IgG (Sigma-Aldrich), or HRP goat anti-rabbit IgG (Pierce). Immunostaining was revealed by enhanced chemiluminescence (Super-Signal West Pico Chemiluminescent, Pierce). Acquisition and quantification were performed by ChemiDoc and Image Lab software (Bio-Rad, Hercules, CA).

Confocal analysis

Mice were anesthetized with chloralium hydrate (320 mg/kg, i.p.) and transcardially perfused with 4% paraformaldehyde (PFA) in 0.1 M phosphate buffer (PB), pH 7.4. Brains were removed, post-fixed 3 h in 4% PFA. Sagittal sections (50 µm thick) were cut with a Vibratome (VT1000S, LeicaMicrosystems, Heidelberg, Germany), and part of them werecryoprotected for long-term conservation at -20°C. Sections were stained with the following antibodies:deTyrtubulin rabbit IgG (Chemicon); Tyr tubulin rat IgG (clone YL 1/2, Abcam); Ac tubulin mouse IgG and with VDAC1/porin rabbit IgG (Abcam). To identify dopaminergic neurons and fibres, each section was concurrently stained with anti-tyrosine hydroxylase (TH) antibody, made in mice (clone LCN1, Millipore,Darmstadt, Germany) or rabbits (Millipore) as appropriate. As secondary antibodies we used Alexa Fluor™ 568 donkey anti-mouse IgG, Alexa Fluor™ 488 goat anti-rabbit IgG and Alexa Fluor™ 568 donkey anti-rat IgG (Invitrogen, Waltham, MA). Samples were examined with a confocal laser scan microscope imaging system (TCS SP2 AOBS, Leica Microsystems, Heidelberg, Germany) equipped with an Ar/Ar-Kr 488 nm, 561 nm and 405 nm diode lasers. Photomultiplier gain for each channel was adjusted to minimize background noise and saturated pixels and, once defined for control conditions, parameters were kept constant for all acquisitions. To estimate the overlapping area between red and green signals, analyses were carried out on single-plane raw images and Manders' coefficients were calculated applying the JACoP plug-in (developed and reviewed by Bolte and Cordelieres, 2006) for ImageJ software. Quantification of the fluorescence inside dopaminergic neurons was performed using the appropriate module of the NIH ImageJ software. As previously described (Cartelli et al., 2013), to

evaluate the mitochondria distribution, the porin signal was superimposed on dopaminergic fibres, using the Mask tool of the Leica Confocal Software (Leica); mitochondria accumulations were identified as white pixel-containing areas, as thick as long, clearly separated from other white pixels. A TH-positive signal longer than 5 µm was considered as dopaminergic fibre, and signals separated by more than 10 µm were counted as two distinct fibres.

Immuno-electron microscopy

Mice were perfused with 4% PFA and 0.5% glutaraldehyde in PB 0.1 M as described for confocal analysis. Vibratome sagittal sections were incubated sequentially with anti-TH rabbit IgG (Millipore), biotinylated goat anti-rabbit IgG (Vector Laboratories, Burlingame, CA) and with avidin biotinylated peroxidase complex (ABC method, Vector Laboratories). After completion of the immunoenzymatic procedure, the visualization of reaction was performed using a solution of 0.075% 3-3'-diaminobenzidine tetrahydrochloride (DAB; Sigma-Aldrich) and 0.002% H_2O_2 in 0.05 M Tris-HCl buffer, pH 7.6, as chromogen. Next, the sections were washed in PB, osmicated, dehydrated and flat embedded in Epon-Spurr resin between acetate foils (Aclar, Ted Pella, Redding, CA). Selected areas of the embedded sections were then cut with a razor blade and glued to blank blocks of resin for further sectioning. Thin sections (70 nm) were obtained withan ultramicrotome (Reichert Ultracut E, Leica Microsystems)and were observed with a Philips CM10 transmission electron microscope at 80 kv; images were acquired using a Morada Olympus digital camera.

Live cell imaging

PC12 cells were maintained in cultures and differentiated for 3 days with NGF, as previously described (Cartelli et al., 2010). PC12 cells were transiently transfected using Lipofectamine 2000 (Invitrogen) (1:3 DNA to Lipofectamine ratio), with the shRNA previously reported (Helton et al., 2008; Maraschi et al., 2014) and together with EB3-mCherry construct(Komarova et al., 2009) or Mito-dsRed (Cartelli et al., 2010). 3 days after transfection, cultures were transferred to a live cell imaging workstation composed of an inverted microscope (Axiovert 200M, Zeiss), a heated (37°C) chamber (Okolab, Naple, Italy), and a Plan neofluar 63x/1.25 numerical aperture oil-immersion objective (Zeiss). Images were collected with a cooled camera (Axiocam HRM Rev. 2; Zeiss, Oberkochen, Germany), every 6 s for the analyses of MT growth and every 10-15 s for mitochondrial trafficking; single movie duration was set at 1-3 min and the total recording time did not exceed 60 min for each dish. For rescue experiments, cells were incubated for 2 h with 1 μM paclitaxel (Sigma-Aldrich) dissolved in methanol. MT growth dynamics were analyzed from EB3 time-lapse movies using plusTipTracker software (Applegate et al., 2011), whereas mitochondrial movement was analyzed by the Imaris software, kindly provided by Immagini & Computer (Bareggio, Italy).

Statistical analysis and data management

The statistical significance of genetic background or treatment was assessed by Student's t-test, one-way ANOVA with Fischer LSD *post-hoc* testing or χ^2test when appropriate. Analyses were performed using STATISTICA software (StatSoft Inc., Tulsa, OK).

RESULTS

Loss of parkin function leads to the unbalance of α tubulinPTMs in knockout mice

The majority ofpathological *PARK2* mutations are loss-of-function and result in the absence or, at least, in an inactive form of parkin. *PARK2* KO mouse is mouse model extensively used to investigate the effects of loss of parkin function (Goldberg et al., 2003; Itier et al., 2003; Oliveras-Salvàet al., 2011). We evaluated MT stability in *Corpus striatum* and *Substantia nigra* of WT and *PARK2*KO mice at different ages, ranging from young adult to old mice (2-24 months). Biochemical analyses of αtubulin PTMs,which are markers of MTs with different stability (Janke, 2014), showed that these modifications change over time in *PARK2* KO mice both in the*Corpus striatum*and in *Ventral mesencephalon* (Figure S1). Nevertheless, we observed a huge variability that could be due to the contribution of multiple cell types (i.e. glial cells or different neuronal subpopulations) which can be influenced in different ways by the absence of parkin. In order to get more punctual informations about the changes in the nigrostriatal system, we moved to immunohistochemistry and confocal microscopy.We analysed the distribution ofαtubulin PTMsin the *Corpus striatum* of *PARK2* KO mice (Figures1a, red signals) and,to uncover whetherthe observablechanges of tubulin PTMscan be attributedto dopaminergic terminals (Figure 1a, green signal), we measured theManders' parameters (Figure 1b) which are a reliable tool for the analyses of signal distribution and colocalization (Bolte and Cordelieres, 2006). Dopaminergic terminals of *PARK2* KO mice showed an early decrease of Tyrosinate (Tyr) tubulin, the most dynamic MT pool, which isexacerbatedover time. On the other hand, we observed the accumulation of PTMs associated to stable MTs, as

deTyrosination (deTyr) and Acetylation (Ac), which is highlighted by the increased colocalization between deTyr or Ac tubulin and tyrosine hydroxylase (TH) signal.This is intriguing as it suggests that th eMT cytoskeleton inside dopaminergic terminals of *PARK2*KO mice specifically loses itsdynamic component and accumulates stable MTs,making terminals less prone to rapidly reorganize.

We then moved to the analyses of *Substantia nigra* and we observed a similar scenario (Figure 2a and 2b).Confocal analyses, and the quantification of fluorescence intensity inside dopaminergic neurons, showed an early accumulation andalater decreaseof Tyr tubulin whichoccurred specifically in dopaminergic neurons. Although we observed a time-dependent decrease of deTyr tubulin, the time course of Ac MTs is the opposite; indeed, in young aninal Ac tubulin is reduced in dopaminergic neurons of *PARK2* KO mice but it is doubled at 24 months of age (Figure 2a and 2b).Taken together, our data uncover the ability of parkin to modulateαtubulin PTMs *in vivo*,which well agrees with aputative direct regulation of MT dynamics as we will investigate short after.

Loss of parkin function impacts mitochondrial transport in knock out mice

Axonal transport is a process which is strictly dependent on the MT system. It has been shown that the PINK1/parkin pathwayarrests mitochondrial movement to quarantine damaged mitochondria in hippocampal neurons (Wang et al., 2011). Thus, we analysed mitochondrial transport in *PARK2* KO mice, evaluatingthe distribution of mitochondria inside dopaminergic fibres,as previously described (Cartelli et al., 2013). We observed dopaminergic fibres with a homogeneous distribution of mitochondria as well as fibres showing mitochondriathat are sparse or clusteredinto varicosities (Figure 3a), a typical

sign of axonal transport impairment (De Vos et al., 2008).We quantified the different types of fibres (Figure 3b) and found no differences in mitochondria distribution in 2-months old mice, whereas fibres with mitochondria clustering significantly increased in *PARK2* KO mice, starting from 7 months of age.We also performed qualitative ultrastructural analysis of TH-positive fibres by pre-embedding immunocytochemistry, and observed dopaminergic axons engulfed by several clustered mitochondria (arrows) or withouth mitochondrial accumulation (arrowheads). In agreement with previous evidence (Palacino et al., 2004), the mitochondria of both WT and *PARK2* KO mice display a normal gross morphology (Figure3c). To exclude that the differences in mitochondrial distribution were due to alteration of mitochondrial dynamics, we investigated well-known regulators of mitochondrial fusion and fission (Knott et al., 2008), namely mitofusin-2 (MFN2), dynamin-related protein-1 (DRP1) and its fission-promoting phosphorylation on serine 616 (Figure S2). Since we did not observe any significant change in the levels of these proteins between WT and *PARK2* KO mice at any age studied, we concluded that parkin absencedoes not impair mitochondrial fusion and fission processes, at least in our *in vivo* model. Therefore, showing mitochondria clusters our data reveal a possible failure of axonal transport in *PARK2* KO old mice. According to the evidence we thus far accumulated, we could hypothesize that the mitochondria accumulation observed in *PARK2* KO mice may be directly caused by the imbalance in post-translational regulation of tubulin, which is already noticeable in 2-months old *PARK2* KOmice.

Parkin regulates mitochondrial trafficking through MT dynamics

In order to verify the hypothesis that parkin modulates MT dynamics directly and to investigate the interplay between MT system and mitochondrial transport

in depth, we carried out live cell imaginganalysis. We used parkin-silenced NGF-differentiated PC12 cells (Figure S3) expressing either EB3-mCherry, a fluorescent protein that specifically binds growing MT plus-end (Komarova et al., 2009), or Mito-DsRed, which enables us to follow mitochondrial movement (Cartelli et al., 2010). We show that parkin absence significantly accelerates MTgrowth (Figure 4a); furthermore, since it has no effects on the frequency of MT catastrophes (Figure 4b), parkin-silencing also increases the MT growing distance (Figure 4c). At the same time, parkin absence speeds up the anterograde velocity of mitochondrial transport (Figure4d), with no effects on the retrograde one (Figure 4e); noteworthy, silenced cells display a higher fraction of mitochondria moving towards the soma (Figure 4f), meaning that parkin absence causes a disorientated mitochondrial trafficking. Therefore, to ascertain whether the mitochondrial motility defects were strictly related to alterations in the MT system, we performed rescue experiments using the MT-stabilizing agent paclitaxel, which is able to reduce dynamics at MT plus-ends (Ganguly et al., 2010). As shown in Figure 4, paclitaxel restores the physiological MT-growth rate and, very interestingly, rescues mitochondria transport defects, reverting the direction of mitochondria movement and slowing down its velocity. Altogether, our data pinpoint that parkin directly regulates MT dynamics and, in turn, modulates mitochondrial trafficking in cells.

DISCUSSION

As for other PD-related proteins, the functional role of parkin is somewhat controversial. It is clearly related to the protein degradation system, via its ubiquitin-ligase activity (Shimura et al., 2000), and to mitochondrial

homeostasis (Scarffe et al., 2014).On the other hand, although the ability of parkin to modulate the MT system was proposed many years ago (Feng et al., 2006), it remained largely neglected. Here, we have first demonstrated that parkin is involved in the regulation of MT system and precedes mitochondrial accumulation during mouse aging. Using a parkin-silenced cell system, we have next demonstrated that parkin modulates MT dynamics speeding up MT growth and causes the impairment of mitochondrial transport.

We have shown that parkin balances tubulin post-translational modifications and directly modulates MT growth. In accordance with the proposed MT-stabilizing effect of parkin (Yang et al., 2005), its absence results in a faster MT growth rate (Figure4). This is consistent with the enrichment of the most dynamic MT pool, i.e. Tyr-MTs, we have previously shownin human fibroblasts (Cartelli et al., 2012) and with the increase of free tubulin recently observed in iPSC-derived neurons (Ren et al., 2015). As a whole, these data strongly suggest that parkin may be a MT stability modulator in humans, both in physiological and in PD contexts. Moreover, in *PARK2* KO mice we observed an early increase in dynamic MTs followed by the specific accumulation of AcMT pools, whichisconsistent withour previous findings in MPTP-treated mice (Cartelli et al., 2013). Therefore, our data unmask parkin as a novel regulator of MT stability/dynamics, via the modulation of tubulin PTMs, which could be achived also by the regulation of tubulin modifying enzymes, even though a deeper investigation of that system will be necessary.

We also demonstrated defective mitochondria distribution and transport in the absence of parkin, which is a possible and expected consequence of the alteration of MT stability. Indeed, proteins and organelles run along MT tracks and we have already reported that mitochondrial transport block can be the

result of MT dysfunctionin toxin-induced parkinsonism (Cartelli et al., 2010; 2013). Our work adds on to the previous accrued evidence on the role of parkin, and reveals that parkin, a PD-related protein, physiologically modulates mitochondrial trafficking in a MT-dependent manner. Indeed, the analyses performed on brain slices and overall live cell imaging experiments on cultured cells revealed that the transport defects observed in the absence of parkin are dependent on MT dynamics,asthey are rescued by MT stabilization. It has been already reported that parkin regulates the trafficking of mitochondria in hippocampal neurons, especially of those which are damaged and have to be degraded, and that this process is dependent on Miro phosphorylation (Wang et al., 2011). In the present work, we provide further details on this physiological event showing that parkin is able to regulate mitochondrial mobility *in vivo* (Figure 3). Nevertheless, our results are not necessarily in contrast with those of Wang and colleagues (2011); indeed, Schwarz's lab had already demonstrated that the Miro/Milton complex acts as an adaptor recruiting the heavy chain of conventional kinesin-1 (Glater et al., 2006). Kinesin-1, which is highly expressed in neuronal cells, is sensitive to tubulin PTMs, which modulate its axonal recruitment (Konishi and Setou, 2009), its preferential binding to specific MT subsets (Dunn et al., 2008) and the velocity of its movement (Reed et al., 2006). Furthermore, MT acetylation regulates the binding of WT or mutant forms of Leucine-Rich Repeat Kinase 2 (LRRK2) (Law et al., 2014;Godena et al., 2014), a common cause of genetic PD, and increased level of Ac MTs rescues axonal transport and locomotor deficits caused by mutations of LRRK2 (Godena et al., 2014). Hence, the changes in tubulin PTMs and MT dynamics reported here could be a neuronal attempt aimed at restoring the correct mitochondrial trafficking in the absence of parkin. It is intriguing that the two proteins which are responsible of the vast majority of genetic PD,

parkin and LRRK2, regulate axonal transport and converge their action on Ac MTs. The same story is also true for MPTP which increases Ac tubulin both in cells and in mice (Cartelli et al., 2010; 2013) and leads to Ac MTs fragmentation (Kin-Han et al., 2011). Therefore, under a terapheutical light, in order to rescue a physiological axonal transport it could be possible the (re)balancing of MT acetylation, through the modulation of enzymes that specifically acetylate (αTAT1) or deacetylate (HDAC6) MTs (Akella et al., 2010; Hubbert et al., 2002).

Another important aspect to be consideredabout parkin biology is the regulation of mitochondrial homeostasis. The direct involvement of parkin in mitophagy is debated (Grenier et al., 2013; Rakovic et al., 2013), although the PINK1/parkinpathway has been very recently implicated in the initiation of local mitophagy in the distal axon (Ashrafi et al., 2014). Nevertheless, parkin is crucial for the maintenance of mitochondrial dynamics (Scarffe et al., 2014). It has also been reported that MTs participate in the regulation of this process (Bowes and Gupta, 2008), which isessential for modulating mitochondrial function and movement. In concordance with the evidence that *PARK2* KO mice do not accumulate mitochondria with an abnormal morphology (Palacino et al., 2004), our qualitative ultrastructural analysis showed mitochondria with a conventional gross morphology (Figure 3) and the biochemical approach did not reveal alteration of mitochondria fusion and fission (Figure S2). Nevertheless, this mouse strain shows early respiratory defects in striatal mitochondria (Palacino et al., 2004; Damiano et al., 2014) and MT alterations (present data). The fact that these problems do not worsen over time can be explained in two ways. First, there are many pathways converging on the regulation of either mitochondria or MTs; therefore the early defects, due to parkin absence, can likely be buffered overtime. Second, mouse models have a

shorter lifespans than humans and this does not allow the full unmasking of this particular phenotype and the accumulation of sufficient defects overcoming a hypothetical pathological threshold. The difficulties in developing animal models that exhibit all the key features of human PD are further exacerbated by the different scales of human and rodent nigral dopaminergic neurons, whose axons reach an average arborization of 460 and 46 cm,respectively (Pissadaki and Bolam, 2013; Matsuda et al., 2009). This particular morphology gives rise to the selective vulnerability of these neuronal subtypes, and the different time- and space-scale could explain why in many animal models those neurons do not degenerate.Nevertheless, since MT destabilization and energy failure are associated with the latency period of axonal degeneration (Park et al., 2013), all data emerging from *PARK2* KO mice, as the ones presented here, can be used for the analyses of the earlier eventsoccurring in degenerating dopaminergic neurons, eventually leading to PD.

Altogether, our data indicatethat parkin balances stable and dynamic MTs through the regulation of tubulin PTMs. When this equilibrium deviates from physiological conditions, as we have demonstrated here in the absence of parkin, it results in the alteration of mitochondrial transport and, likely, in mitochondrial damage and axonal degeneration, mirroring the pathological chain of events we reported in toxin-induced parkinsonism (Cartelli et al., 2013).

Aknowledgements

This work was supported by Fondazione Grigioni per ilMorbo di Parkinson, Milan, Italy [to G.C.]; ‘‘Dote ricerca’’, FSE, RegioneLombardia[to D.C.]; and the Program for Intractable Disease Research Utilizing Disease-specific iPS

cells funded by the Japan Science and Technology Agency [JST, to H.O.]. The authors are thankful to Dr.Maura Francolini (Department of Medical Biotechnology and Translational Medicine, UniversitàDegliStudi Di Milano, Milano, Italy) for the use of transmission electron microscope, technical advicesand helpful discussion. The authors are grateful to Dr. Jennifer S. Hartwigfor reading and editing the manuscript and apologize for each possible involuntary paper omission.

H.O. is a paid scientific consultant to San Bio Co., Ltd.

REFERENCES

Alves da Costa C. and Checler F. (2012) Parkin: much more than a simple ubiquitin ligase. Neurodegener. Dis. 10, 49-51.

Akella J.S., Wloga D., Kim J., Starostina N.G., Lyons-Abbott S., Morrissette N.S., Dougan S.T., Kipreos E.T. and Gaertig J. (2010) MEC-17 is an alpha-tubulin acetyltransferase. Nature 467, 218-22.

Applegate K.T., Besson S., Matov A., Bagonis M.H., Jaqaman K. and Danuser G. (2011) plusTipTracker: Quantitative image analysis software for the measurement of microtubule dynamics. J.Struct Biol.176, 168-84.

Ashrafi G., Schlehe J.S., LaVoie M.J. andSchwarz T.L. (2014) Mitophagy of damaged mitochondria occurs locally in distal neuronal axons and requires PINK1 and Parkin. J. Cell Biol.206, 655-70.

Bolte S. and Cordelières F.P. (2006) A guided tour into subcellular colocalization analysis in light microscopy. J.Microsc.224, 213-32.

Bowes T. andGuptaR.S. (2008) Novel mitochondrial extensions provide evidence for a link between microtubule-directed movement and mitochondrial fission. Biochem.Biophys. Res.Commun. 376, 40-5.

Cartelli D., Casagrande F., BuscetiC.L., Bucci D., Molinaro G., Traficante A., Passarella D., Giavini E., Pezzoli G., Battaglia G. and Cappelletti G. (2013) Microtubulealterationsoccurearly in experimentalparkinsonism and the microtubulestabilizer Epothilone D is neuroprotective. Sci. Rep. 3, 1837.

Cartelli D., Goldwurm S., Casagrande F., Pezzoli G. and Cappelletti G. (2012) Microtubule destabilization is shared by genetic and idiopathic Parkinson's disease patient fibroblasts. PLoS ONE 7, e37467.

Cartelli D., Ronchi C., Maggioni M.G., Rodighiero S., Giavini E. and Cappelletti G. (2010) Microtubule dysfunction precedes transport impairment and mitochondria damage in MPP^+-induced neurodegeneration. J.Neurochem.115, 247-58.

Damiano M., Gautier C.A., Bulteau A.L., Ferrando-Miguel R., Gouarne C., Paoli M.G., Pruss R., Auchère F., L'Hermitte-Stead C., Bouillaud F., Brice A., Corti O. and Lombes A. (2014) Tissue- and cell-specific mitochondrial defect in Parkin-deficient mice. PLoS ONE.9, e99898.

De Vos K.J., Grierson A.J., Ackerley S. and Miller C.C. (2008) Role of axonal transport in neurodegenerative diseases. Annu Rev.Neurosci. 31, 151-73.

Dunn S., Morrison E.E., Liverpool T.B., Molina-París C., Cross R.A., Alonso M.C. and Peckham M. (2008) Differential trafficking of Kif5c on tyrosinated and detyrosinated microtubules in live cells. J. Cell Sci.121, 1085-95.

Feng J. (2006) Microtubule: a common target for Parkin and Parkinson’s disease toxins. Neuroscientist 12, 469-76.

Glater E.E.,Megeath L.J., Stowers R.S. andSchwarz T.L. (2006) Axonal transport of mitochondria requires milton to recruit kinesin heavy chain and is light chain independent. J. Cell Biol.173, 545-57.

Godena V.K.,Brookes-Hocking N., Moller A., Shaw G., Oswald M., Sancho R.M., Miller C.C., Whitworth A.J. and De Vos K.J. (2014) Increasing microtubule acetylation rescues axonal transport and locomotor deficits caused by LRRK2 Roc-COR domain mutations. Nat.Commun.5, 5245.

Goldberg M.S., Fleming S.M., Palacino J.J., Cepeda C., Lam H.A., Bhatnagar A., Meloni E.G., Wu N., Ackerson L.C., Klapstein G.J.,Gajendiran M., Roth B.L., Chesselet M.F., Maidment N.T., Levine M.S. and Shen J. (2003) Parkin-deficient mice exhibit nigrostriatal deficits but not loss of dopaminergic neurons. J. Biol. Chem.278, 43628-35.

Grenier K., McLelland G.L. andFon E.A. (2013) Parkin- and PINK1-Dependent Mitophagy in Neurons: Will the Real Pathway Please Stand Up? Front Neurol4, 100.

Helton T.D., Otsuka T., Lee M.C., Mu Y. and Ehlers M.D. (2008) Pruning and loss of excitatory synapses by the parkin ubiquitin ligase. Proc. Natl. Acad. Sci. USA 105, 19492-7.

Hubbert C., Guardiola A., Shao R., Kawaguchi Y., Ito A., Nixon A., Yoshida M., Wang X.F. and Yao T.P. (2002) HDAC6 is a microtubule-associated deacetylase. Nature 417, 455-8.

ItierJ.M., Ibanez P., Mena M.A., Abbas N., Cohen-Salmon C., Bohme G.A., Laville M., Pratt J., Corti O., Pradier L., Ret G., Jourbet C., PeriquetM., Araujo F., Negroni J., Casarejos M.J., Canals S., Solano R., Serrano A., Gallego E., Sanchez M., Danefle P., Benavides J., Tremp G., Rooney T., Brice A. and de Yebenes J.G.(2003) Parkin gene inactivation alters behaviour and dopamine neurotransmission in the mouse. Hum. Mol. Genet.12:2277-91.

Janke C. (2014) The tubulin code: molecular components, readout mechanisms, and functions. J. Cell Biol.206, 461-72.

Kim-Han J.S., Antenor-Dorsey J.A. andO'Malley K.L. (2011)The parkinsonian mimetic, MPP+, specifically impairs mitochondrial transport in dopamine axons.J.Neurosci. 31, 7212-21

KnottA.B., Perkins G., Schwarzenbacher R. and Bossy-Wetzel E. (2008) Mitochondrial fragmentation in neurodegeneration. Nat. Rev.Neurosci.9, 505-18.

Komarova Y., De Groot C.O., Grigoriev I., Gouveia S.M., Munteanu E.L., Schober J.M., Honnappa S., Buey R.M., Hoogenraad C.C., Dogterom M.,Borisy G.G., Steinmentz M.O. and Akhmanova A. (2009) Mammalian end binding proteins control persistent microtubule growth. J. Cell Biol.184, 691-706.

Konishi Y. andSetou M. (2009) Tubulin tyrosination navigates the kinesin-1 motor domain to axons. Nat.Neurosci.12, 559-67.

Law B.M., Spain V.A., Leinster V.H., Chia R., Beilina A., Cho H.J., Taymans J.M., Urban M.K., Sancho R.M., Blanca Ramírez M., Biskup S., Baekelandt V., Cai H., Cookson M.R., Berwick D.C., and Harvey K. (2014) A direct interaction between leucine-rich repeat kinase 2 and specific β-tubulin isoforms regulates tubulin acetylation.J. Biol. Chem. 289, 895-908.

Lesage S. andBrice A. (2009) Parkinson's disease: from monogenic forms to genetic susceptibility factors. Hum. Mol. Genet. 18, R48-59.

Maraschi A., Ciammola A., Folci A., Sassone F., Ronzitti G., Cappelletti G., Silani V., Sato S., Hattori N., Mazzanti M., ChieregattiE., Mulle C., Passafaro M. and Sassone J. (2014) Parkin regulateskainatereceptors by interacting with the GluK2 subunit. Nat.Commun.5, 5182.

Matsuda W., Furuta T., Nakamura K.C., Hioki H., Fujiyama F., Arai R. and Kaneko T. (2009) Single nigrostriatal dopaminergic neurons form widely

spread and highly dense axonal arborizations in the neostriatum. J.Neurosci.29, 444-53.

Oliveras-Salvà M., Van Rompuy A.S., Heeman B., Van den Haute C. and Baekelandt V. (2011) Loss-of-function rodent models for parkin and PINK1. J.Parkinson Dis. 1, 229-51.

Palacino J.J., Sagi D., Goldberg M.S., Krauss S., Motz C., Wacker M., Klose J. aand Shen J. (2004) Mitochondrial dysfunction and oxidative damage in parkin-deficient mice. J. Biol. Chem.279, 18614-22.

Park J.Y., Jang S.Y., Shin Y.K., Koh H., Suh D.J., Shinji T., Araki T. andPark H.T. (2013) Mitochondrial swelling and microtubule depolymerization are associated with energy depletion in axon degeneration. Neuroscience 238, 258-69.

Pissadaki E.K. and Bolam J.P. (2013) The energy cost of action potential propagation in dopamine neurons: clues to susceptibility in Parkinson's disease. Front.Comput.Neurosci.7, 13.

Rakovic A., Shurkewitsch K., Seibler P., Grünewald A., Zanon A., Hagenah J., Krainc D. and Klein C. (2013) Phosphatase and tensin homolog (PTEN)-induced putative kinase 1 (PINK1)-dependent ubiquitination of endogenous Parkin attenuates mitophagy: study in human primary fibroblasts and induced pluripotent stem cell-derived neurons. J. Biol. Chem.288, 2223-37.

Reed N.A., Cai D., Blasius T.L., Jih G.T., Meyhoferm E,.Gaertig J. and Verhey K.J. (2006) Microtubule acetylation promotes kinesin-1 binding and transport. Curr. Biol.16, 2166-72.

Ren Y., Jiang H., Hu Z., Fan K., Wang J., Janoschka S., Wang X., Ge S. and Feng J. (2015) Parkin Mutations Reduce the Complexity of Neuronal Processes in iPSC-derived Human Neurons. Stem Cells33, 68-78.

Ren Y., Jiang H., Yang F., Nakaso K. and Feng J. (2009) Parkin protects dopaminergic neurons against microtubule-depolymerizing toxins by attenuating microtubule-associated protein kinase activation. J. Biol. Chem.284, 4009-17.

Ren Y., Zhao J. and FengJ. (2003) Parkin binds to alpha/beta tubulin and increases their ubiquitination and degradation. J.Neurosci.23, 3316-24.

Scarffe L.A., Stevens D.A., Dawson V.L. and Dawson T.M. (2014) Parkin and PINK1: much more than mitophagy. Trends Neurosci.37, 315-24.

Shimura H., Hattori N., Kubo S., Mizuno Y., Asakawa S., Minoshima S., Shimizu N., Iwai K., Chiba T., Tanaka K. and Suzuki T. (2000) Familial Parkinson disease gene product, parkin, is a ubiquitin-protein ligase. Nat. Genet.25, 302-5.

Wang X., Winter D., Ashrafi G., Schlehe J., Wong Y.L., Selkoe D., Rice S., Steen J., LaVoie M.J. and Schwarz T.L. (2011) PINK1 and Parkin target Miro for phosphorylation and degradation to arrest mitochondrial motility. Cell147, 893-906.

Yang F., Jiang Q., ZhaoJ., Ren Y., Sutton M.D. and Feng J. (2005) Parkin stabilizes microtubules through strong binding mediated by three independent domains. J. Biol. Chem.280, 17154-62.

LEGENDS

Figure 1. Loss of parkin function leads to the unbalance in tubulin PTMs in the *Corpus striatum*.(a) Confocal images of striatum of wild type (WT) and *PARK2* knockout (*PARK2*) mice of different ages (2, 7 and 24 months). Green represents TH staining and red signals tubulin PTMs. Scale bar, 50 μm. (b)Analysis of M1 parameter (Tubulins vs. TH) in striatal sections. Data are expressed as mean ± SEM, n= 2-3 sections for each mouse from 3-4 mice per group. *p<0.05 according to Student's t-Test.Actual *p*values are: Tyr Tub, 2 months= 0.017 and 24 months= 0.0047; deTyr Tub, 2 months= 0.034 and 7 months= 0.001; Ac Tub, 2 months= 0.021 and 7 months= 0.04.

Figure 2. Loss of parkin functionleads to the unbalance in tubulin PTMsin the *Substantia nigra*.(a)Confocal images of *Substantia nigra* of wild type (WT) and *PARK2* knock out (*PARK2*) mice of different ages (2, 7 and 24 months). Green represents TH staining and red signals tubulin PTMs. Scale bar, 50 μm. (b) Quantification of fluorescence of Tyrosinated (Tyr Tub), deTyrosinated (deTyr Tub) and Acetylated (Ac Tub) tubulin inside dopaminergic neurons in the *Substantia nigra*. Data are expressed as fold change on wild type level (mean ± SEM, n= 2-3 sections for each mouse from 3-4 mice per group). *p<0.05 according to Student's t-Test, performed on rough data.Actual *p*values are: Tyr Tub, 2 months=0.000068 and 7 months=0.000026; deTyr Tub, 2 months= 0.00000018, 7 months= 0.000055 and 24 months= 0.0001; Ac Tub, 2 months= 0.000024, 7 months= 0.000026 and 24 months= 0.00006.

Figure 3. Loss of parkin function impacts mitochondrial transport *in vivo*. (a) Representative confocal images showing the different distribution of mitochondria (Porin, red signal) inside dopaminergic fibres (TH, green signal).

Arrowhead indicates a fibre with an homogeneous distribution of mitochondria whereas arrow highlights acluster. Scale bar, 20 μm. (b) Percentage of dopaminergic fibres displaying an homogeneous distribution of mitochondria (homogeneous, white) or mitochondria accumulation (clustered, black) in wild type (WT) and *PARK2* knockout (*PARK2*) mice of different ages (2, 7 and 24 months). n= 3 sections for each mouse from 3-4 mice per group. ns= not significant and *p<0.05 according to χ^2 test. The actual *p* values are 7 months = 0.000005 and 24 months = 0.0000005. (c) Electron micrographs of TH-positive fibres. Arrowheads indicate fibres with an homogeneous distribution of mitochondria whereas arrows highlight mitochondrial clusteringin both longitudinal (left) and trasversal (right) sectioned dopaminergic axons. Scale bar, 500nm.

Figure 4. Parkin modulates mitochondrial trafficking via the regulation of MT dynamics. Box plots of the MT growth rate (a), histograms showing the catastrophe frequency (f_{CAT}, b) andbox plots of the MT growth displacement (c) in parkin-silenced (sh*PARK2*) and scramble-treated (shSCR) NGF-differentiated PC12 cells, in basal conditions (CONT) or after 2 h of treatment with 1 μM paclitaxel (PTX). n ≥ 1500 MTs deriving from at least 10-15 cells per experimental group. *p<0.05 vs shSCR/CONT, #p<0.05 vs sh*PARK2*/CONT according to ANOVA, Fischer LSD *post hoc* test. The actual statistical values correspond to: a) F = 40.74, p = 0.00000001, and the indivual*p* value are shSCR/PTX vs shSCR/CONT = 0.000004, sh*PARK2*/CONT vs shSCR/CONT = 0.0000005 and sh*PARK2*/PTX vs sh*PARK2*/CONT = 0.000002; c) F = 65.15, p = 0.00000001, and the indivual *p* value are shSCR/PTX vs shSCR/CONT = 0.008576, sh*PARK2*/CONT vs shSCR/CONT = 0.000008 and sh*PARK2*/PTX vs sh*PARK2*/CONT = 0.000008,

sh*PARK2*/PTX vsshSCR/CONT = 0.008516. Box plots of anterograde velocity (d) and retrograde velocity (e) of mitochondrial transport in parkin-silenced (sh*PARK2*) and scramble-treated (shSCR) NGF-differentiated PC12 cells, in basal conditions (CONT) or after 2 h of treatment with 1 µM paclitaxel (PTX). n ≥ 200 mitochondria tracks per condition, deriving from at least 10-15 cells per experimental group. *p<0.05 vs shSCR/CONT, #p<0.05 vs sh*PARK2*/CONT according to ANOVA, Fischer LSD *post hoc* test. The actual statistical values correspond to: d) F = 4.64, p = 0.00033, and the indivual*p* value are sh*PARK2*/CONT vs shSCR/CONT = 0.0014 and sh*PARK2*/PTX vs sh*PARK2*/CONT = 0.00018.f) Histogram showing the percentage of immobile mitochondria (Stop, black), mitochondria forward (FWD, light grey) or backward (BWD, dark grey) moving and vibrating mitochondria (Vibr, white) in the same conditions reported in dand e. *p<0.05 vs shSCR/CONT (*p* value = 0.00025), #p<0.05 vs sh*PARK2*/CONT (*p* value = 0.0013) according to χ^2 test.

Figure S1. Representative western blot (a and c) and densitometric analyses (b and d) of Tyrosinated (Tyr Tub), deTyrosinated (deTyr Tub) and Acetylated (Ac Tub) tubulin on lysates of *corpus striatum*(A and B) or *ventral mesencephalon* (C and D) of wild type (WT) and *PARK2*knockout (*PARK2*) mice of different ages (2, 7 and 24 months). The level of tubulin PTMs were normalized on the level of total α tubulin (α Tub) in the respective sample and are expressed as fold chance on wild type level (mean ± SEM, n= 3-5 individuals per group). *p<0.05 according to Student's t-Test, performed on the rough data. Actual *p*valuesin b are: Tyr Tub, 2 months= 0.035 and 7 months= 0.0099; Ac Tub, 7 months= 0.0124.Actual *p*valuesin dare: Tyr Tub, 2 months=0.039; Ac Tub, 7 months= 0.02.

Figure S2. Representative western blot (a and c) and densitometric analyses (b and d) of phospho-dynamin related protein 1 (pDRP1), dynamin related protein 1 (DRP1), mitofusin 2 (MFN2) on lysates of *corpus striatum* and ventral mesencephalon of wild type (WT) and *PARK2* knockout (*PARK2*) mice of different ages (2, 7 and 24 months). The level of total proteins was normalized on the level of voltage dependent anion channel (VDAC) and the level of pDRP1 on total DRP1 in the respective sample. Data are expressed as fold chance of wild type (mean ± SEM, n= 3-5 individuals per group).

Figure S3. Representative Western blot (a) and relative quantification of parkin (b), in *PARK2*-silenced (sh*PARK2*) and scramble-treated (shSCR) NGF-differentiated PC12 cells. The level of parkin has been normalized on the total amount of loaded proteins (as revealed by Comassie Blue staining).*$p<0.05$ according to Student's t-Test (*p* value = 0.026).

Figure 1.

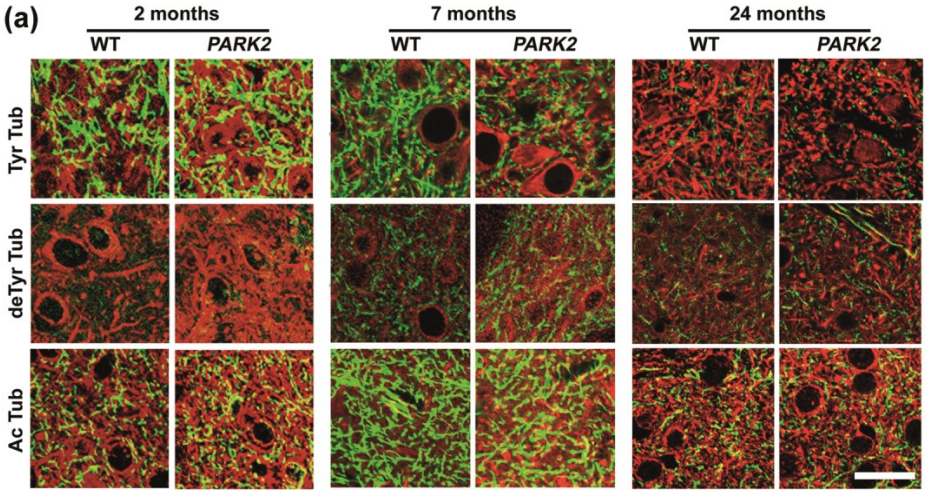

(b)

	Tyr Tub	deTyr Tub	Ac Tub
WT, 2 months	0.66±0.015	0.60±0.041	0.24±0.032
PARK2, 2 months	0.59±0.007 (*)	0.84±0.075 (*)	0.37±0.031 (*)
WT, 7 months	0.61±0.178	0.30±0.047	0.38±0.049
PARK2, 7 months	0.63±0.171	0.65±0.111 (*)	0.53±0.050 (*)
WT, 24 months	0.39±0.046	0.40±0.032	0.49±0.041
PARK2, 24 months	0.18±0.014 (*)	0.39±0.082	0.44±0.057

Figure 2.

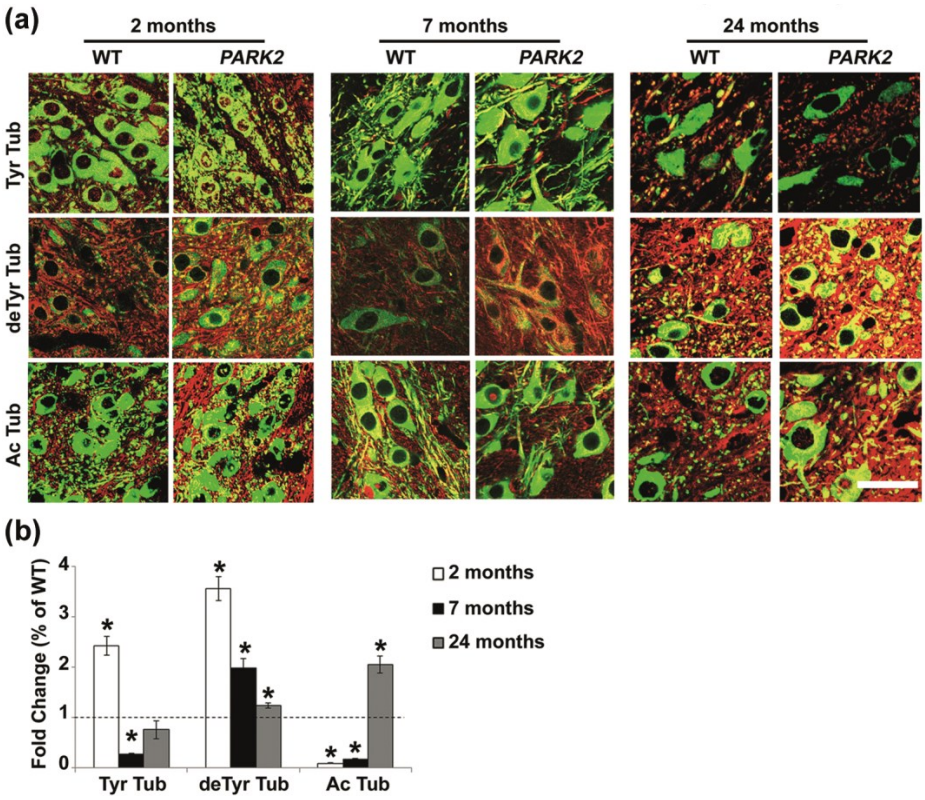
(a)
2 months
7 months
24 months
WT
PARK2
Tyr Tub
deTyr Tub
Ac Tub
(b)
Fold Change (% of WT)
0
1
2
3
4
2 months
7 months
24 months
Tyr Tub
deTyr Tub
Ac Tub

Figure 3.

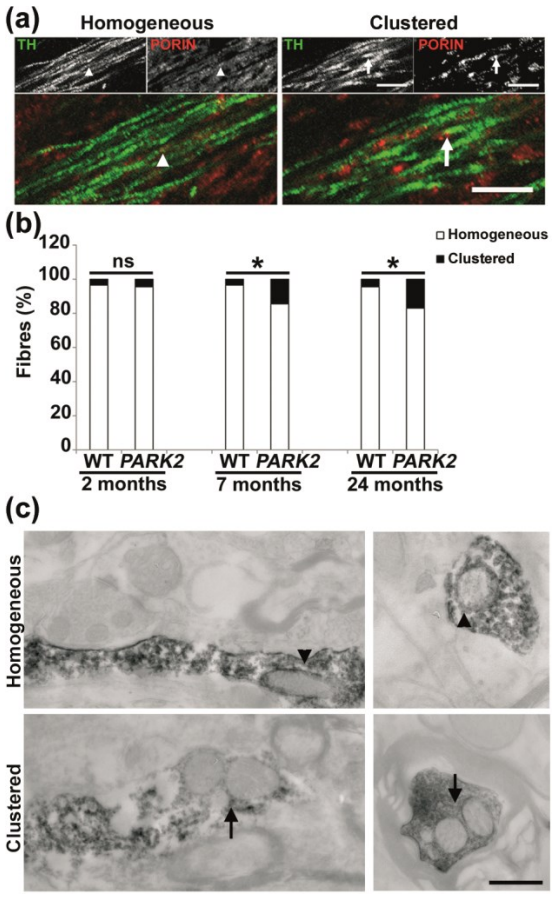
(a)
Homogeneous
Clustered
TH
PORIN
TH
PORIN
(b)
Homogeneous
Clustered
Fibres (%)
120
100
80
60
40
20
0
ns
*
*
WT PARK2
2 months
WT PARK2
7 months
WT PARK2
24 months
(c)
Homogeneous
Clustered

Figure 4.

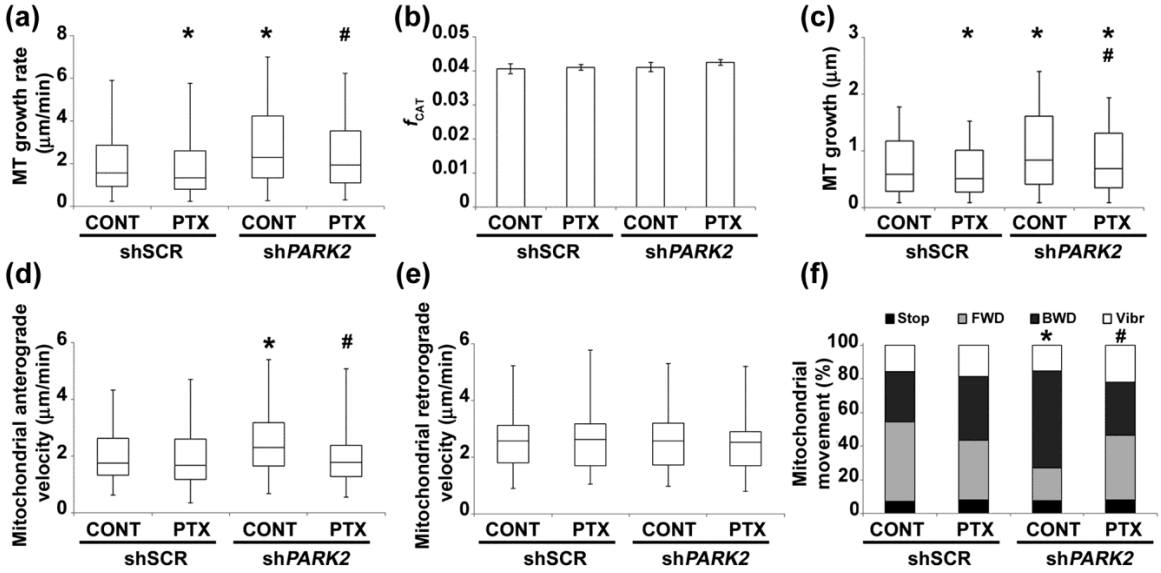
(a)
MT growth rate (μm/min)
8
6
4
2
0
*
*
#
CONT
PTX
CONT
PTX
shSCR
shPARK2
(b)
f_{CAT}
0.05
0.04
0.03
0.02
0.01
0
CONT
PTX
CONT
PTX
shSCR
shPARK2
(c)
MT growth (μm)
3
2
1
0
*
*
*
#
CONT
PTX
CONT
PTX
shSCR
shPARK2
(d)
Mitochondrial anterograde velocity (μm/min)
6
4
2
0
*
#
CONT
PTX
CONT
PTX
shSCR
shPARK2
(e)
Mitochondrial retrorograde velocity (μm/min)
6
4
2
0
CONT
PTX
CONT
PTX
shSCR
shPARK2
(f)
Stop
FWD
BWD
Vibr
Mitochondrial movement (%)
100
80
60
40
20
0
*
#
CONT
PTX
CONT
PTX
shSCR
shPARK2

Figure S1.

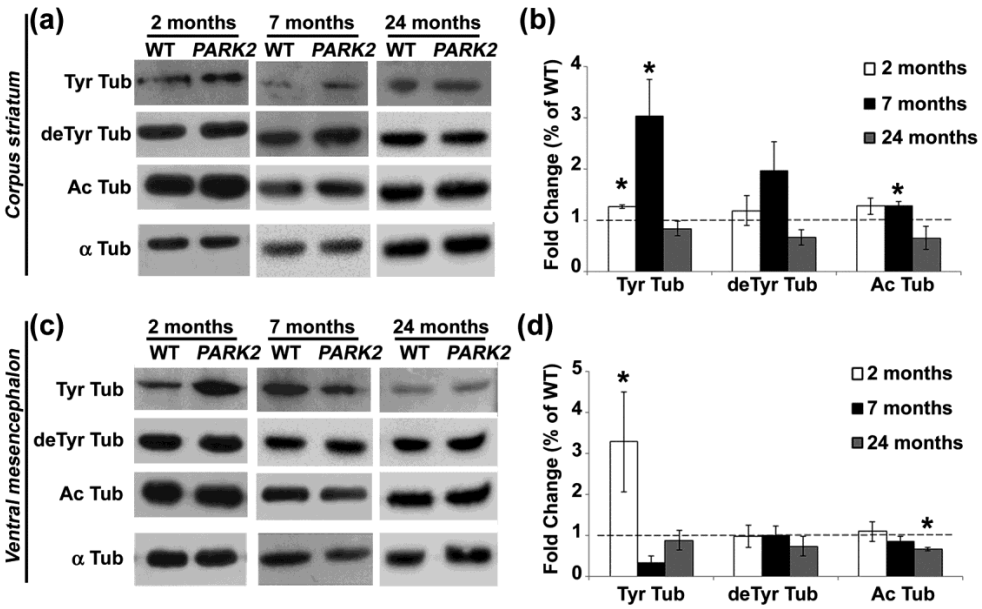
(a)
2 months
7 months
24 months
WT PARK2 WT PARK2 WT PARK2
Tyr Tub
deTyr Tub
Ac Tub
α Tub
Corpus striatum
(b)
Fold Change (% of WT)
2 months
7 months
24 months
Tyr Tub
deTyr Tub
Ac Tub
(c)
Ventral mesencephalon
(d)

Figure S2.

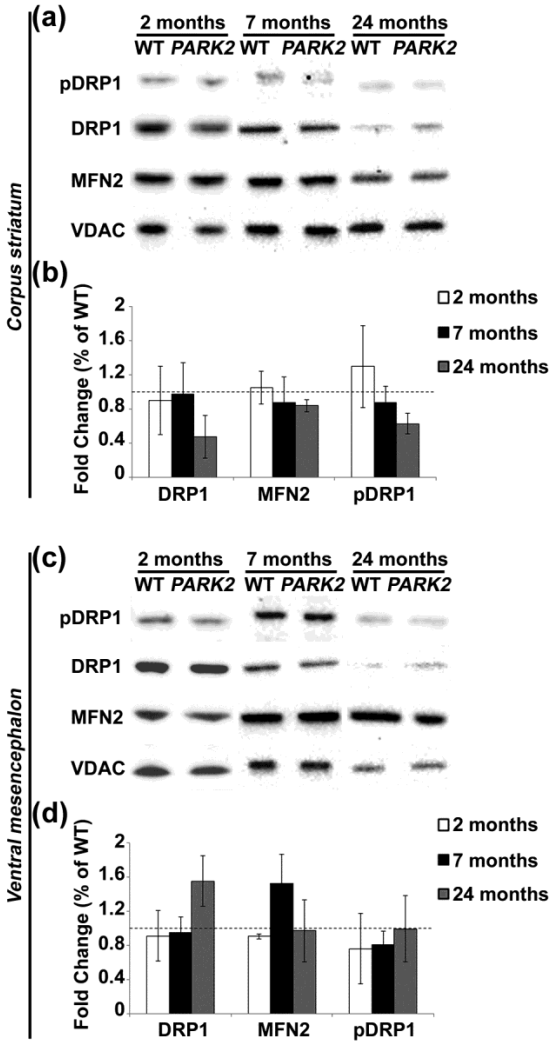
(a)
2 months
7 months
24 months
WT PARK2 WT PARK2 WT PARK2
pDRP1
DRP1
MFN2
VDAC
Corpus striatum
(b)
Fold Change (% of WT)
2
1.6
1.2
0.8
0.4
0
2 months
7 months
24 months
DRP1
MFN2
pDRP1
(c)
2 months
7 months
24 months
WT PARK2 WT PARK2 WT PARK2
pDRP1
DRP1
MFN2
VDAC
Ventral mesencephalon
(d)
Fold Change (% of WT)
2
1.6
1.2
0.8
0.4
0
2 months
7 months
24 months
DRP1
MFN2
pDRP1

Figure S3.

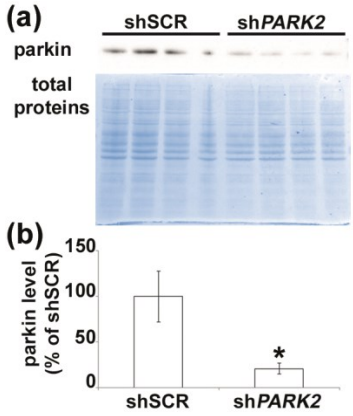
(a)
shSCR
shPARK2
parkin
total
proteins
(b)
parkin level
(% of shSCR)
150
100
50
0
*
shSCR
shPARK2

PART III

Contents

Manuscript in preparation

De Gregorio C., Casagrande F., Calogero A., Cartelli D., Ferretti M., Calcaterra V., Beltramone S., Pezzoli G and Cappelletti G.
"Parkin deficiency impacts on axonal transport in primary midbrain neurons by regulating microtubule dynamics."

Published Review

Cappelletti G., Casagrande F., Calogero A., **De Gregorio C**., Pezzoli G. and Cartelli D. (2015)
“Linking microtubules to Parkinson’s disease: the case of parkin.” *Biochem Soc Trans* 43(2):292-6.

Published Paper

Cartelli D, Aliverti A, Barbiroli A, Santambrogio C, Ragg EM, Casagrande FV, Cantele F, Beltramone S, Marangon J, De **Gregorio C**, Pandini V, Emanuele M, Chieregatti E, Pieraccini S, Holmqvist S, Bubacco L, Roybon L, Pezzoli G, Grandori R, Arnal I, Cappelletti G.(2016).
"α -Synuclein is a Novel Microtubule Dynamase." *Sci Rep,* **6**:33289.

Parkin deficiency impacts on axonal transport in primary midbrain neurons by regulating microtubule dynamics.

Carmelita De Gregorio[1], Francesca V.M. Casagrande[1], Alessandra M. Calogero[1], Daniele Cartelli[1], Marta Ferretti[1], Valerio Calcaterra[1], Silvia Beltramone[1], Gianni Pezzoli[3]and Graziella Cappelletti[1,2].

[1]Department of Biosciences, Università degli Studi di Milano, Milano, Italy
[2]Center of Excellence on Neurodegenerative Diseases,Università degli Studi di Milano, Milano, Italy
[3]Parkinson Institute, ASST G. Pini-CTO, ex ICP, Milano, Italy.

ABSTRACT

Microtubule (MT) cytoskeleton is a complex network essential for neuronal morphogenesis and function, including neuronal plasticity and axonal transport. The tightly control of MT system is crucial for neuron survival and its alteration has been proved to be involved in many neurodegenerative diseases, such as Parkinson's disease (PD). *PARK2*gene, whose mutation is responsible for the majority of Autosomal Recessive Juvenile Parkinsonism, encodes for parkin, an ubiquitin E3-ligase known to play multiple roles including the regulation of mitophagy and MT system. Here, we investigated the impact of parkin deficiency on neuronal differentiation, MT system and axonal transport in murine neurons. Morphometric analyses on primary midbrain cultures from *PARK2* knockout (KO) and heterozygous mice showed that parkin deficiency interferes with the complexity of neuronal processes. To test whether this effect was dependent on MT dysfunction, we investigated MT dynamics using live cell imaging in neurons expressing mCherry-EB3, a fluorescent protein that

specifically binds to growing MT plus-ends. Our results showed that parkin absence induces a faster MT growth, making MTs more dynamic. The further analysis of post-translational modifications of tubulin by immunofluorescence showed that the level of tyrosinated tubulin, that is associated to dynamic MT pool, increases in neuronal cells derived from *PARK2* KO mice. Finally, we investigated the axonal transport of mitochondria by live cell imaging. We found that the absence of parkin slightly increases mitochondrial velocity and that this effect is rescued by treating with paclitaxel, a MT-stabilizer agent.

Collectively, these results suggest that parkin interferes with neuronal differentiation and impairs the axonal transport of mitochondria through the modulation of MT dynamics. Moreover, these data reinforce the concept that MT dysfunction could play a crucial role in PD progression.

INTRODUCTION

Recessive mutations in parkin gene (*PARK2*) are responsible for Autosomal Recessive Juvenile Parkinsonism, characterized by early-onset. Parkin loss of function is a recognized genetic mechanism in the early-onset of Parkinson's disease (PD) pathogenesis, whereas the role of heterozygous parkin mutation as a risk factor for PD remains still controversial (Klein et al. 2007; Houlden et al. 2012). Sometimes, asymptomatic individuals bearing *PARK2* mutations in heterozygosis present nigrostriatal abnormalities, making the heterozygosity for this gene a possible risk factor for developing late-onset PD. Thus, deciphering the role of parkin haploinsufficiency in parkinsonism is important for a better understanding of disease pathogenesis progression (Klein et al. 2007).

PARK2 gene encodes for parkin, an ubiquitin E3-ligase known to be involved in different pathways, including the regulation of mitochondrial homeostasis and MT behavior. Interestingly, it has been shown that parkin interacts with

MTs and, in particular, is involved in their stabilization against depolymerizing agents (Yang et al. 2005), other than in the ubiquitination of misfolded α/β tubulin heterodimers (Ren et al. 2003). MTs are dynamic components of the cytoskeleton and their coordinated organization and regulation are essential for neuronal function and morphology. Furthermore, the involvement of MT system impairment has been clearly proved in the context of many neurodegenerative diseases, such as PD (Dubey et al. 2015). Recently, it has been demonstrated that parkin maintains the morphological complexity of human midbrain derived-iPSc neurons from PD patients through its MT-stabilizing effect (Ren et al. 2015). Noteworthy, parkin PD-linked mutants reduce the complexity of neuronal processes and promote MT destabilization whereas the overexpression of wild-type parkin significantly increases MT stability and rescues the morphological defects due to mutant parkin, the same effect obtained by treating the cells with MT-stabilizing taxol. According to this study, Cartelli and colleagues (2012) previously demonstrated that skin fibroblasts derived from PD patients, bearing *PARK2* mutations, displayed an altered MT stability. Notably, MT-stabilizing taxol treatment or the transfection of wild-type parkin rescued control phenotype of PD fibroblasts (Cartelli et al. 2012).

Consistent with these evidences, we aimed to investigate the interplay between parkin and MT system in murine primary neurons. Thus, we have characterized MT and mitochondrial system in primary neurons obtained from *PARK2*-heterozygous and *PARK2* KO mice (Goldberg et al. 2003). Although the current *PARK2*-KO model does not exhibits dopaminergic neurodegeneration, the cardinal feature of PD pathology, and shows only some abnormalities in the nigrostriatal pathway, it represents a good model to investigate the earliest changes that might occur due to parkin deficiency (Martin et al. 2011), other

than an useful tool to study the biological role of parkin protein, and in particular for our purpose, its interplay with MT cytoskeleton.

The dysregulation of axonal transport could be a reliable consequence of the alteration of MT stability (Cartelli et al. 2013). Mitochondrial transport is fundamental for neuron and defects in this process has been linked to energy failure and, consequently, implicated in the pathogenesis of neurodegenerative diseases (Itoh et al. 2013). Moreover, parkin together with phosphatase and tensin homolog (PTEN)-induced putative kinase 1 (PINK1), arrest mitochondrial transport via degradation of Miro protein (Wang et al. 2011).

Here we found that parkin interferes with neuronal differentiation and controls MT stability, through the modulation of tubulin PTMs and MT dynamics, in neurons. In addition, we revealed that mitochondrial axonal transport is altered in neurons derived from *PARK2* KO mice and, specifically, parkin absence speeds up mitochondrial axonal transport. On the ground that the treatment with a stabilizer-MT agent (taxol) speeds down the mitochondrial velocity to the control level, we state that parkin regulates axonal transport of mitochondria in a MT-dependent way. Collectively, these data reinforce the concept that MT dysfunction could play a crucial role in PD progression.

RESULTS

Parkin deficiency interferes with neuronal differentiation

The complexity of neuronal processes is a prerequisite for neurons to form connections among them and, interestingly, parkin maintains morphological complexity of human neurons by stabilizing MTs (Ren et al. 2015).We looked at the impact of parkin deficiency on the neuron morphology using primary

midbrain neurons from *PARK2* KO (*PARK2*$^{-/-}$), heterozygous (*PARK2*$^{+/-}$) and wild-type (*PARK2*$^{+/+}$) mouse embryos at E12.5. Their genotype was screened using PCR-based technique. Midbrain cultures were daily observed by phase-contrast microscope and morphometric analyses were performed in selected randomly fields, in order to calculate different parameters of neuritogenesis in the early phase of cell differentiation. We checked whether parkin deficiency could impact neuronal differentiation after 1 and 2 days of differentiation *in vitro* (DIV). Cultures obtained from *PARK2*$^{-/-}$ embryos are less differentiated than those isolated from wild-type embryos, at both time points (**Figure 1A-2A**). The percentage of cells displaying axon outgrowth decreased in *PARK2*$^{-/-}$ compared to wild-type cells at 1 DIV (**Figure 1B**) and 2 DIV (**Figure 1B**), whereas we observed a mild increase of differentiated cells in *PARK2*$^{+/-}$ cultures at 2 DIV (**Figure 1B**). This surprising difference between control and*PARK2*$^{+/-}$ cells could be due to the potential of the cells to compensate for the deficiency of parkin. Furthermore, we have measured the neurite sprouting, namely the emission of dynamic processes that might be followed by neurite stabilization and outgrowth in developing neurons. Interestingly, our analysis showed that the number of sprouting increased in undifferentiated cells obtained from *PARK2*$^{-/-}$ and *PARK2*$^{+/-}$ mice compared to the control cultures at 1 DIV (**Figure 1C**), that to say in cells that are actively involved in neurite emission. As expected, the sprouting process is not affected at 2 DIV when the most of cells are differentiated (**Figure 2C**). Moreover, we have investigated the impact of parkin deficiency on the complexity of neuronal processes as measured by total neurite length and number of branch points. Our analysis showed that the average neurite length (**Figure 1D-2D**) and the average number of branch points (**Figure 2E**) were not significantly affected in our cultures. Based on these observations, we conclude that parkin deficiency affects axonal outgrowth

and, according to its proposed MT-stabilizing effect, increases the sprouting of the undifferentiated cells, a process that involved the dynamic behavior of MTs.

Parkin deficiency increases microtubule dynamics in primary neurons.

Since MTs are strictly involved in neuronal development and the proper control of their dynamics plays an active role in the different phases of neuritogenesis, we wondered whether the absence of parkin, which has been reported to stabilize MTs (Yang et al. 2005; Ren et al. 2009), could impact differentiation of primary neuronal cultures by regulating MT dynamics. To address this issue, we transfected primary neurons taking advantage of end-binding protein 3 (EB3)-mCherry (Wauer and Komander 2013), a fluorescent protein that specifically binds to growing MT plus-ends. We visualized the neurons after 3 days of differentiation *in vitro* and MT growth dynamics were analyzed from time-lapse movies, using plusTipTracker software, following the movement of the EB3 comets (**Figure 3A**).Our results showed that *PARK2*$^{+/-}$ and *PARK2*$^{-/-}$ neurons displayed an increased MT growth speed (**Figure 3B**) compared to wild-type cells (*PARK2*$^{+/+}$). Furthermore, parkin deficiency has no effect on the lifetime of the comets (**Figure 3D**), whereas it increases the MT growing distance (**Figure3 C**). Collectively, our data pinpoint that parkin deficiency speeds up MT-growth, making MT more dynamic.

Parkin deficiency impacts MT stability.

Previous data indicate that, once bound to MTs, parkin reduces the efficiency of MT-depolyimerizing PD-toxins, such as colchicine and nocodazole, and protects midbrain dopaminergic neurons (Ren et al. 2009). This process seems to be mediated by the regulation of mitogen-activated protein (MAP) kinases

signaling pathway, which in turn regulates MT stability through the modulation of tubulin post translational-modifications (PTMs).

Thus, to further investigate in such details MTs, we analyzed the level of tyrosinated tubulin(Tyr-tub), which is a PTM associated with the native form of α tubulin and, in particular, found in the non-assembled pool of tubulin and in highly labile MTs (Bulinski and Gundersen 1991). The midbrain cultures were fixed at 7 DIV and concurrently stained with anti-Tyr-tub and anti-tyrosine hydroxylases (TH) antibodies, in order to examine MT stability in whole midbrain cultures and specifically in dopaminergic TH-positive neurons (**Figure 4 A**). Noteworthy, the quantification of fluorescence intensity revealed an enrichment of Tyr-tub in *PARK2*$^{-/-}$ neurons compared to the *PARK2*$^{+/-}$ and *PARK2*$^{+/+}$ genotypes in whole mesencephalic culture (**Figure 4 B**). Next, we analysed in detail dopaminergic neurons and showed that TH^{+} neurons display the same trend observed in the entire culture for Tyr-tub level although the limited number of neurons suitable for quantification of fluorescence made the sample too small for reaching a statistical significance (**Figure 4C**). However, these cultures allowed us to examine selectively the complexity of TH^{+} neurons. Thus, we performed morphometric analyses and found that the total neurite length, the average number of branch points and the average number of terminals in dopaminergic neurons at 7 DIV were not significantly different from the control (data not shown). Our results suggest that the absence of parkin leads to an increased level of Tyr-tub, likely related to more dynamic MTs, but does not interfere with length and complexity of neuronal processes in murine midbrain neurons at late stages of differentiation.

Parkin modulates mitochondrial axonal transport via the regulation of microtubule dynamics

In order to evaluate the impact of parkin absence on intracellular transport, we visualized the dynamics of mitochondria and hence axonal transport using live cell imaging. This approach was performed on primary midbrain neurons in 5 DIV cultures over-expressing the N-terminal mitochondrial signal sequence of cas2 fused to DsRed plasmid pMitoDsRed (Cartelli et al. 2010), a suitable tool to follow mitochondria movement along axons. We analyzed exclusively neuronal axons and excluded cell body and the growth cone for assessing the velocity of mitochondrial transport. Axonal mitochondria could be subdivided into four categories: immobile, vibrant, anterograde and retrograde moving. In neurons, mobile mitochondria (anterograde or retrograde) can become stationary or pause in areas that have a high energy demand and can move again quickly in response to physiological changes (Sheng and Cai 2016). Our results show that parkin absence (*PARK2*$^{-/-}$) speeds up the velocity of mitochondrial axonal transport (**Figure 5 A**) compared to the control cells (*PAR2K*$^{+/+}$), with a mild but not significant increase in anterograde or retrograde transport specifically (**Figure 5B**). Therefore, to investigate the interplay between MT system and mitochondrial transport in deep, we performed rescue experiments using a MT stabilizer agent paclitaxel (PTX). As shown in **Figure 5 C**, after the treatment with 1 µM paclitaxel for 2 hours the total velocity of mitochondria in *PARK2*$^{-/-}$ (PTX) cells decreased compared to the *PARK2*$^{-/-}$ (-PTX) and to the control cells *PARK2*$^{+/+}$ (-PTX). Specifically, looking at anterograde or retrograde transport, both the velocities speed down in *PARK2*$^{-/-}$ cells after the treatment with paclitaxel (**Figure 5 D**). Actually, the treatment decreases mitochondrial velocity of *PARK2*$^{-/-}$ compared also to the control cells

(*PARK2*$^{+/+}$ -PTX). Probably, the effect could be due to the high concentration of paclitaxel that we have used for our experiments.

Interestingly, parkin-silencing of PC12 cells speeds up the anterograde velocity of mitochondrial transport (Cartelli et al., to be submitted), and silenced cells display a higher fraction of backword mitochondria moving, meaning that parkin absence leads to a disorientated mitochondrial trafficking. Thus, we evaluate din primary neurons the percentage of vibrant, immobile and mobile mitochondria moving backwards or towards the soma at basal condition (PTX-) and after the treatment with 1µM paclitaxel for 2 hours (PTX)and, as reported in **Figure 5 E**, the results show that parkin does not cause a mitochondrial disorientated trafficking, at least in this cell model. Collectively, our results showed that parkin absence increases the mitochondrial transport velocity and the treatment with a MT-stabilizer agent speeds down the velocity to the control level, allowing us to suggest that parkin regulates axonal transport of mitochondria in a MT-dependent way.

FIGURE 1

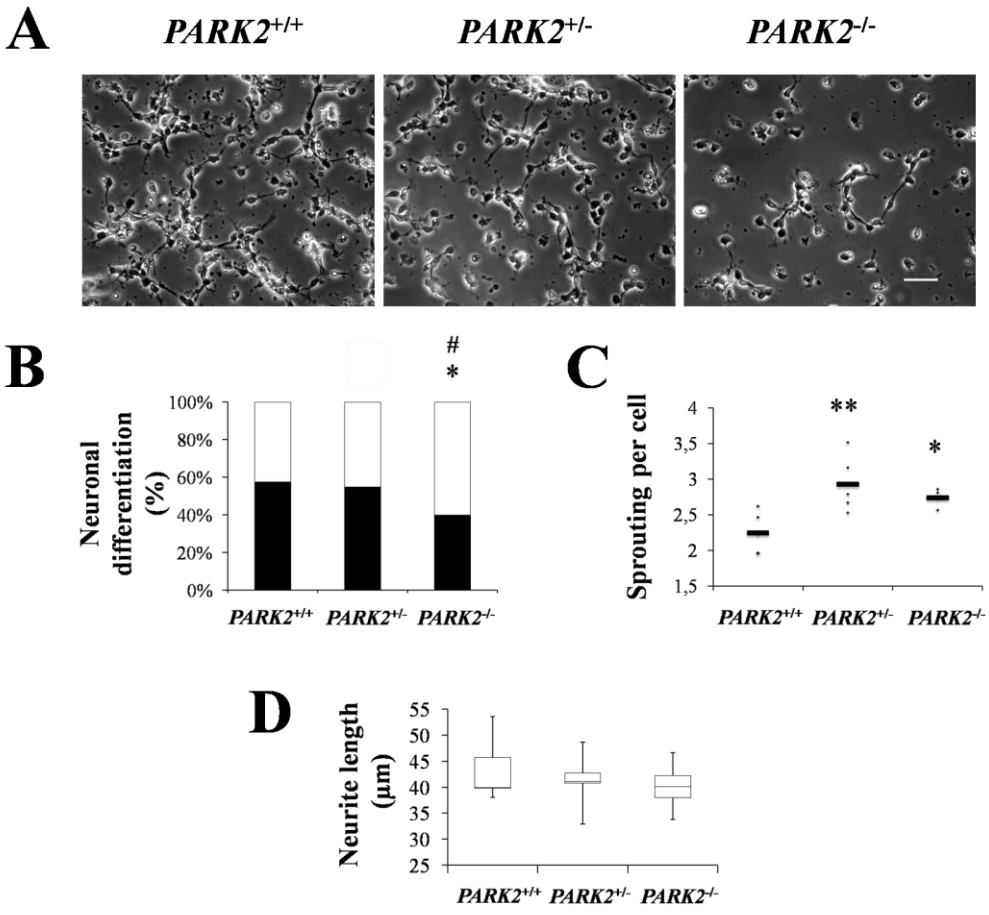
A
PARK2+/+
PARK2+/-
PARK2-/-
B
Neuronal differentiation (%)
100%
80%
60%
40%
20%
0%
#
*
PARK2+/+
PARK2+/-
PARK2-/-
C
Sprouting per cell
4
3,5
3
2,5
2
1,5
**
*
PARK2+/+
PARK2+/-
PARK2-/-
D
Neurite length (µm)
55
50
45
40
35
30
25
PARK2+/+
PARK2+/-
PARK2-/-

FIGURE 2

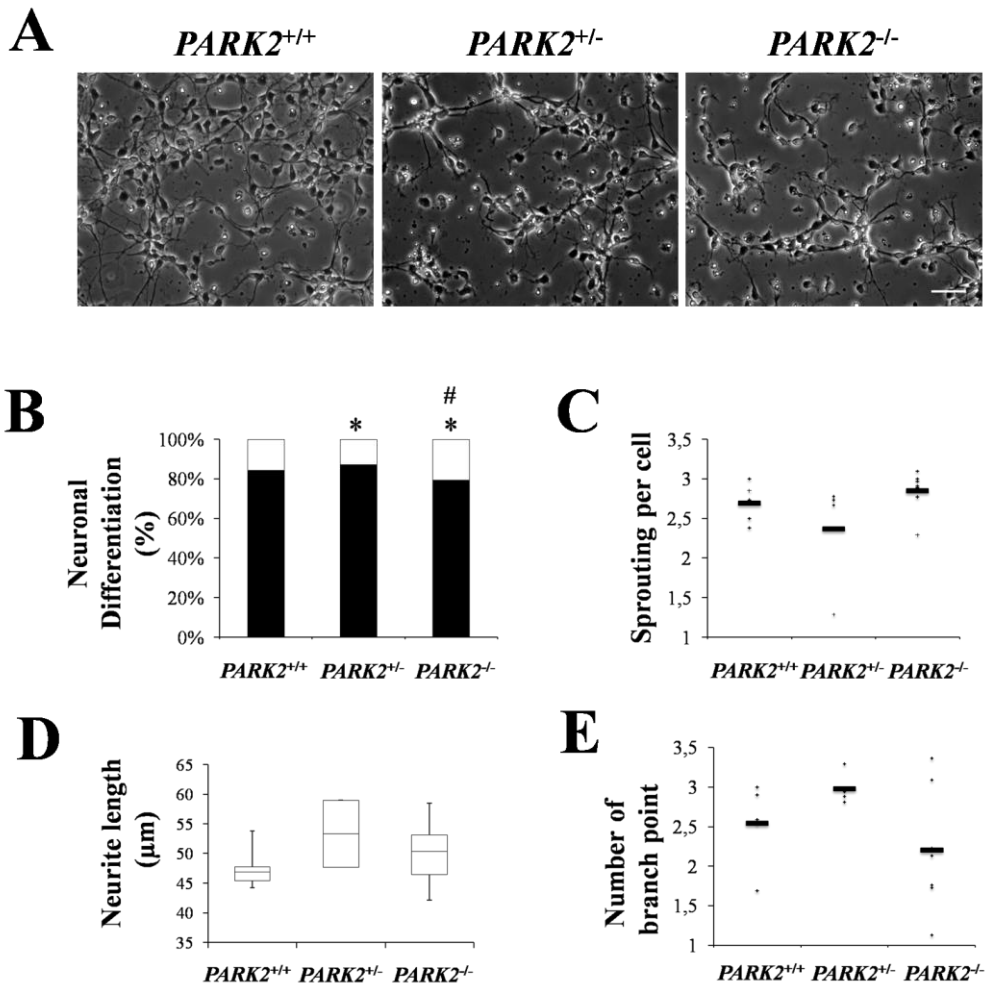
A
PARK2+/+
PARK2+/-
PARK2-/-
B
Neuronal Differentiation (%)
100%
80%
60%
40%
20%
0%
*
#
*
PARK2+/+ PARK2+/- PARK2-/-
C
Sprouting per cell
3,5
3
2,5
2
1,5
1
PARK2+/+ PARK2+/- PARK2-/-
D
Neurite length (µm)
65
60
55
50
45
40
35
PARK2+/+ PARK2+/- PARK2-/-
E
Number of branch point
3,5
3
2,5
2
1,5
1
PARK2+/+ PARK2+/- PARK2-/-

FIGURE 3

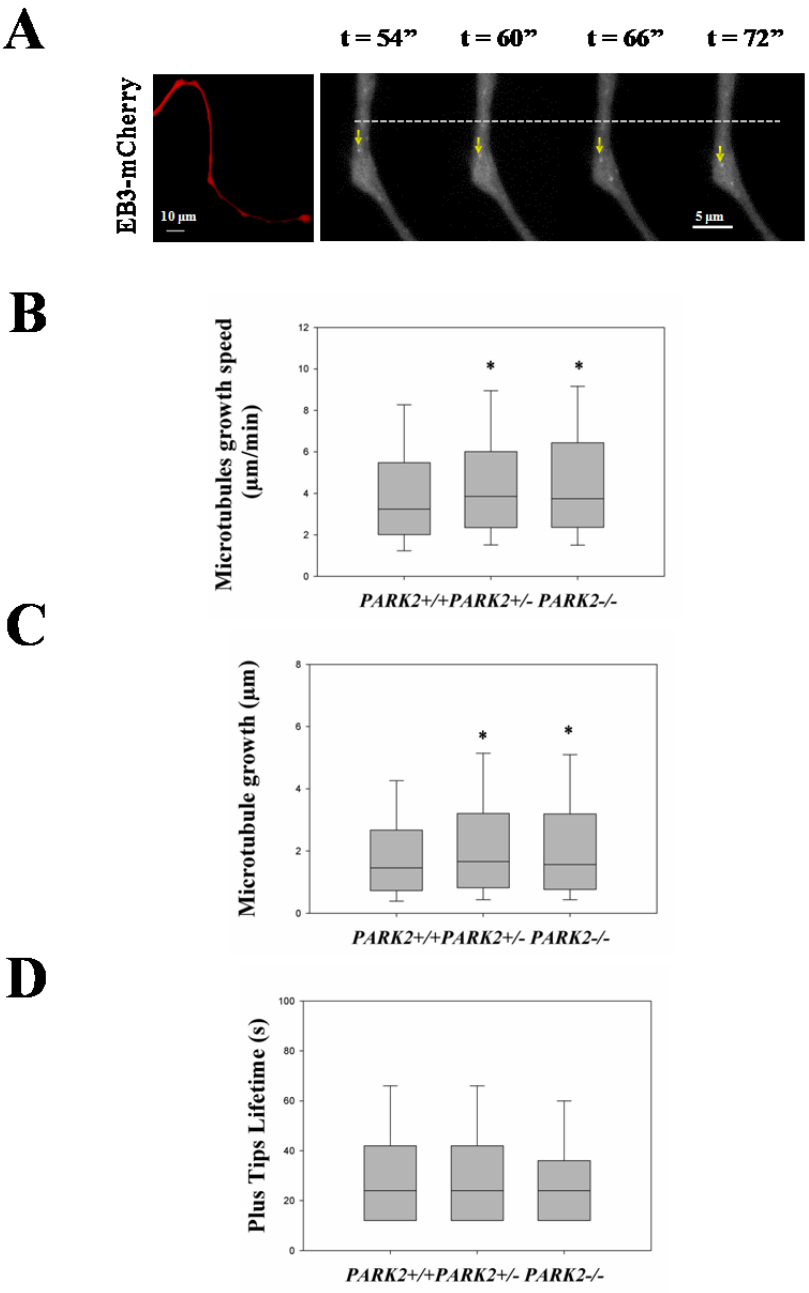
A
t = 54”
t = 60”
t = 66”
t = 72”
EB3-mCherry
10 µm
5 µm
B
Microtubules growth speed (µm/min)
PARK2+/+ PARK2+/- PARK2-/-
C
Microtubule growth (µm)
PARK2+/+ PARK2+/- PARK2-/-
D
Plus Tips Lifetime (s)
PARK2+/+ PARK2+/- PARK2-/-

FIGURE 4

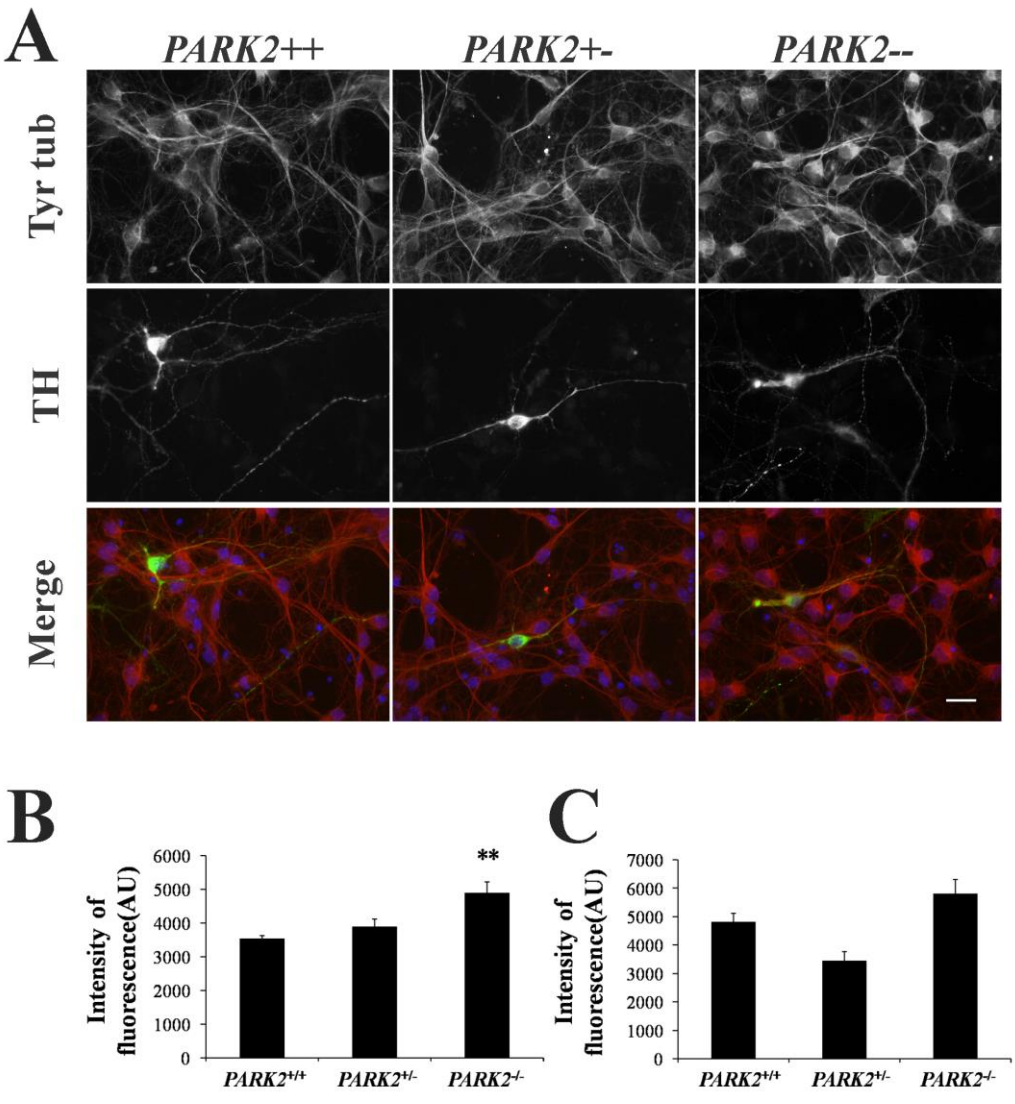
A
PARK2++
PARK2+-
PARK2--
Tyr tub
TH
Merge
B
Intensity of fluorescence(AU)
6000
5000
4000
3000
2000
1000
0
**
PARK2+/+
PARK2+/-
PARK2-/-
C
Intensity of fluorescence(AU)
7000
6000
5000
4000
3000
2000
1000
0
PARK2+/+
PARK2+/-
PARK2-/-

FIGURE 5

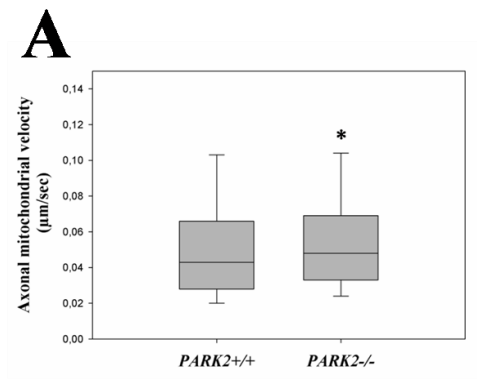

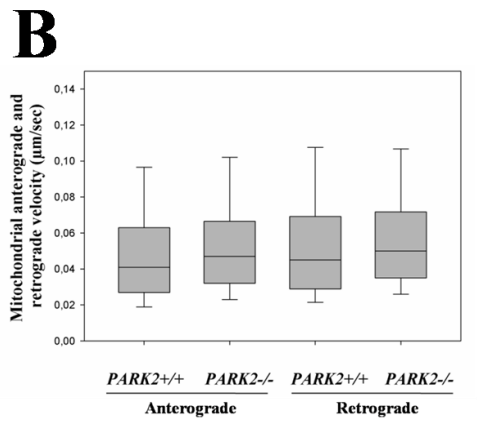

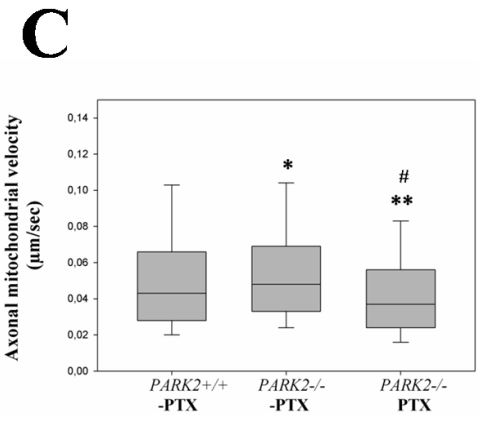

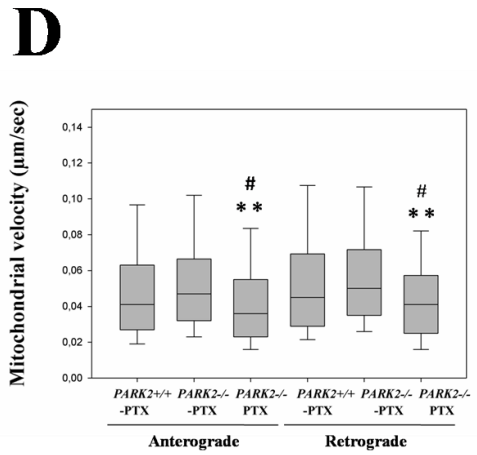

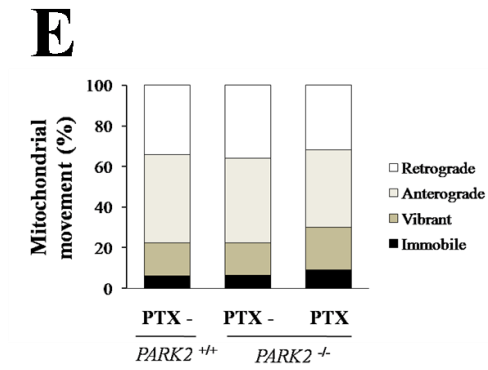

%	PTX -	PTX -	PTX
Immobile	6	6	9
Vibrant	16	16	21
Anterograde	44	42	38
Retrograde	34	36	32

MATERIALS & METHODS

Animals

Male and female wild-type and *PARK2* knockout (Goldberg et al. 2003) C57 Black mice were purchased from Charles River (Calco, Italy). Mice colony was obtained interbreeding heterozygous mice and gave rise to wild-type, heterozygous, and homozygous knockout mice at the expected Mendelian ratio. Their genotype was screened using PCR-based genotyping with the following primers: *PARK2*$^{+/+}$ reverse: 5'-CCT ACA CAG AAC TGT GAC CTG G-3'; *PARK2*$^{+/+}$forward: 5'-GCA GAA TTA CAG CAG TTA CCT GG-3'; *PARK2*$^{-/-}$: 5'-ATG TTG CCG TCC TCC TTG AAG TCG-3'. Mice were host under environmentally controlled conditions (ambient temperature = 22°C, humidity = 40%) on a 12-h light/dark cycle with food and water *ad libitum.* Animals were kept in pathogen-free conditions and all procedures and the study were carried out in accordance with Italian law (D. Lgs n° 2014/26, implementation of the 2010/63/EU) and were approved by the University of Milan Animal Welfare Body and by the Italian Minister of Health. All efforts were made to minimize animal suffering. Mice were killed by decapitation to perform our experiments.

Primary mesencephalic cultures

Primary cultures of mesencephalic neurons from C57 Black mice were prepared according to described protocols (Studer 2001) with some modifications.

Ventral mesencephalon tissues were dissected from E12.5 mouse embryos and kept on ice in cold Phosphate-Buffered Saline (PBS) with1% of penicillin-streptomycin,1% of gentamicin and 1μg/ml amphotericin B (EuroClone). The dissected parts were collected in PBS containing 0,6% glucose.

Tissues were incubated in Accumax (Millipore) at room temperature and after 30 min were mechanically dissociated. The cells were resuspended in MACS Neuro Medium containing 1% L-glutamine, 1% penicillin-streptomycin and 2% of MACS NeuroBrew-21 and plated on poly-D-lysine (Millipore)/laminin (Sigma Aldrich) pre-coated coverslip. The cells were seeded in one drop and placed in a humidified 37°C, 5% CO_2 incubator for 3 h to allow the attachment of the cells in the droplets to the coverslip. Afterwards, the culture medium is added. The cells were cultured *in vitro* and the fifty percent of the medium was changed every two days.

Morphometric analysis

The morphology of living cells has been evaluated by phase contrast microscopy at 1 and 2 days of differentiation *in vitro* (DIV). Random fields (at least 3 images for each embryo) were acquired for each well using S100 microscope (Zeiss, Oberkochen, Germany) equipped with AxiocamHR (Zeiss) and then analyzed using digital image processing software (Interactive measurement module, Axiovision Release 4.8, Zeiss). For the analysis, the following four principal features of neuritogenesis were considered: the percentage of differentiated and undifferentiated cells, the number of neuronal sprouting of both undifferentiated and differentiated cells, the length and the number of branch points of the longest neurite for each differentiated cell. In detail, one cell was considered differentiated when the neurite length measured at least twice of the cell body diameter.

Immunofluorescence and labeling

The cells were fixed with cold methanol (-20°C) at 7 DIV for 7 min and incubated with the following primary antibodies: anti-Tyr tubulin rat IgG (clone

YL 1/2, Abcam, Cambridge, UK) 1: 500 to detect dynamic MTs, anti-tyrosine hydroxylase (TH) rabbit IgG (Millipore) 1:200 to identify dopaminergic neurons. As secondary antibodies we used AlexaFluor^{TM} 488 goat anti-rabbit IgG 1:1000 and AlexaFluor^{TM} 568 donkey anti-rat IgG (Invitrogen) 1:1000. The coverslips were mounted in Mowiol® (Calbiochem, San Diego, CA)–DABCO (Sigma-Aldrich) and samples were examined with the Axiovert 200M microscope (Zeiss).

Live cell imaging

Primary mesencephalic cultures were transiently transfected using Lipofectamine 3000 (Invitrogen) (1:3 DNA to Lipofectamine ratio), with EB3-mCherry construct (Komarova et al. 2009) or Mito-dsRed (Cartelli et al. 2010). According to the experimental protocols, at different days after transfection, cultures were transferred to a live cell imaging workstation composed of an inverted microscope (Axiovert 200M, Zeiss), a heated (37°C) chamber (Okolab, Naple, Italy), and a Plan neofluar 63x/1.25 numerical aperture oil-immersion objective (Zeiss). Images were collected with a cooled camera (Axiocam HRM Rev. 2; Zeiss), every 6 s for the analyses of MT growth and every 10-15 s for mitochondrial trafficking; single movie duration was set at 1-3 min and the total recording time did not exceed 60 min for each dish. Next, cells were incubated for 2 h with 1 μM paclitaxel (Sigma-Aldrich) dissolved in methanol. MT dynamics were analyzed from EB3 time-lapse movies using plusTipTracker software (Applegate et al. 2011) whether mitochondrial movement by the Imaris software. For the analyses of mitochondrial transport in the axons, we defined a ROI (region of interest) excluding the cell bodies and the growth cone. We have also classified the mitochondria as follows: mobile (with anterograde and retrograde movement), vibrant and immobile.

Statistical analysis and data management

All data were expressed as mean ± SEM (standard error of measurement). Statistical analyses were performed using STATISTICA software (StatSoft Inc., Tulsa, OK). The statistical significance was assessed by Student's t test, one-way ANOVA with Tukey HSD, Fischer LSD *post-hoc* testing or χ^2 test when appropriate.

LEGENDS

Figure 1. Parkin deficiency interferes with neuronal differentiation at 1 day of differentiation *in vitro*.

Morphometric analysis showed alteration of neuronal differentiation and increase of neuronal sprouting on primary mesencephalic cultures isolated from *PARK2* knockout (*PARK2*$^{-/-}$) and heterozygous (*PARK2*$^{+/-}$) mice at 1 DIV. **(A)** Representative phase-contrast micrographs of mesencephalic cultures at 1 DIV. Scale bar, 50µm. Three principal features of neuritogenesis were considered for morphometric analysis. **(B**) The percentage of differentiated cells (black bars) and undifferentiated cells (white bars) are shown; *p<0.05 *vs* *PARK2*$^{+/+}$ and $^{\#}$p<0.001 *vs* *PARK2*$^{+/-}$ according to χ^2 test, (*PARK2*$^{+/+}$, n>1000; *PARK2*$^{+/-}$, n>1100; *PARK2*$^{-/-}$, n>550). **(C)** The sprouting of undifferentiated cells is shown, *p<0.05 and **p<0.005 *vs* *PARK2*$^{+/+}$ according to ANOVA, Fischer LSD *post hoc* test. The actual statistical values correspond to: F = 6,523, p = 0,013551, and the individual *p* value are *PARK2*$^{+/-}$ *vs* *PARK2*$^{+/+}$ = 0,004875, *PARK2*$^{-/-}$*vsPARK2*$^{+/+}$ = 0,035069 according to ANOVAFisher LSD *post hoc* test. (**D)** The length of the longest neurite for each differentiated cellis shown.

Figure 2. Parkin deficiency interferes with neuronal differentiation at 2 days of differentiation *in vitro*.

Morphometric analysis showed alterations of neuronal differentiation on primary mesencephalic cultures isolated from *PARK2* knockout (*PARK2*$^{-/-}$) and heterozygous (*PARK2*$^{+/-}$) mice at 2 DIV. **(A)** Representative phase-contrast micrographs of mesencephalic cultures at 2 DIV. Scale bar, 50µm. Four principal features of neuritogenesis were considered for morphometric analysis. (**B**) The percentage of differentiated cells (black bars) and undifferentiated cells (white bars) are shown, *p<0.025 *PARK2*$^{+/+}$ *vs PARK2*$^{+/-}$, *p<0.05 *PARK2*$^{-/-}$*vs PARK2*$^{+/+}$ and $^{\#}$p<0.05 *vs PARK2*$^{+/-}$ according to χ^2 test (*PARK2*$^{+/+}$, n>3800; *PARK2*$^{+/-}$, n>1500; *PARK*$^{+/-}$, n>5200 cells). In addition, the sprouting of undifferentiated cells **(C)**, the length of the longest neurite for each differentiated cell (**D**), and the number of the branch points of the longest neurite **(E)** are shown.

Figure 3. Parkin deficiency increases MT dynamics in primary neurons.

(A) Representative micrographs of midbrain neurons axons, showing the EB3 comets (EB3-mCherry). On the left is represented the axon of one transfected neuron (red, mCherry). Scale bar, 10 µm. The yellow arrows indicate the movement of the EB3 comets towards the plus end of MTs within the different frame (right panel, elapsed time is shown). Scale bar, 5 µm. Box plots of MT growth rate **(B)**, MT growth **(C)**, lifetime of MT **(D)** in primary mesencephalic cultures obtained from n=13/1448 tracks (PARK2$^{+/+}$), n=10 cells/819 tracks (*PARK2*$^{+/-}$) and n=8 cells/504 tracks (*PARK2*$^{-/-}$) mice. **B)** *p< 0.05 according to ANOVA Tukey HSD *post hoc* test. **C)** *p< 0.05 according to ANOVA, Fisher LSD *post hoc* test. All values are expressed as mean ± SEM.

Figure 4. Parkin deficiency impacts MT stability.

(A) Primary mesencephalic cultures were concomitantly stained for tyrosinated tubulin (Tyr-tub) and for tyrosine hydroxylase (TH), to investigate MT stability in whole culture and inside the dopaminergic neuron at 7 DIV. All cells were stained with DAPI (blue), to visualize the nucleus. Scale bar, 20 μm. **(B)** Analyses of immunofluorescence intensity performed in whole mesencephalic cultures: n=2 embryos (*PARK2*$^{+/+}$); n=3 embryos (*PARK2*$^{+/-}$); n=2 embryos (*PARK2*$^{-/-}$) and selectively in the dopaminergic neurons **(C)**. **p< 0.005 according to ANOVATukey HSD *post hoc* test. All values are expressed as mean ± SEM.

Figure 6. Parkin deficiency increases mitochondrial transport velocity in axon.

(A) Mitochondria transport in the axons of *PARK2*$^{-/-}$ and control cells (*PARK2*$^{+/+}$). n=7 cells/669tracks (*PARK2*$^{+/+}$); n=12 cells/767 tracks (*PARK2*$^{+/-}$); n=13 cells/1021 tracks (*PARK2*$^{+/-}$). *p<0.05 according to Student's t-Test. **(B)** Anterograde velocity and retrograde velocity of mitochondrial transport in *PARK2*$^{-/-}$and *PARK2*$^{+/+}$ axons. **(C)** Axonal transport of mobile mitochondria, at basal conditions (-PTX) or after 2 h of treatment with 1 μM paclitaxel (PTX). *p< 0.05 *vs* *PARK2*$^{-/-}$ (-PTX)/ *PARK2* $^{+/+}$ (-PTX); **p< 0.0001 *vs* *PARK2*$^{-/-}$ (PTX)/*PARK2*$^{+/+}$ (-PTX); $^{\#}$p<0.0001 *PARK2*$^{-/-}$ (PTX) *vs* *PARK2*$^{-/-}$ (-PTX) according to ANOVA, Tukey HSD *post hoc* test. **(D)** Anterograde and retrograde mitochondrial velocities in the axons, at basal condition (-PTX) or after 2h of treatment with 1 μM paclitaxel (PTX). **p<0.01 *vs* *PARK2*$^{-/-}$ (PTX)/*PARK2*$^{-/-}$ (-PTX) and $^{\#}$p<0.0001 for anterograde and retrograde movement according to ANOVA Tukey HSD *post hoc* test. **(E)** Histogram representing the percentage of immobile, vibrant and anterograde or retrograde moving mitochondria before (PTX-) and after 2 h of treatment with 1 μM

paclitaxel (PTX), while the table (right) reports the percentage values for the different categories.

REFERENCES

Applegate, K.T. et al., 2011. plusTipTracker : Quantitative image analysis software for the measurement of microtubule dynamics. *J Struct Biol*, **176,** 168–184.

Cartelli, D. et al., 2010. Microtubule dysfunction precedes transport impairment and mitochondria damage in MPP+-induced neurodegeneration. *J Neurochem*, **115**, 247–258.

Cartelli, D. et al., 2012. Microtubule Destabilization Is Shared by Genetic and Idiopathic Parkinson's Disease Patient Fibroblasts. *PLoS* ONE, **7**:e37467.

Cartelli, D. et al., 2013. Microtubule Alterations Occur Early in Experimental Parkinsonism and The Microtubule Stabilizer Epothilone D Is Neuroprotective. *Sci Rep*, **3**, 1837.

Dawson, T., Ko, H. and Dawson, V., 2010. Genetic animal models of Parkinson's disease. *Neuron*, **66**, 646–661.

Dubey, J. et al., 2015. Neurodegeneration and microtubule dynamics : death by a thousand cuts. *Front Cell Neuroscin*, **9**, 10-26.

Goldberg, M.S. et al., 2003. Parkin-deficient Mice Exhibit Nigrostriatal Deficits but not Loss of Dopaminergic Neurons. *J Biol Chem*, **278**, 43628–43635.

Houlden H., Singleton A.B. 2012. The genetics and neuropathology of Parkinson's disease. *Acta Neuropathol*, **124**, 325-38.

Itoh K., Nakamura K., Iijima, Miho and H.S., 2013. Mitochondrial Dynamics in Neurodegeneration. *Trends Cell Biol*, **23**, 64–71.

Khan, N.L. et al., 2005 Dopaminergic dysfunction in unrelated , asymptomatic carriers of a single parkin. *Neurology*, **64**,134–136.

Klein, C. et al., 2007. Deciphering the role of heterozygous mutations in genes associated with parkinsonism. *Lancet Neurol*, **6,** 652–662.

Komarova, Y. et al., 2009. Mammalian end binding proteins control persistent microtubule growth. *J Cell Biol*, **184**, 691–706.

Ren, Y., Zhao, J. and Feng, J., 2003. Parkin Binds to α / β Tubulin and Increases their Ubiquitination and Degradation. *J Neurosci*, **23**, 3316–3324.

Ren, Y. et al., 2009. Parkin Protects Dopaminergic Neurons against Microtubule-depolymerizing Toxins by Attenuating Microtubule-associated Protein Kinase Activation. *J Biol Chem*, **284**, 4009–4017.

Ren, Y. et al., 2015. Parkin Mutations Reduce the Complexity of Neuronal Processes in IPSC-Derived Human. *Stem Cells*, **33**, 68–78.

Sheng, Z.-H. and Cai, Q., 2016. Mitochondrial transport in neurons: impact on synaptic homeostasis and neurodegeneration. *Nat Rev Neurosci*, **13**, 77–93.

Studer, L., 2001. Culture of substantia nigra neurons. *Curr Prot Neurosci*, Chapter 3, p.Unit 3.3.

Wang, X. et al., 2011. PINK1 and Parkin target miro for phosphorylation and degradation to arrest mitochondrial motility. *Cell*, **147**, 893–906.

Yang, F. et al., 2005. Parkin Stabilizes Microtubules through Strong Binding Mediated by Three Independent Domains Parkin. *J Biol Chem*, **280**, 17154–17162.

Linking microtubules to Parkinson's disease: the case of parkin

Graziella Cappelletti*[1], Francesca Casagrande*, Alessandra Calogero*, Carmelita De Gregorio*, Gianni Pezzoli† and Daniele Cartelli*

*Department of Biosciences, Università degli Studi di Milano, I-20133 Milano, Italy
†Parkinson Institute, Istituti Clinici di Perfezionamento, I-20125 Milano, Italy

Abstract

Microtubules (MTs) are dynamic polymers consisting of α/β tubulin dimers and playing a plethora of roles in eukaryotic cells. Looking at neurons, they are key determinants of neuronal polarity, axonal transport and synaptic plasticity. The concept that MT dysfunction can participate in, and perhaps lead to, Parkinson's disease (PD) progression has been suggested by studies using toxin-based and genetic experimental models of the disease. Here, we first learn lessons from MPTP and rotenone as well as from the PD related genes, including *SNCA* and *LRRK2*, and then look at old and new evidence regarding the interplay between parkin and MTs. Data from experimental models and human cells point out that parkin regulates MT stability and strengthen the link between MTs and PD paving the way to a viable strategy for the management of the disease.

Introduction

The molecular pathways implicated in neurodegenerative disorders are gradually being elucidated and several contributing factors have been identified. To date, aetiopathogenic mechanisms in Parkinson's disease (PD) converge on accumulation of aberrant or misfolded proteins, mitochondrial injury, and oxidative/nitrosative stress, making PD a multifactorial disease [1,2]. However, the primary degenerative events remain unclear, thus making it really hard to develop an efficient therapy for this devastating disorder.

PD is a progressive neurodegenerative disorder that is characterized by tremor, muscular rigidity and bradykinesia, with a prevalence of 2–5 % in the population aged 60 years, worldwide. PD can be defined in biochemical terms as a dopamine-deficiency state resulting from loss of dopamine neurons in the *substantia nigra pars compacta* accompanied by characteristic intraneuronal protein inclusions, termed Lewy bodies. On these grounds, starting in the 1950s, the strategy for treating PD has been to restore the dopamine concentrations in the brain by administering pharmacological treatment. However, thanks to a huge amount of clinical and basic research work, a redefinition of PD as a multiorgan disease has been proposed recently and novel therapeutic strategies are emerging [3].

In recent years, growing attention has been dedicated to neuronal cytoskeleton dysfunction and increasing evidence suggests a role for the microtubule (MT) system in the pathogenesis of neurodegenerative disorders. Mutations in tubulin, the major constituent of MTs, have been found to induce severe neurological disorders, such as peripheral neuropathy and loss of axons in many kinds of brain neurons [4] and, very recently, to be associated with familial amyotrophic lateral sclerosis [5]. Moreover, defects in the proper regulation of MT organization and stability are tightly linked to neuronal damages. Indeed, significant impairment in MT-associated proteins has been extensively reported in Alzheimer's disease, frontotemporal dementia and other tauopathies [6] and, notably, the failure in polyglutamilation of tubulin can dramatically lead to a rapid neuronal cell death in an ataxia mouse model [7]. Besides MT organization and stability, MT-dependent functions, such as overall axonal transport, are increasingly investigated in the field of neurodegeneration. The intracellular transport of organelles along an axon is a complex and crucial process for the maintenance and function of a neuron. Several different mechanisms including defects in the proper organization of MTs, mutations in MT-associated proteins and molecular motors, and activation of MT-targeting kinases act in concert and produce deficits in axonal transport underlying several neurodegenerative diseases, as extensively reviewed by Millecamps and Julien [8]. In addition, recent evidence suggests that axon degeneration underlying PD could depend mainly on the failure of axonal transport [9].

The question arises as to whether we can reasonably include MT dysfunction among the culprits triggering neurodegeneration in PD or not. Here, we bear in mind such a key question and move from a brief insight into the basis of MT functions in neurons to the evidence that MT dysfunction occurs in experimental parkinsonism and, finally, to the critical discussion on the interplay between parkin and MT system in cellular and animal models and in human tissues.

Key words: microtubules, microtubule stability, microtubule-dependent functions, neurodegeneration, parkin, Parkinson's disease.

Abbreviations: iPSC, induced-pluripotent stem cells; MPP^+, 1-methyl-4-phenylpyridinium; MPTP, *N*-methyl-4-phenyl-1,2,3,6-tetrahydropyridine; MT, microtubule; PD, Parkinson's disease.

[1]To whom correspondence should be addressed (email graziella.cappelletti@unimi.it).

Microtubules and microtubule-dependent functions in neurons

MTs are non-covalent cytoskeletal filaments, which occur in all eukaryotic cell types from fungi to mammals. They consist of α/β tubulin heterodimers that assemble in a head-to-tail fashion into linear protofilaments whose lateral association forms polarized 25 nm wide hollow cylindrical polymers. MTs are heterogeneous in length and highly dynamic *in vivo* and *in vitro*, undergoing cycles of polymerization and rapid depolymerization. This 'dynamic instability' property was first described in 1984 [10] as a feature that is crucial to many MT functions. The tight regulation of their organization and dynamics depends on the incorporation of alternative tubulin isotypes, a highly complex and diverse set of MT-interacting proteins, and posttranslational modifications occurring on MTs [11].

MTs play several essential roles in cell shape acquisition and in the performance of many intracellular processes. Neurons are a striking example of cells in which MTs are essential to achieve a high degree of morphological and functional complexity. Neuronal MTs display different orientation and dynamics in axons and dendrites, and interact with specific associated proteins [12]. In addition, the incorporation of tubulin isotypes and posttranslational modifications of tubulin are selectively combined and distributed among different subcellular compartments, thus generating a tubulin code, that might regulate basic as well as higher-order neuronal functions. Highly dynamic MTs are enriched in tyrosinated tubulin and accumulate a set of factors known as MT plus-end tracking proteins; they are essential for rapid remodelling and reorganization in the growth cone underlying axonal elongation during neuronal differentiation [12] and synaptic plasticity in mature neurons [13]. On the contrary, a high stability is favoured for MT functions in the shaft of axons and for the preferential binding of MT-based motors transporting membrane-bound organelles and regulatory macromolecular complexes [12]. Neuronal MT stability is related to the accumulation of several posttranslational modifications of tubulin including acetylation, detyrosination, Δ2-tubulin, polyglutamylation and the very recently described polyamination [14], and to spatial gradient of tau [15].

Beyond their known conventional roles for supporting neuronal architecture, organelle transport and synaptic plasticity, a novel function as 'information carriers' has been attributed to neuronal MTs [16]. This amazing theory posits that both the short, stable and mobile MTs and the highly dynamic ends of longer MTs can act as information carriers in the neuron thanks to their ability to interact with a vast array of proteins. Short MTs, which appear to be unusually stable, move rapidly along axons and presumably in dendrites as well. It is reasonable to assume that they may convey information and signalling molecules with them. In addition, highly dynamic regions would act as scaffolds concentrating MT plus end tracking proteins, which, in turn, interact with many other proteins and structures contributing to the plasticity of the neuron, including kinases and small G proteins that impact the actin cytoskeleton and proteins that reside at the cell cortex [17].

Microtubule dysfunction in experimental models of Parkinson's disease

The concept that MT dysfunctions can participate in, and perhaps lead to, PD progression has been suggested by studies on toxin-based and genetic experimental models of the disease.

Within the context of studies on PD-inducing neurotoxins, intriguing results have been reported with *N*-methyl-4-phenyl-1,2,3,6-tetrahydropyridine (MPTP), a neurotoxin widely used as a tool for studies on sporadic PD [1], and the herbicide rotenone. We showed that 1-methyl-4-phenylpyridinium (MPP^+), the toxic metabolite of MPTP, reduces MT polymerization and interferes with dynamic instability of MTs *in vitro* acting as a destabilizing factor [18]. Then, we confirmed and extended these results reporting that MPP^+ leads to MT alteration in neuronal cell and, in turn, to mitochondrial trafficking impairment [19]. Finally, we showed that systemic injection of MPTP to mice induces MT dysfunction that occurs very early, before axonal transport deficit, depletion of tyrosine hydroxylase and, ultimately, dopaminergic neuron degeneration [20]. Moving to the herbicide rotenone, old studies demonstrated its ability to induce MT depolymerization *in vitro* [21], whereas more recent data suggest that MT disruption may be an alternative mechanism underlying rotenone-induced dopamine neuron death in cellular models [22,23].

We can find further signs of MT involvement in PD looking at PD-linked genes. Interestingly, several independent GWAS and meta-analysis studies have shown a genome-wide significant association of single nucleotide polymorphisms in the gene coding for α-synuclein (*SNCA*) and the MT-associated protein tau [24]. α-Synuclein, the first protein associated to familial form of PD [25], interacts with tubulin with crucial consequences: the promotion of its aggregation in fibrils [26], the interference with tubulin assembly [27] and the recycling of monoamine transporter [28]. More recently, MT disruption has been reported in cells overexpressing α-synuclein [29] or following incubation with extracellular α-synuclein [30]. In addition, the kinase LRRK2 has been shown to interact with and to phosphorylate β-tubulin [31,32] and tubulin-associated tau, whereas a novel role of DJ-1 in the regulation of MT dynamics has been proposed [33].

Although these studies provide evidences that the MT cytoskeleton could be involved in neuronal damage caused by PD-related proteins or toxins, very little is known about MT dysfunction in patients. Using cybrid cell lines generated from idiopathic PD patients, Esteves et al. [34] showed significant alterations in MT integrity as compared with healthy subjects. Notably, we have recently analysed primary fibroblasts deriving from patients with idiopathic or genetic

PD and disclosed reduction in MT mass and significant changes in signalling pathways related to MT stability [35].

We believe that it is not a coincidence that tubulin and MTs represent a point of convergence in so many different PD experimental models, thus making the study of MT dysfunction a challenge leading to a better comprehension of PD pathogenesis.

The interplay between parkin and microtubules

Exonic deletions in the *Parkin* gene were first reported in Japanese families with autosomal recessive juvenile-onset parkinsonism with onset frequently occurring before the age of 20 [36]. The *Parkin* gene encodes for a member of the E3 ligase family that catalyses the addition of ubiquitin to numerous target proteins [37]. The molecular understanding of the regulation of parkin E3 ligase activity is emerging [38]. However, it has been suggested that parkin, in addition to its ligase activity, has a number of other roles including the regulation of mitochondria dynamics and quality control designed to preserve mitochondria integrity [39]. Most of the supporting observations derive from mammalian cell lines overexpressing parkin, but endogenous parkin does not induce mitophagy in induced-pluripotent stem cell (iPSC)-derived human neurons [40]. This raises the issue of whether parkin involvement in this process is actually relevant in neurons or in PD pathogenesis [41]. Very recently, it has also been reported that parkin interacts with the kainate receptor GluK2 subunit and regulates the receptor function *in vitro* and *in vivo* [42].

Parkin interaction with tubulin and MTs has been proposed many years ago and remained largely neglected for a long time. Interestingly, parkin binds and increases the ubiquitination and degradation of both α- and β-tubulin [43], whose complex folding reactions are prone to produce misfolded intermediates. In addition to its E3 ligase activity on tubulin, however, Yang et al. [44] proposed that parkin strongly binds tubulin/MTs through three redundant interaction domains resulting in MT stabilization. At the moment, we can simply speculate that the anchorage of parkin to MTs could provide an important environment for its E3 ligase activity on misfolded substrates that are usually transported on MTs themselves. Further work demonstrates that parkin protects midbrain dopaminergic neurons against PD-causing substances, as rotenone and colchicine, by stabilizing MTs [45]. This process seems to be mediated by the regulation of the MAP kinase pathway, which, interestingly, is a direct regulator of MT stability via the modulation of tubulin posttranslational modifications.

Bringing into focus the impact of parkin on MT-dependent functions, a reliable consequence of the alteration of MT stability could be the dysregulation of axonal transport. Indeed, previously, parkin has proved to regulate the trafficking of mitochondria in hippocampal neurons, especially when they are damaged and have to be degraded. This process was found to be dependent on the Miro phosphorylation [46].

Striking data coming from human cells have recently contributed to our understanding of the interplay between parkin and MTs strengthening interest in this aspect. We reported that PD-patient skin fibroblasts bearing *Parkin* mutations display reduced MT mass and imbalance in the pattern of tubulin posttranslational modifications, and that MT pharmacological stabilization or the overexpression of wild-type parkin rescue control phenotype [39]. This is not restricted to skin cells from patients but, interestingly, has been confirmed in iPSC-derived neurons. Ren et al. [47] found that the complexity of neuronal processes was greatly reduced in both dopaminergic and non-dopaminergic neurons from PD patients with parkin mutations and that MT stability was significantly decreased as demonstrated by the reduction in MT mass. Overexpression of parkin, but not its PD-linked mutants, restored the complexity of neuronal processes and MT mass. Notably, the MT depolymerizing agent colchicine mirrored the effect of parkin mutations by decreasing neurite complexity in control neurons while the MT stabilizing drug taxol mimicked the effect of parkin overexpression. These results strongly support the concept that the interaction of parkin with MTs in neurons may have an important physiological role. Thus, although the hypothesis of the interaction of parkin with MTs is supported mainly by studies in cellular models, it seems to be a promising theory, which provides a mechanistic explanation for the multiple intracellular functions and, possibly, dysfunctions of parkin. Indeed, we are currently undergoing the analyses of brain samples from *Parkin* knockout mice; our preliminary results have shown an early alteration of MT stability, thus confirming and expanding the importance of parkin in modulating the MT system.

Concluding remarks

A growing body of evidence from experimental models and human cells indicates that parkin regulates MT stability and strengthens the link between MTs and PD. Indeed, the MT cytoskeleton represents a point of convergence in the action of various proteins mutated in PD and of PD-inducing neurotoxins, suggesting that it has a major role in the onset of the disease and providing the rationale for novel therapeutic interventions. Thus, MT stabilizing strategies may offer an opportunity for treating neurodegenerative diseases [48–50]. Importantly, we have recently demonstrated that this may be true also in PD showing that Epothilone D, a MT stabilizer drug, exerts neuroprotective effects in a toxin-based murine model of PD [20].

Funding

This work was supported by the Fondazione Grigioni per il Morbo di Parkinson, Milan, Italy (2011–2015 grants to G.C.) and the 'Dote ricerca', FSE, Regione Lombardia (to D.C.).

References

1 Dauer, W. and Przedborski, S. (2003) Parkinson's disease: mechanisms and models. Neuron **39**, 889–909 CrossRef PubMed
2 Obeso, J.A., Rodriguez-Oroz, M.C., Goetz, C.G., Marin, C., Kordower, J.H., Rodriguez, M., Hirsch, E.C., Farrer, M., Schapira, A.H.V. and Halliday, G. (2010) Missing pieces in the Parkinson's disease puzzle. Nat. Med. **16**, 653–661 CrossRef PubMed
3 Shapira, A.H.V., Olanow, C.W., Greenamyer, J.T. and Bezard, E. (2014) Slowing of neurodegeneration in Parkinson's disease and Huntington's disease: future therapeutic perspectives. Lancet **384**, 545–555 CrossRef PubMed
4 Tischfield, M.A., Baris, H.N., Wu, C., Rudolph, G., Van Maldergem, L., He, W., Chan, W.M., Andrews, C., Demer, J.L., Robertson, R.L. et al. (2010) Human TUBB3 mutations perturb microtubule dynamics, kinesin interactions, and axon guidance. Cell **140**, 74–87 CrossRef PubMed
5 Smith, B.N., Ticozzi, N., Fallini, C., Gkazi, A.S., Topp, S., Kenna, K.P., Scotter, E.L., Kost, J., Keagle, P., Miller, J.W. et al. (2014) Exome-wide rare variant analysis identifies TUBA4A mutations associated with familial ALS. Neuron **84**, 324–331 CrossRef PubMed
6 Spillantini, M.G. and Goedert, M. (2013) Tau pathology and neurodegeneration. Lancet Neurol **12**, 609–622 CrossRef PubMed
7 Rogowski, K., Van Dijk, J., Magiera, M.M., Bosc, C., Deloulme, J.C., Bosson, A., Peris, L., Gold, N.D., Lacroix, B., Bosch Grau, M. et al. (2010) A family of protein-deglutamylating enzymes associated with neurodegeneration. Cell **143**, 564–578 CrossRef PubMed
8 Millecamps, S. and Julien, J-P. (2013) Axonal transport deficits and neurodegenerative diseases. Nat. Rev. Neurosci. **14**, 161–176 CrossRef PubMed
9 Burke, R.E. and O'Malley, K. (2013) Axon degeneration in Parkinson's disease. Exp. Neurol. **246**, 72–83 CrossRef PubMed
10 Mitchison, T. and Kirschner, M. (1984) Dynamic instability of microtubules growth. Nature **312**, 237–242 CrossRef PubMed
11 Janke, C. and Bulinski, J.C. (2011) Post-translational regulation of the microtubule cytoskeleton: mechanisms and functions. Nat. Rev. Mol. Cell Biol. **12**, 773–786 CrossRef PubMed
12 Conde, C. and Cáceres, A. (2009) Microtubule assembly, organization and dynamics in axons and dendrites. Nat. Rev. Neurosci. **10**, 319–332 CrossRef PubMed
13 Jaworski, J., Kapitein, L.C., Montenegro Gouveia, S., Dortland, B.R., Wulf, P.S., Grigoriev, I., Camera, P., Spangler, S.A., Di Stefano, P., Demmers, J. et al. (2009) Dynamic microtubules regulate dendritic spine morphology and synaptic plasticity. Neuron **61**, 85–100 CrossRef PubMed
14 Song, Y., Kirkpatrick, L.L., Schilling, A.B., Helseth, D.L., Chabot, N., Keillor, J.W., Johnson, G.V.W. and Brady, S.T. (2013) Transglutaminase and polyamination of tubulin: posttranslational modification for stabilizing axonal microtubules. Neuron **78**, 109–123 CrossRef PubMed
15 Scholz, T. and Mandelkow, E. (2014) Transport and diffusion of Tau protein in neurons. Cell Mol. Life Sci. **71**, 3139–3159 CrossRef PubMed
16 Dent, E.W. and Baas, P.W. (2014) Microtubules in neurons as information carriers. J. Neurochem. **129**, 235–239 CrossRef PubMed
17 Akhmanova, A., Stehbens, S.J. and Yap, A.S. (2009) Touch, grasp, deliver and control: functional cross-talk between microtubules and cell adhesions. Traffic (Copenhagen, Denmark) **10**, 268–274 CrossRef PubMed
18 Cappelletti, G., Surrey, T. and Maci, R. (2005) The parkinsonism producing neurotoxin MPP+ affects microtubule dynamics by acting as a destabilising factor. FEBS Lett. **579**, 4781–4786 CrossRef PubMed
19 Cartelli, D., Ronchi, C., Maggioni, M.G., Rodighiero, S., Giavini, E. and Cappelletti, G. (2010) Microtubule dysfunction precedes transport impairment and mitochondria damage in MPP+-induced neurodegeneration. J. Neurochem. **115**, 247–258 CrossRef PubMed
20 Cartelli, D., Casagrande, F., Busceti, C.L., Bucci, D., Molinaro, G., Traficante, A., Passarella, D., Giavini, E., Pezzoli, G., Battaglia, G. and Cappelletti, G. (2013) Microtubule alterations occur early in experimental parkinsonism and the microtubule stabilizer epothilone D is neuroprotective. Sci. Rep. **3**, 1837 CrossRef PubMed
21 Marshall, L.E. and Himes, R.H. (1978) Rotenone inhibition of tubulin self-assembly. Biochim. Biophys. Acta **543**, 590–594 CrossRef PubMed
22 Ren, Y., Liu, W., Jiang, Q. and Feng, J. (2005) Selectively vulnerability of dopaminergic neurons to microtubule depolymerization. J. Biol. Chem. **280**, 34105–34112 CrossRef PubMed
23 Choi, W.S., Palmiter, R.D. and Xia, Z. (2011) Loss of mitochondrial complex I activity potentiates dopamine neuron death induced by microtubule dysfunction in a Parkinson's disease model. J. Cell Biol. **192**, 873–882 CrossRef PubMed
24 Nalls, M.A., Plagnol, V., Hernandez, D.G., Sharma, M., Sheerin, U.M., Saad, M., Simon-Sanchez, J., Schulte, C., Lesage, S., Sveinbjornsdottir, S. et al. (2011) Imputation of sequence variants for identification of genetic risks for Parkinson's disease: a meta-analysis of genome-wide association studies. Lancet **377**, 641–649 CrossRef PubMed
25 Polymeropoulos, M.H., Lavedan, C., Leroy, E., Ide, S.E., Dehejia, A., Dutra, A., Pike, B., Root, H., Rubenstein, J., Boyer, R. et al. (1997) Mutation in the alpha-synuclein gene identified in families with Parkinson's disease. Science **276**, 2045–2047 CrossRef PubMed
26 Alim, M.A., Hossain, M.S., Arima, K., Takeda, K., Izumiyama, Y., Nakamura, M., Kaji, H., Shinoda, T., Hisanaga, S. and Ueda, K. (2002) Tubulin seeds alpha-synuclein fibril formation. J. Biol. Chem. **277**, 2112–2117 CrossRef PubMed
27 Alim, M.A., Ma, Q.L., Takeda, K., Aizawa, T., Matsubara, M., Nakamura, M., Asada, A., Saito, T., Kaji, H., Yoshii, M. et al. (2004) Demonstration of a role for alpha-synuclein as a functional microtubule-associated protein. J. Alzheimers Dis. **6**, 435–442 PubMed
28 Jeannotte, A.M. and Sidhu, A. (2007) Regulation of the norepinephrine transporter by alpha-synuclein-mediated interactions with microtubules. Eur. J. Neurosci. **26**, 1509–1520 CrossRef PubMed
29 Prots, I., Veber, V., Brey, S., Campioni, S., Buder, K., Riek, R., Bohm, K.J. and Winner, B. (2013) α-Synuclein oligomers impair neuronal microtubule-kinesin interplay. J. Biol. Chem. **288**, 21742–21754 CrossRef PubMed
30 Gassowska, M., Czapski, G.A., Pajak, B., Cieślik, M., Lenkiewicz, A.M. and Adamczyk, A. (2014) Extracellular α-synuclein leads to microtubule destabilization via GSK-3β-dependent Tau phosphorylation in PC12 cells. PLoS One **9**, e94259 CrossRef PubMed
31 Gillardon, F. (2009) Leucine-rich repeat kinase 2 phosphorylates brain tubulin-beta isoform and modulates microtubule stability: a point of convergence in parkinsonian neurodegeneration? J. Neurochem. **110**, 1514–1522 CrossRef PubMed
32 Law, B.M., Spain, V.A., Leinster, V.H., Chia, R., Beilina, A., Cho, H.J., Taymans, J.M., Urban, M.K., Sancho, R.M., Blanca Ramírez, M. et al. (2014) A direct interaction between leucine-rich repeat kinase 2 and specific β-tubulin isoforms regulates tubulin acetylation. J. Biol. Chem. **289**, 895–908 CrossRef PubMed
33 Sheng, C., Heng, X., Zhang, G., Xiong, R., Li, H., Zheng, S. and Chen, S. (2013) DJ-1 deficiency perturbs microtubule dynamics and impairs striatal neurite outgrowth. Neurobiol. Aging **34**, 489–498 CrossRef PubMed
34 Esteves, A.R., Arduino, D.M., Swerdlow, R.H., Oliveira, C.R. and Cardoso, S.M. (2010) Microtubule depolymerisation potentiates alpha-synuclein oligomerization. Front. Aging Neurosci. **1**, 5 CrossRef PubMed
35 Cartelli, D., Goldwurm, S., Casagrande, F., Pezzoli, G. and Cappelletti, G. (2012) Microtubule destabilization is shared by genetic and idiopathic Parkinson's disease patient fibroblasts. PLoS One **7**, e37467 CrossRef PubMed
36 Kitada, T., Asakawa, S., Hattori, N., Matsumine, H., Yamamura, Y., Minoshima, S., Yokochi, M., Mizuno, Y. and Shimizu, N. (1998) Mutations in the parkin gene cause autosomal recessive juvenile parkinsonism. Nature **392**, 605–608 CrossRef PubMed
37 Shimura, H., Hattori, N., Kubo, S., Mizuno, Y., Asakawa, S., Minoshima, S., Shimizu, N., Iwai, K., Chiba, T., Tanaka, K. and Suzuki, T. (2000) Familial Parkinson's disease gene product parkin, is a ubiquitin-protein ligase. Nat. Genet. **2**, 302–305
38 Walden, H. and Martinez-Torres, R.J. (2012) Regulation of Parkin E3 ligase activity. Cell. Mol. Life Sci. **69**, 3053–3067 CrossRef PubMed
39 Scarffe, L.A., Stevens, D.A., Dawson, V.L. and Dawson, T.M. (2014) Parkin and PINK1: much more than mitophagy. Trends Neurosci. **37**, 315–324 CrossRef PubMed
40 Rakovic, A., Shurkewitsch, K., Seibler, P., Grunewald, A., Zanon, A., Hagenah, J., Krainc, D. and Klein, C. (2013) PTEN-induced putative kinase 1 (PINK1)-dependent ubiquitination of endogenous Parkin attenuates mitophagy: study in human primary fibroblasts and induced pluripotent stem (iPS) cell-derived neurons. J. Biol. Chem. **288**, 2223–2237 CrossRef PubMed
41 Grenier, K., McLelland, G.L. and Fon, E.A. (2013) Parkin- and PINK1-dependent mitophagy in neurons: will the real pathway please stand up? Front. Neurol. **4**, 100 CrossRef PubMed
42 Maraschi, A.M., Ciammola, A., Folci, A., Sassone, F., Ronzitti, G., Cappelletti, G., Silani, V., Sato, S., Hattori, N., Mazzanti, M. et al. (2014) Parkin regulates kainate receptors by interacting with the GluK2 subunit. Nat. Commun. **5**, 5182 CrossRef PubMed
43 Ren, Y., Zhao, J. and Feng, J. (2003) Parkin binds to α/β tubulin and increases their ubiquitination and degradation. J. Neurosci. **23**, 3316–3324 PubMed

44 Yang, F., Jiang, Q., Zhao, J., Ren, Y., Sutton, M.D. and Feng, J. (2005) Parkin stabilizes microtubules through strong binding mediated by three independent domains. J. Biol. Chem. **280**, 17154–17162 CrossRef PubMed
45 Ren, Y., Jiang, H., Yang, F., Nakaso, K. and Feng, J. (2009) Parkin protects dopaminergic neurons against microtubule-depolymerizing toxins by attenuating microtubule-associated protein kinase activation. J. Biol. Chem. **284**, 4009–4017 CrossRef PubMed
46 Wang, X., Winter, D., Ashrafi, G., Schlehem, J., Wong, Y.L., Selkoe, D., Rice, S., Steen, J., LaVoie, M.J. and Schwarz, T.L. (2011) PINK1 and Parkin target Miro for phosphorylation and degradation to arrest mitochondrial motility. Cell **147**, 893–906 CrossRef PubMed
47 Ren, Y., Jiang, H., Hu, Z., Fan, K., Wan, J., Janoschka, S., Wang, X., Ge, S. and Feng, J. (2015) Parkin mutations reduce the complexity of neuronal processes in iPSC derived human neurons. Stem Cells **33**, 68–78 CrossRef PubMed
48 Gozes, I. (2011) Microtubules (tau) as an emerging therapeutic target: NAP (davunetide). Curr. Pharm. Des. **17**, 3413–3417 CrossRef PubMed
49 Baas, P.W. and Ahmad, F.J. (2013) Beyond taxol: microtubule-based treatment of disease and injury of the nervous system. Brain **136**, 2937–2951 CrossRef PubMed
50 Brunden, K.R., Trojanowski, J.Q., Smith, III, A.B., Lee, V.M.-Y. and Ballatore, C. (2014) Microtubule-stabilizing agents as potential therapeutics for neurodegenerative disease. Bioorg. Med. Chem. **22**, 5040–5049 CrossRef PubMed

Received 13 January 2015
doi:10.1042/BST20150007

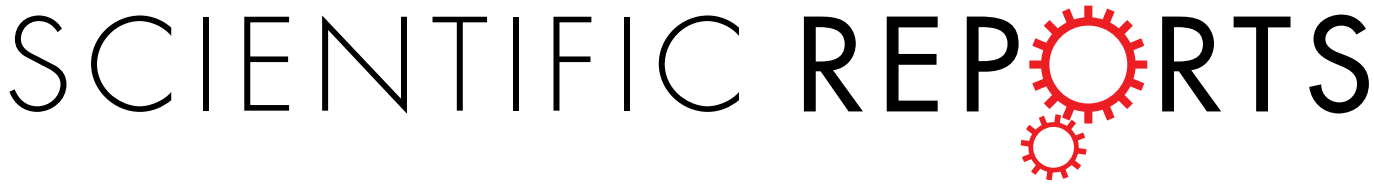

OPEN

α-Synuclein is a Novel Microtubule Dynamase

Daniele Cartelli[1], Alessandro Aliverti[1], Alberto Barbiroli[2], Carlo Santambrogio[3], Enzio M. Ragg[2], Francesca V.M. Casagrande[1], Francesca Cantele[1], Silvia Beltramone[1], Jacopo Marangon[1], Carmelita De Gregorio[1], Vittorio Pandini[1], Marco Emanuele[4], Evelina Chieregatti[4], Stefano Pieraccini[5], Staffan Holmqvist[6,7], Luigi Bubacco[8], Laurent Roybon[6,7], Gianni Pezzoli[9], Rita Grandori[3], Isabelle Arnal[10] & Graziella Cappelletti[1,11]

Received: 18 April 2016
Accepted: 23 August 2016
Published: 15 September 2016

α-Synuclein is a presynaptic protein associated to Parkinson's disease, which is unstructured when free in the cytoplasm and adopts α helical conformation when bound to vesicles. After decades of intense studies, α-Synuclein physiology is still difficult to clear up due to its interaction with multiple partners and its involvement in a *pletora* of neuronal functions. Here, we looked at the remarkably neglected interplay between α-Synuclein and microtubules, which potentially impacts on synaptic functionality. In order to identify the mechanisms underlying these actions, we investigated the interaction between purified α-Synuclein and tubulin. We demonstrated that α-Synuclein binds to microtubules and tubulin $\alpha_2\beta_2$ tetramer; the latter interaction inducing the formation of helical segment(s) in the α-Synuclein polypeptide. This structural change seems to enable α-Synuclein to promote microtubule nucleation and to enhance microtubule growth rate and catastrophe frequency, both *in vitro* and *in cell*. We also showed that Parkinson's disease-linked α-Synuclein variants do not undergo tubulin-induced folding and cause tubulin aggregation rather than polymerization. Our data enable us to propose α-Synuclein as a novel, foldable, microtubule-dynamase, which influences microtubule organisation through its binding to tubulin and its regulating effects on microtubule nucleation and dynamics.

Microtubules (MTs) are dynamic polymers consisting of αβ tubulin dimers, which play an essential role in cell shape acquisition and many intracellular processes[1]. In large cells, such as neurons, little is known about how MTs can nucleate in the axonal compartment, far away from the MT-organizing center in the cell body. Further, to date, the regulation of the MT dynamics underlying synaptic functions is still elusive. Many MT-interacting proteins are believed to regulate these phenomena; for example, dispersed γ tubulin complexes are reliable nucleating structures in the axon[2].

Nowadays, there is increasing evidence for a direct interplay between MTs and α-Synuclein (Syn), a presynaptic unfolded protein widely expressed in brain tissues[3]. Despite the controversial issues on its physiology, Syn has been clearly associated with neurodegeneration. Indeed, Syn overproduction due to multiplications of the *SNCA* locus encoding for Syn and point mutations in the gene itself cause familial forms of Parkinson's disease (PD)[3]. The underlying pathogenic mechanism is still unclear. Cytotoxicity is currently attributed to Syn oligomers[4], whose overexpression induces MT disruption in cells[5]. Furthermore, tubulin is known to promote Syn fibrillation *in vitro*[6], although it is not clear whether destabilization of the MT cytoskeleton potentiates[7] or prevents[8] Syn aggregation *in vivo*.

Even though many efforts have been devoted to the identification of a link between tubulin and Syn in pathological contexts, their physiological interaction has been largely ignored. Alim and colleagues[9] have revealed that

[1]Dept. Biosciences, Università degli Studi di Milano, Milano, Italy. [2]Dept. of Food, Environmental and Nutritional Sciences, Università degli Studi di Milano, Milano, Italy. [3]Dept. Biotecnology and Biosciences, Università degli Studi di Milano-Bicocca, Milano, Italy. [4]Dept. Neuroscience and Brain Technologies, Istituto Italiano di Tecnologia, Genova, Italy. [5]Dept. Chemistry, Università degli Studi di Milano, Milano, Italy. [6]Stem Cell laboratory for CNS Disease Modeling, Wallenberg Neuroscience Center, Department of Experimental Medical Science, Lund University, Lund, Sweden. [7]Strategic Research Area MultiPark and Lund Stem Cell Center, Lund University, Lund, Sweden. [8]Dept. Biology, University of Padova, Padova, Italy. [9]Parkinson Institute, ASST G. Pini-CTO, ex ICP, Milano, Italy. [10]Grenoble Institut des Neurosciences, Grenoble, France. [11]Center of Excellence on Neurodegenerative Diseases, Università degli Studi di Milano, Milano, Italy. Correspondence and requests for materials should be addressed to D.C. (email: daniele.cartelli@gmail.com) or G.C. (email: graziella.cappelletti@unimi.it)

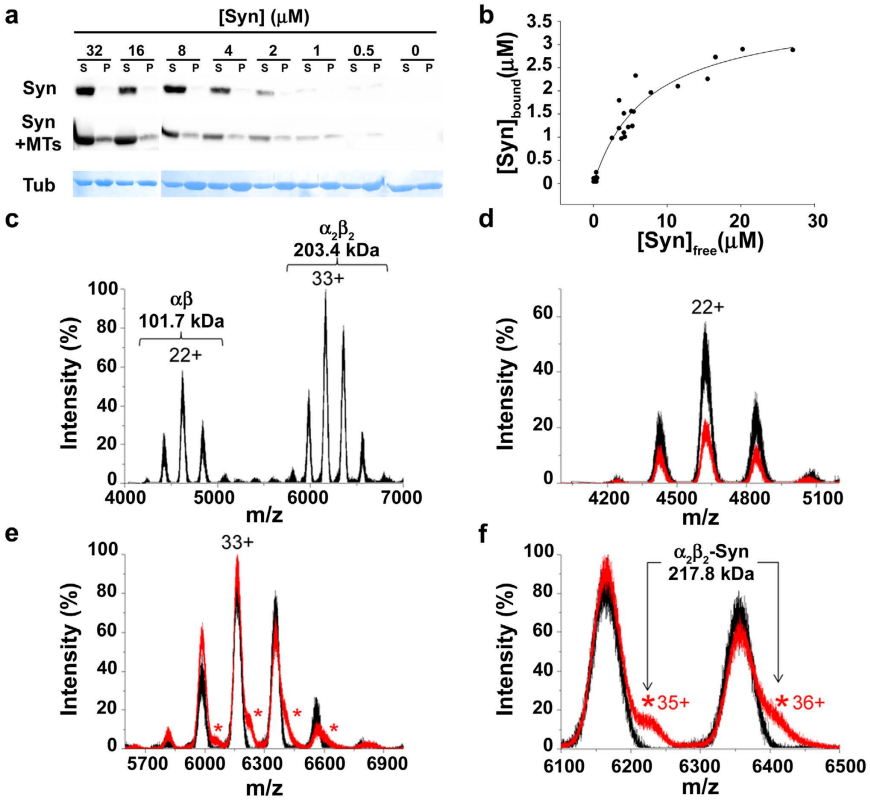

Figure 1. WT Syn interacts with preformed MTs and tubulin $\alpha_2\beta_2$ tetramer. (**a**) Representative Western blotting of Syn (0–32 μM) recovered in the supernatant (S) or pellet (P) fraction from co-sedimentation assays without (Syn) or after (Syn + MTs) incubation with preformed MTs (Tub) at constant total MT concentration (4 μM tubulin dimers). (**b**) Bound Syn plotted versus free Syn ($r^2 = 0.94$). The data reported in the plot derive from at least three different replicates. (**c**) Nano-ESI-MS spectra of 14 μM tubulin: the peak distributions relative to the tubulin dimer and the $\alpha_2\beta_2$ tetramer are grouped by brackets, with the indication of the measured mass. (**d**) Overlay of spectra of 14 μM tubulin (black), and a mixture of 14 μM tubulin and 14 μM Syn (red), in the *m/z* range 4000–5200 (αβ dimer) or (**e**) in the *m/z* range 5600–7000 ($\alpha_2\beta_2$ tetramer). The peaks corresponding to the $\alpha_2\beta_2$/Syn complex are labelled by asterisks. (**f**) Magnification of panel e, in the *m/z* range 6100–6500. The arrows point to the peaks of the $\alpha_2\beta_2$/Syn complex, labelled by the corresponding charge state. The measured mass of the complex is also indicated. In each panel, the most intense peak of each distribution is labelled by the corresponding charge state.

wild type (WT) Syn promotes MT assembly, whereas Chen and colleagues have claimed that neither monomeric nor oligomeric Syn influences MT polymerization *in vitro*[10]. Co-immunoprecipitation studies as well as affinity chromatography have also revealed a direct interaction between Syn and free tubulin[11], but it is still unclear whether Syn forms a complex with tubulin dimers or with higher-order assemblies.

Here we analyse the interaction between Syn and tubulin and we clear up the physiological relevance of the interaction between Syn and MTs. We found that WT Syn undergoes a structural change upon tubulin binding, promoting both microtubule nucleation and dynamics. Furthermore, our data obtained with PD-related Syn mutants provide hints for the pathogenic mechanism in PD.

Results

Syn binds to MTs and folds upon interaction with the tubulin $\alpha_2\beta_2$ tetramer. In order to investigate the mechanism by which Syn regulates MT cytoskeleton and to determine whether Syn interacts with tubulin dimer or with higher-order assemblies, we studied the interaction between purified Syn and tubulin *in vitro*. First of all, we performed co-sedimentation assay (Fig. 1a,b, and Supplementary Fig. S1), an approach which allows investigating the capability of a protein to bind polymerized and stabilized MTs[12], showing that Syn interacts with preformed MTs (Fig. 1a). The plot of $[Syn]_{bound}$ *versus* $[Syn]_{free}$ (Fig. 1b), which was fitted by nonlinear regression to a standard binding equation, enabled us to calculate an apparent K_d of 7.48 ± 1.38 μM, which is indicative of loose binding between Syn and MTs. In addition, differential interference contrast (DIC) and fluorescence microscopy analyses confirmed that WT Syn co-polymerizes with MTs (Supplementary Fig. S2), as revealed by Syn staining along conventional MTs polymerized in the presence of Syn. We also verified the ability of Syn to co-purify with brain tubulin[9]; two purification batches of tubulin were analysed by western blotting using anti-Syn antibodies and resulted to be positive for Syn staining, thus confirming that Syn co-purifies with tubulin (Supplementary Fig. S2). As the tubulin purification involves cycles of polymerization and depolymerization in conditions that should remove the majority of the MT-associated proteins[13], this result reinforces the idea that

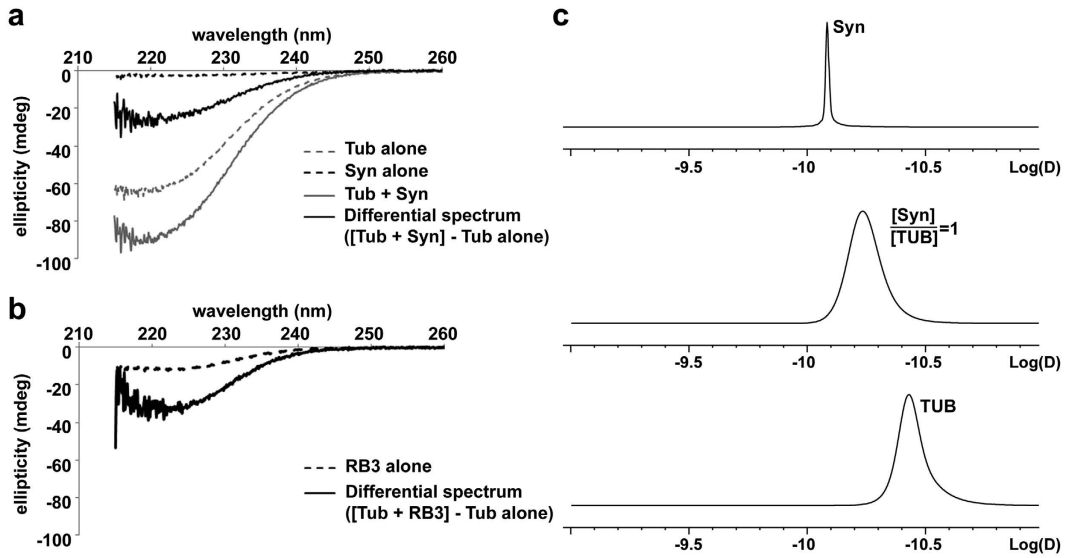

Figure 2. WT Syn interacts with tubulin and acquires secondary structure. (**a**) Far UV CD spectra of isolated 14 μM WT Syn (dashed black line, Syn alone), isolated 14 μM tubulin (dashed grey line, Tub alone), 14 μM WT Syn in the presence of equimolar tubulin (solid grey line, Tub + Syn) and differential spectra (solid black line, differential spectrum, [Tub + Syn] – Tub Alone). (**b**) Far UV CD spectra of isolated RB3-SLD (dashed line, RB3 alone) and differential spectra of 7 μM RB3-SLD in the presence of 14 μM tubulin (solid line, differential spectrum, [Tub + RB3] – Tub Alone). (**c**) ^{1}H-NMR diffusion coefficient measurements at 25 °C from 2D-DOSY projections of 27 μM Syn (Syn), Syn/tubulin equimolar mixture ([Syn]/[TUB] = 1) and 27 μM tubulin (TUB).

Syn can interact also with unpolymerized tubulin[11]. Thus, we investigated the direct interaction between Syn and free tubulin dimers by using native mass spectrometry (MS) and nano-electrospray ionization (nano-ESI). The spectra of 14 μM tubulin and a mixture of 14 μM tubulin and 14 μM Syn (black and red spectra, respectively, in Fig. 1c–f) reveal that Syn forms a specific complex with the tubulin $\alpha_2\beta_2$ tetramer. The measured mass of this complex (217.8 kDa) was in agreement with the calculated one for a complex of two tubulin dimers ($\alpha_2\beta_2$) and one Syn molecule. Moreover, the average charge (34.5+) of the complex is close to the expected value for a globular protein of the same mass (36.1+)[14], suggesting that the complex itself has a compact conformation. However, bound Syn does not necessarily have a globular conformation but it can wrap around the tubulin tetramer in an ordered, but extended conformation. To address this issue, we studied potential conformational changes resulting from tubulin/Syn interaction by far UV circular dichroism (CD). Our data confirmed that Syn is unfolded in the absence of the ligand, whereas an equimolar Syn/tubulin mixture gives an overall secondary structure CD signal, which is more intense than the sum of the signals of the two individual proteins (Fig. 2a). Moreover, the CD signal originating in the mixture shows a gain of signal at 220 nm, which is typical of α-helix structures. Considering that (i) the interaction of tubulin with ligands is widely studied and an increase in its α-helix content has never been observed, and (ii) Syn is a soluble, intrinsically unfolded protein which is able to adopt α-helix structure in adequate conditions[15–17], we hypothesize that, upon its interaction with tubulin, Syn folds into a structure which is rich in α-helix content. Such a secondary structural transition is reminiscent of the conformational changes associated with the RB3-stathmin like domain (RB3-SLD) upon interaction with tubulin[18] (Fig. 2b). According to the hypothesis that Syn/tubulin interaction induces α-helical structures in Syn, the CD spectra of Syn complexed with tubulin has been extrapolated (Fig. 2a, solid black line, differential spectrum obtained by subtracting the tubulin spectrum from the one of the complex) and the related α-helix content estimated to 35%. It is worth remembering that such helical content should not reflect the amount of α-helix in a single folded molecule, but rather the average content of α-helix in the whole sample, taking into account both the Syn folded molecules which interact with tubulin and the unfolded ones remaining free in solution. The formation of a Syn/tubulin complex in solution, at neutral pH, has been also investigated by ^{1}H-NMR diffusion measurements approach (Fig. 2c). Tubulin alone had a diffusion coefficient ($D = 0.37 \times 10^{-10}\,m^2sec^{-1}$) consistent with the presence of α β dimers in solution, whereas Syn showed a value ($D = 0.83 \times 10^{-10}\,m^2sec^{-1}$) smaller than the one expected for a globular ~14 kDa protein and consistent with the presence of unfolded species[19]. In the presence of tubulin, the diffusion coefficient measured for Syn significantly decreased from $0.83 \times 10^{-10}\,m^2sec^{-1}$ to $0.59 \times 10^{-10}\,m^2sec^{-1}$. This clearly indicates the formation of a complex between these proteins. However, since the measured value is actually less than that one expected for a stable 1:1 complex, it should be concluded that, at least in our conditions, a certain fraction of Syn still remains in its free state in solution and that the Syn molecules exchange between the free and bound states at a rate which is fast compared to both the NMR chemical shift and diffusion measurement time scales (fast exchange limit, $k_{ex} < 100\,sec^{-1}$). The fraction of free Syn has been estimated within the 45–55% range, leading to a Syn/tubulin dissociation constant between 10 and 20 μM, which is in agreement with the data obtained by the co-sedimentation assay (Fig. 1).

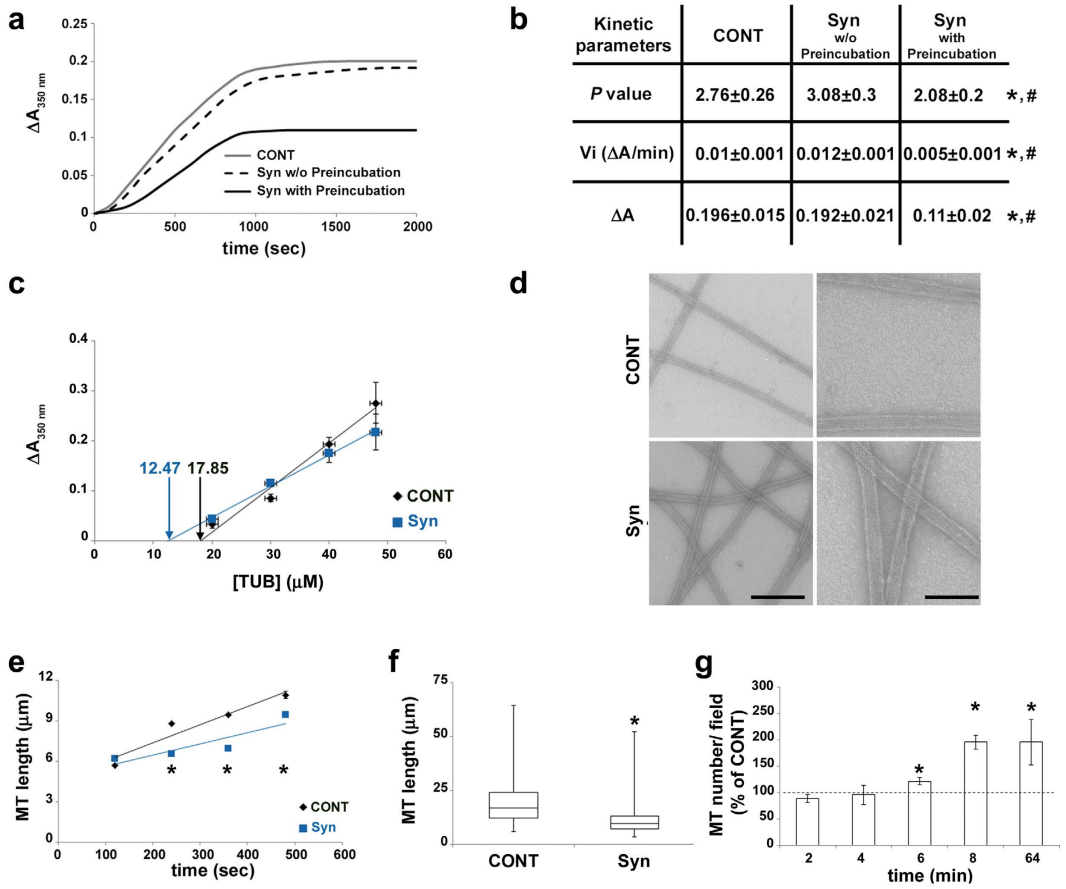

Figure 3. Folded Syn promotes MT nucleation *in vitro*. (**a**) Tubulin assembly was recorded over time by measuring the increase in absorbance variation (ΔA) at 350 nm. Tubulin (40 μM) was polymerized in the absence (CONT) and in the presence of 5 μM of naïve (Syn w/o preincubation) or preincubated (Syn preincubated with tubulin) WT Syn. (**b**) Parameters describing nucleation (*P*, $^{*}p = 0.031$ vs CONT and $^{\#}p = 0.002$ vs Syn w/o preincubation), initial velocity (V_i, $^{*}p = 0.018$ vs CONT and $^{\#}p = 0.033$ vs Syn w/o preincubation) and absorbance variation (ΔA, $^{*}p = 0.0016$ vs CONT and $^{\#}p = 0.028$ vs Syn w/o preincubation) were calculated from polymerisation kinetics analysis. Values are expressed as mean ± SEM (at least five independent experiments). $^{*}p < 0.05$ vs CONT, according to ANOVA, Fischer *post hoc* test. (**c**) Final ΔA, obtained at various initial tubulin concentrations, were plotted against tubulin concentration. The tubulin critical concentration (arrows, x-intercept of fitting lines) was calculated in the absence (CONT, black) and in the presence of 5 μM WT Syn (Syn, blue). Plotted values are mean ± SEM (at least three independent experiments). (**d**) Electron microscope images of MTs assembled (40 μM Tubulin) in the absence (CONT) or in the presence of 5 μM WT Syn (Syn). Scale bar, 200 (left) and 100 nm (right). (**e**) MT length measurements during the initial phase of tubulin polymerization (40 μM) in the absence (CONT, black) and in the presence of 5 μM of WT Syn (Syn, blue). Actual p values are 5.1×10^{-14} (240 sec), 2.4×10^{-17} (360 sec) and 2.3×10^{-7} (480 sec). (**f**) MT length measurements in similar conditions at steady state ($^{*}p = 3.12 \times 10^{-13}$). MT number is at least 600 for each condition, obtained from two independent experiments. $^{*}p < 0.05$ vs CONT, according to Student's t-test. (**g**) Quantification over time of the number of MT assembled with WT Syn. Values (mean ± SEM) are expressed as a percentage of the control experiment (without Syn). At least 15 fields obtained from two independent experiments were analysed for each condition (see Supplementary Fig. S2). $^{*}p < 0.05$ vs CONT, according to Student's t-test, performed on the raw data. Actual p are 0.024 (6 min), 0.002 (8 min), 0.042 (64 min).

Altogether, our data provide a relatively detailed insight into the binding of Syn to tubulin and MTs, demonstrating, for the first time, the formation of a complex between Syn and the tubulin $\alpha_2\beta_2$ tetramer, and enabling us to posit a Syn folding step.

Folded Syn promotes MT nucleation and increases MT dynamics. Until now, the effects of Syn on MT polymerization have been studied without pre-incubating Syn and tubulin dimers[9,10]. On the other hand, our CD results (Fig. 2) indicate that during the period of the analyses (performed on a time scale of 5–10 min at 20 °C) Syn folds. Thus, we incubated Syn for 10 min at 20 °C with tubulin in order to allow Syn conformational rearrangement prior to carefully analyse tubulin assembly kinetics using a standard tubulin:protein ratio of 8:1 (Fig. 3a,b). We found that Syn molecules that have not been pre-incubated with tubulin did not influence

	Tub 10 μM			Tub 15 μM			
	Syn 0 μM	Syn 5 μM	Syn 10 μM	Syn 0 μM	Syn 5 μM	Syn 10 μM	Syn 15 μM
V_{growth} (μm/min)	1.2 ± 0.1	1.38 ± 0.5	1.08 ± 0.18	1.1 ± 0.086	1.17 ± 0.14	1.38 ± 0.14*	1.32 ± 0.24*
	n = 1097	n = 362	n = 395	n = 1420	n = 663	n = 695	n = 973
$V_{shrinkage}$ (μm/min)	8.7 ± 2.24	7.35 ± 2.1	7.5 ± 1.65	11 ± 1.77	8.6 ± 2	11.7 ± 2.6	8.5 ± 2.24
	n = 357	n = 209	n = 309	n = 287	n = 216	n = 298	n = 336
$F_{catastrophe}$ (min^{-1})	0.16 ± 0.05	1.04 ± 0.3	0.69 ± 0.17	0.09 ± 0.03	0.27 ± 0.07	0.26 ± 0.07	0.22 ± 0.06
	n = 9	n = 12	n = 15	n = 9	n = 14	n = 12	n = 11
F_{rescue} (min^{-1})	0.15	0.67 ± 0.33	0.33 ± 0.19	0.1	0.6 ± 0.26	0.44 ± 0.22	1.26 ± 0.44
	n = 1	n = 4	n = 3	n = 1	n = 5	n = 4	n = 8
Growth Duration (s)	3327	692	1304	5797	3056	2751	2944
Shrinkage Duration (s)	382	356	537	594	512	540	380
MT number	32	14	16	41	22	25	20

Table 1. Folded Syn increases MT dynamics *in vitro*. Dynamic parameters were determined by VE-DIC light microscopy for MTs assembled from purified axonemes in the presence of tubulin (10 and 15 μM) and increasing concentrations of Syn (0–15 μM). In each condition, Syn was preincubated with tubulin prior the observation at 37 °C. Velocities are expressed as mean ± SEM. The total growth and shrinkage times analysed, as well as the number of MTs used for each condition, are given in the last three rows. Catastrophe and rescue frequencies were calculated by dividing the total number of events by the time spent in growth and shrinkage, respectively. The standard deviation is calculated by dividing $F_{catastrophe}$ or F_{rescue} by $\sqrt{n}$ assuming a Poisson distribution[55]. (*n*) represents the total number of measurements for the growth and shrinkage rates, and the total number of observed events for the catastrophe and rescue frequencies. *$p < 0.05$ vs Syn 0 μM, according to ANOVA, Dunnett *post hoc* test. Actual p are 0.005 (Syn 10 μM) and 0.0051 (Syn 15 μM).

tubulin kinetics. By contrast, pre-incubated Syn strongly impacts MT assembly (Fig. 3a) by reducing by half the initial velocity of polymerization (V_i) and the MT assembly at the plateau (ΔA), as shown in Fig. 3b. Next, by plotting log(A(t)/A∞) against log(t) we extrapolated the parameter *P*, which is indicative of the successive steps during the nucleation phase[20], and is significantly decreased compared to tubulin alone (Fig. 3b). The effect of pre-incubated Syn on *P* value and its concomitant ability in significantly reducing tubulin critical concentration (Fig. 3c), underscored the ability of folded Syn to nucleate MTs. We confirmed the presence of MTs in these conditions by electron microscopy and negative staining analysis (Fig. 3d). We next estimated the length and the number of MTs assembled in the presence of folded Syn, which revealed that Syn induces the formation of shorter and more abundant MTs with respect to controls (Fig. 3e–g, see also Supplementary Fig. S3). The significant increase of MT number perfectly agrees with the induction of MT nucleation. However, the significant reduction of the MT mean length also suggests that, besides stimulating MT nucleation, Syn should reduce MT elongation, either by slowing down MT growth rate or increasing catastrophe frequency, as strongly supported by the reduction in the initial velocity of polymerization. Notably, this would explain the decrease in total polymer mass (ΔA in Fig. 3a,b and Supplementary Fig. S3), which is in contrast to the expected effect of a nucleation inducer.

Thus, we used video-enhanced differential interference contrast (VE-DIC) light microscopy to clear up the effects of WT Syn on MT dynamics (Table 1). Tubulin (10 and 15 μM) was assembled from purified axonemes, in the absence or in the presence of increasing concentrations of Syn (0–15 μM). These protein to protein ratios are comparable to those observed *in vivo,* since the actual cellular concentration of tubulin is up to 40 μM[21] and the estimated presynaptic Syn concentration varies between 30 and 60 μM in neurons[22]. At low tubulin concentration (10 μM), Syn enhanced catastrophe frequency, 4 to 6.5-fold in comparison to the control. A similar, albeit smaller, effect was observed at the highest tubulin concentration (15 μM), with a 3-fold increase in the catastrophe frequency in the presence of Syn compared to tubulin alone. With the two highest Syn concentrations (10 and 15 μM), we also noticed a significant increase in the MT growth rate in the presence of 15 μM tubulin. These results would indicate that Syn increases MT dynamics by speeding up the growth rate and promoting catastrophe events. In order to confirm these data in a neuronal cell line we used differentiated rat PC12 cells, which naturally express rat Syn starting from 7th day of NGF treatment[23]. We transfected PC12 cells with a construct coding for human Syn and treated them with NGF for three days. As shown in Fig. 4a, parental PC12 cells lack of endogenous Syn whereas transfected ones express human WT Syn. First of all, we confirmed the well-known interaction of Syn with βIII-tubulin[5], either in PC12 cells overexpressing human Syn (Supplementary Fig. S4) or in human neurons derived from embryonic stem cells expressing the endogenous Syn (Supplementary Fig. S5). In addition, we highlighted a high degree of co-localization with tyrosinated α-tubulin, which is associated with the most dynamic MTs. Thus, to directly investigate MT dynamics in cells, we performed live cell imaging taking advantage of end-binding protein 3 (EB3)-mCherry[24], a fluorescent protein that specifically binds growing MT plus-ends. We visualized MT dynamics under basal conditions (cells kept at 37 °C) or during the MT recovering phase (rewarming at 37 °C), which follows a cold-treatment (30 min at 4 °C), in differentiated PC12 cells co-expressing EB3-mCherry and GFP-Syn or GFP alone (Fig.4). This approach shows that Syn increases the number of detectable growing MTs per neurite (Fig. 4c), even though the analysed surfaces do not change (Supplementary Fig. S6), and thus demonstrates that Syn favours MT (re)nucleation *in cell*. Moreover, Syn accelerates MT growth (Fig. 4d) and reduces MT lifetime (Fig. 4e). The latter observation is consistent with the enhancement of the catastrophe frequency reported by VE-DIC microscopy (Table 1). Altogether, our data demonstrate that, upon interaction

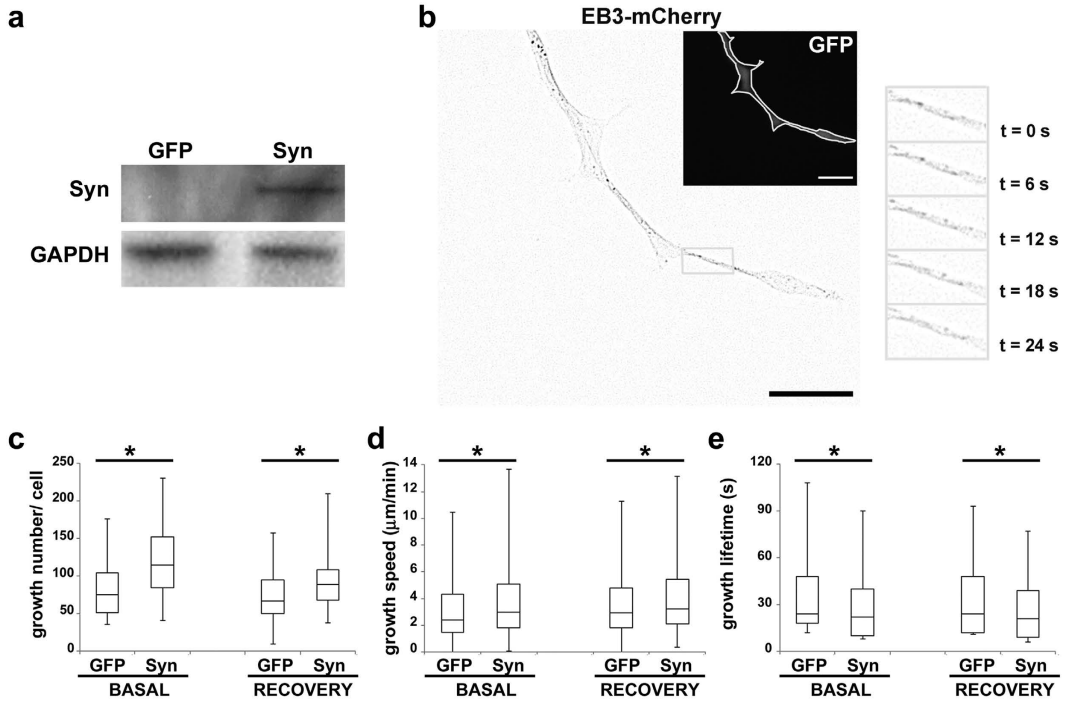

Figure 4. WT Syn increases MT dynamics in neuronal cells. (**a**) Representative western blot showing the levels of expression of human Syn (Syn) in 5 days NGF-differentiated control (GFP) and transfected (Syn) PC12 cells. The antibody used (Sigma-Aldrich) recognized both human and rat Syn. Glyceraldehyde 3-phosphate dehydrogenase (GAPDH) is used as loading reference. (**b**) Representative micrographs of double transfected PC12 cells differentiated 3 days with NGF, showing the EB3 comets (EB3-mCherry, inverted contrast) and, in the inset, the GFP channel (GFP, grey line marks the cell boundary). The grey box indicates the area from which the frames of the time series were taken (elapsed time is shown). Scale bar, 5 μm. Box plots of the number (**c**, *BASAL = 0.007, *RECOVERY = 0.005), speed (**d**, *BASAL = 0.02, *RECOVERY = 0.007) and lifetime (**e**, *BASAL = 0.02, *RECOVERY = 0.02) of MT growths, in each experimental condition. BASAL indicates cell cultures maintained at 37 °C whereas RECOVERY indicates registration during the rewarming phase after 30 min at 4 °C. At least 30 cells were analysed per condition, for a total number of 2200 tracks, or more. *$p < 0.05$ vs GFP, according to Student's t-test. The analyses of the relative neurite's area are reported in Supplementary Fig. S5.

with the tubulin $\alpha_2\beta_2$ tetramer, Syn acquires helical structure and becomes able to govern multiple steps of MT assembly and dynamics, such as nucleation, growth rate and catastrophe frequencies, in a purified system as well as in a neuronal cell model.

Syn displays sequence similarity to stathmin. Syn displays striking structural and functional similarities with the tubulin-interacting protein stathmin. Both of them are about 14-15 kDa, intrinsically disordered proteins and capable of adopting α-helix conformation upon interaction with binding partners[18,25] (Fig. 2a). It is noteworthy that Syn, like stathmin and RB3-SLD, interacts with the tubulin $\alpha_2\beta_2$ tetramer and promotes MT catastrophes. Thus, we explored sequence similarities between Syn and the members of the stathmin family. Pairwise alignment of WT Syn to stathmin showed about 20% identical residues and over 50% conservative substitutions. Two possible tubulin-interacting domains have been proposed for Syn but the pathological point mutations, which impair the tubulin binding, are outside the suggested regions[9,26]. Therefore, searching for a tubulin-related physiological relevance for the region including the mutations, we decided to align two 21-residue stretches surrounding the residues 30 or 53 in the Syn polypeptide chain (Fig. 5). Interestingly, the fragment centered around Syn residue 53, in which four of the five PD-linked point mutations are clustered[27], aligned to one of the functionally relevant regions of the stathmin family (Fig. 5, blue lines), namely the tubulin-binding domains[28]. This region displays multiple invariant residues (Fig. 5 asterisks), including the sites of the Syn pathological mutations A53T and E46K (Fig. 5, red arrows), besides several other conservative or semi-conservative substitutions (Fig. 5, colons and dots, respectively). Furthermore, we completed the analysis in order to align the entire region 1–100 of Syn polypeptide chain to the stathmin-family (Supplementary Fig. S7), since we suggest that Syn acquires an α-helical structure (Fig. 2) and this is the domain of Syn that folds upon interaction with vesicle. As the two domains reported in Fig. 5 showed a good conservation, we anchored them and aligned the other stretches of Syn to the remaining regions of the stathmin-family. These regions display a very poor conservation and, thus, this result reinforces the idea that the region around the pathological mutations might be important for binding to tubulin and that its point mutations likely compromise Syn/tubulin interaction. All these data demonstrate that Syn and stathmin share physicochemical and functional properties, and the good alignment

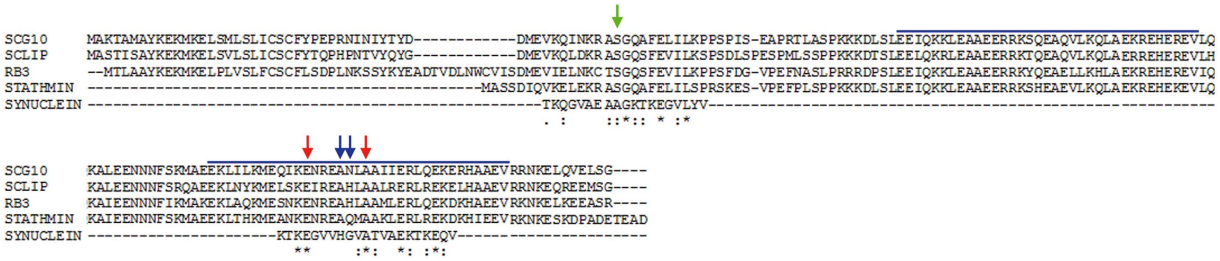

Figure 5. Syn displays sequence similarities with stathmin. Multiple alignment of Syn with four members of stathmin family was performed by ClustalW. Blue lines delimitate the domains of stathmin family involved in tubulin binding. Arrows mark the sites of Syn pathological mutations: Ala30 (green arrow), the conserved Glu46 and Ala53 (red arrows), His50 and Gly51 (blue arrows). Asterisks mark invariant positions, while dots and colons highlight semi-conservative and conservative substitutions, respectively.

of the fragment 43–63 of Syn with a functionally relevant region of stathmins strongly indicates that Syn and proteins belonging to the stathmin-family may be involved in same biological processes, such as the regulation of MT cytoskeleton.

Pathological Syn mutations corrupt Syn/tubulin interaction. Having shown that four out of five PD-linked mutations map to the putative tubulin-binding domain of Syn (Fig. 5), these substitutions are expected to have a profound effect on Syn interaction with tubulin and, reasonably, on tubulin-induced folding of Syn. Indeed, CD analyses revealed that the A53T variant is much less sensitive than WT Syn to the structuring effect of tubulin (Fig. 6a, red lines) whereas the E46K mutant loses almost completely the ability to fold in the presence of tubulin (Fig. 6a, green lines). Although the pathological A30P mutation mapped far away from the putative tubulin-interacting domain we proposed (Fig. 5), this amino acid substitution has the potential to interfere with tubulin-induced folding of Syn, as confirmed by CD analyses (Fig. 6a, blue lines). In order to verify that mutated Syns used in the assays were not aggregated, thus to avoid unwanted effects on tubulin assembly, we analysed them by size exclusion chromatography. We observed a single peak for all the Syn corresponding to a molar mass of 14 kDa (Supplementary Fig. S8), which indicates the presence of monomeric Syn. Moreover, we observed that MTs assembled in the presence of Syn mutants (all pre-incubated with tubulin) are crowded and surrounded by abundant protein aggregates (Fig. 6b and Supplementary Fig. S2), which were not present at the beginning of the experiments (see size exclusion chromatography results, Supplementary Fig. S8) but rather are formed during the incubation. These aggregates should be composed of both tubulin and Syn; indeed, very few and small aggregates are observed both in control conditions, i.e. without adding Syn, meaning that they are made of tubulin, and in the presence of WT Syn (Supplementary Fig. S8). Since aggregates in the presence of mutated Syns (Supplementary Fig. S8) are also recognized by the Syn antibody (Supplementary Fig. S2), they should contain Syn. Interestingly, the aggregation propensity of the mutated Syns seems to be inversely proportional to their ability in folding in the presence of tubulin (Fig. 6a and Supplementary Fig. S8). Therefore, our data reveal that Syn mutants are much less sensitive than WT Syn to tubulin-induced folding and mainly promote tubulin aggregation. This could potentially impair the correct organization of the MT system impacting on the neuronal processes in which MTs and Syn are implicated.

Discussion

As stated by Feng and Walsh[29] a decade ago: "Protein-protein interactions are a little like human relationships. Some are dedicated, faithful and lifelong, while other relationships are brief flings with a promiscuous variety of partners that may leave no lasting trace or may induce profound changes". Here we show that the interplay between Syn and tubulin is a multifaceted protein-protein interaction. Indeed, their encounter triggers the structural rearrangement of Syn which, in turn, regulates the birth, the growth and the lifespan of individual MTs. Therefore, we set forth the hypothesis that Syn is a MT "dynamase", a term introduced by Erent and colleagues[30] for Kinesin-8, which is able to regulate both MT nucleation and catastrophes in *S. pombe*, exactly what Syn does, regulating nucleation, growth rate and catastrophe frequency of MTs, *in vitro* and *in cell*.

MTs exhibit non-equilibrium dynamics, which depends on free-tubulin concentration. In cell systems, a constant free tubulin concentration, and the presence of a multitude of MT-interacting proteins likely buffers and mitigates perturbations in MT dynamics, conferring a degree of robustness and homeostasis to the MT cytoskeleton[31]. Nevertheless, stressful conditions exist (i.e. neuronal aging) and under these conditions the free tubulin content may considerably change. When tubulin concentration is high, the initial response of a MT-associated protein will be potent and it would induce MT assembly, as we observe at the beginning of assembly kinetics in the presence of Syn (Fig. 3) or in VE-DIC experiments performed at high tubulin concentrations (Table 1). In the mechanistic model we propose, the ability of WT Syn to interact with the tubulin $\alpha_2\beta_2$ tetramer enables Syn to fold (Fig. 7, STEP 1) and, possibly, to act as a tubulin carrier by delivering small tubulin oligomers ($\alpha_2\beta_2$ tetramers), which have been recently proposed, although it is controversial, to promote MT nucleation and MT elongation[32–34]. Thus, Syn could either crosslink tubulin heterodimers, inducing nucleation (Fig.7, STEP 2-high $[Tub]_{free}$), and/or stabilize them in a favourable orientation promoting supramolecular interactions involved in MT formation. As net polymerization is promoted, the free tubulin concentration drops down, mitigating the assembly-inducing activity of Syn, as observed at the steady state of assembly kinetics (Fig. 3) or with

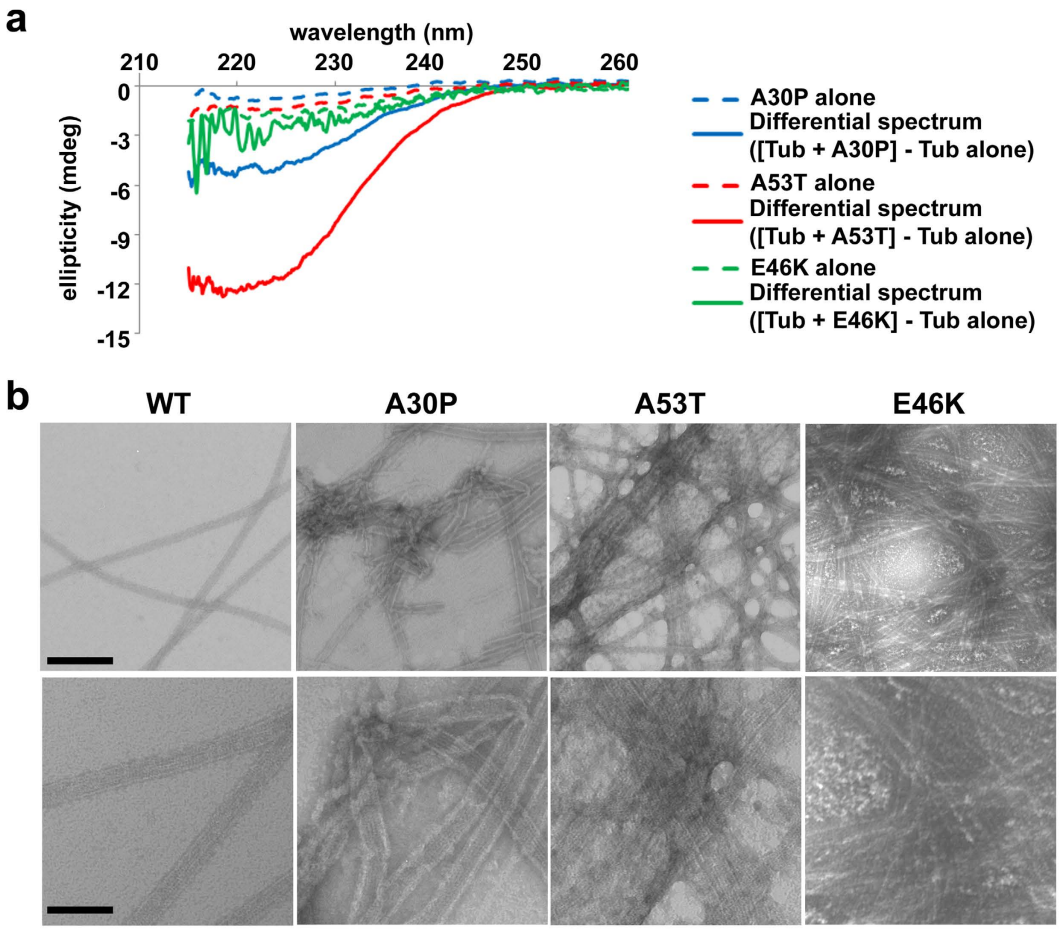

Figure 6. Pathological Syn mutations corrupt Syn/tubulin interaction. (**a**) Far UV CD spectra of 14 μM mutated Syns, A30P (blue lines), A53T (red lines) and E46K (green lines), obtained with naïve proteins (dashed lines, alone) or by the difference between the spectrum of Syns in the presence of equimolar amount of tubulin minus the spectrum of tubulin alone (solid lines, differential spectrum). (**b**) Electron microscope images of MTs assembled *in vitro* (40 μM tubulin) in the presence of 5 μM of WT (WT) or mutated (A30P, A53T and E46K) Syns. Scale bars, 200 (top) and 100 nm (bottom).

low tubulin concentrations in VE-DIC experiments (Table 1), when catastrophe stimulation prevails. How are these catastrophe events induced? Two possible mechanisms have been proposed for the catastrophe-promoting activity of stathmin[35]: (i) sequestering of soluble tubulin into assembly-incompetent tubulin/stathmin complexes, which has the same stoichiometry of Syn/tubulin complexes identified in the present study (Fig. 1), or (ii) direct binding of stathmin to MT ends, which would increase the frequency of switching from growth to shortening. It is unlikely that Syn acts by sequestering tubulin dimers, since such a phenomenon would reduce MT growth rate, in contrast to our observations (Table 1). We hypothesize that, once bound to the MT lattice, Syn could affect the whole stability of the polymer by inducing conformational changes in the intra- or inter-dimer angle and thus amplifying the intrinsic tendency of MTs to undergo catastrophes (Fig. 7, STEP 2-low $[Tub]_{free}$). Nevertheless, further studies are needed to definitively solve the mechanism by which Syn promotes MT catastrophes.

Here, we also demonstrated that PD-linked Syn variants do not exhibit α-helical folding upon tubulin binding and induce tubulin aggregation. A30P mutation is located on the short helix of the lipid-folded Syn[27], and the fact that the polypeptide region including this mutation is not part of the putative tubulin-interacting domain could explain why it is the most "benign" PD point mutation[36]. Conversely, the other 4 described point mutations of Syn (E46K, H50Q, G51D and A53T) fall inside a region corresponding to the tubulin-interacting domain of proteins belonging to the stathmin family. We are aware that this region maps outside the tubulin-binding regions previously proposed for the WT[9,26]., which seem to be unique for Syn and do not share homology with other known tubulin-interacting proteins. Nevertheless, the two previously reported binding domains are diverse, sharing only 4 residues and completely excluding the region in which there are the pathological mutations. Alim and colleagues[9], tried to justify the tubulin-aggregating effect of the A30P and A53T mutants saying that these mutations can alter the Syn folding, exactly what we showed here (Fig. 6). Our results propose an alternative tubulin-binding domain that well matches with the ones of the stathmin-like proteins, and which also includes most of the reported pathological mutations. Future work on pre-incubated Syn fragments will be necessary to validate this as tubulin-binding domain. Thus, our data provide mechanistic insights into the molecular pathology of PD,

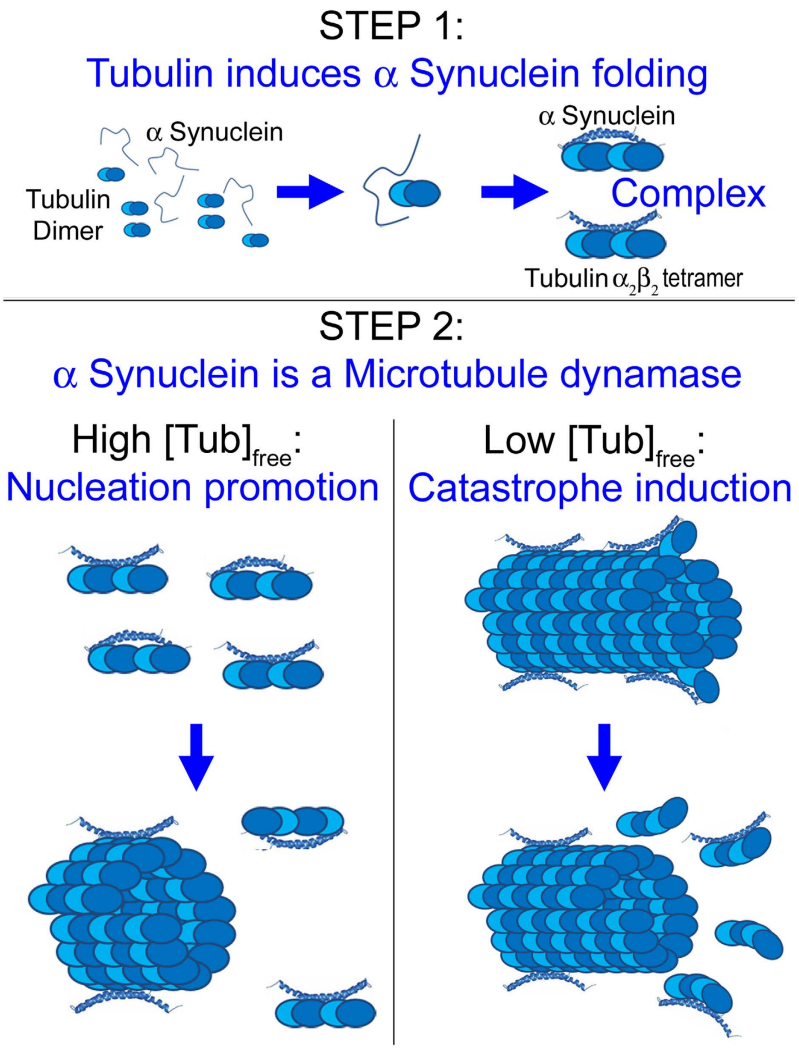

Figure 7. Model for Syn/MTs interaction. Syn senses and binds free tubulin dimers forming a specific complex with tubulin $\alpha_2\beta_2$ tetramer and acquiring α-helix conformation (STEP 1). Afterwards, Syn behaves like a tubulin deliverer promoting MT nucleation (STEP 2-High $[Tub]_{free}$). When entrapped in the MT wall, Syn promotes MT catastrophes probably inducing changes in intra- or inter-dimer angles (STEP 2-Low $[Tub]_{free}$).

which would involve MT-dependent pathways. Indeed, tubulin aggregation induced by mutated Syns (Fig. 6, Supplementary Fig. S2, Supplementary Fig. S8 and Alim *et al.*[9]), could lead to excessive MT bundles, engulfing axons and impairing intracellular transport, as previously described for other neurodegenerative disease[37]. Therefore, axonal transport disruption could be the missing link between Syn/tubulin interaction and PD. In accordance, a very recent paper showed that Syn oligomers, the most toxic Syn species, reduce MT stability, kinesin/MTs interplay and neuritic kinesin-dependent cargoes, promoting early neurite pathology[5]. Although alteration of axonal transport is considered as one of the earliest events in neurodegeneration[38], we showed that it follows MT dysfunction in the 1-methyl-4-phenyl-1,2,3,6-tetrahydropiridine-induced model of PD[39,40]. Hence, by affecting axonal transport, MT dysfunction may trigger the chain of events leading to PD. Accordingly, MT-targeted molecules have beneficial effects in both 1-methyl-4-phenyl-1,2,3,6-tetrahydropiridine-treated[40] and Syn-overexpressing[41] mice and the correction of MT defects rescues control phenotype and cell homeostasis in PD patient derived cell lines[42–44]. Therefore, by providing insights into the interaction between Syn and MTs, our data would highlight some essential steps in neuronal function and degeneration.

Many controversial issues remain to be clarified, such as solving the puzzle of the actual naïve state of Syn: is it a folded tetramer[45] or a labile unstructured monomer[16]? Nevertheless, here we have demonstrated that monomeric WT Syn forms a specific complex with the tubulin $\alpha_2\beta_2$ tetramer, acquiring a defined secondary structure. We could speculate that local accumulation (i.e. at the pre-synapse) of free tubulin dimers would change the equilibrium between unfolded and folded/tetrameric Syn, which may have evolved to act as a sensor of the tubulin dimers/MTs ratio. Thus, the increase in tubulin dimers concentration and the consequent folding of Syn molecules start the Syn-mediated regulation of both MT nucleation and dynamics, as we have demonstrated here. Therefore, we propose that Syn can be considered a MT dynamase, which potentially set MT mass at the pre-synapse.

Methods

Protein purification. Tubulin was purified by two cycles of polymerization/depolymerization in high molar Pipes buffer[13], suspended in BRB buffer (80 mM K-Pipes, pH 6.9, 2 mM EGTA, 1 mM $MgCl_2$) and stored at −80 °C. Recombinant Syn was produced and purified according to Martinez *et al.*[46], and recombinant RB3-SLD (kindly gifted by prof. Patrick A. Curmi, Evry University, France) was produced and purified according to Charbaut *et al.*[47] (see also Supplementary information). Aliquots of Syn (in 20 mM Hepes, pH 7.4, 100 mM KCl) and RB3-SLD (in 10 mM Hepes, pH 7.2,150 mM NaCl) were kept at −80 °C until needed. Each aliquot was clarified by ultracentrifugation (230000× *g* at 4 °C for 30 min) immediately before use.

MT self-assembly. The kinetics of tubulin polymerization was followed turbidimetrically at 350 nm in a multimode plate reader (Infinite 200Pro, Tecan, Mannedorf, Switzerland) equipped with a temperature controller, as previously described[48]. Tubulin was diluted to different concentrations in standard assembly buffer and kept on ice; as WT or mutated Syns were added, the reaction was started by warming the solution at 37 °C. For the preincubation, two solutions were prepared: T1, buffer with 2x glycerol and GTP and w/o proteins, and T2, with double of the final protein concentration but w/o glycerol and GTP. T2 was incubated 10 min at 20 °C, and the reaction was started mixing T1 and T2 1:1 and raising the temperature to 37 °C. Polymerization time-course was dissected and the kinetic parameters calculated according to Bonfils *et al.*[20]: *P* (number of successive steps during nucleation) was determined by plotting $\log(A(t)/A\infty)$ against log(t) and extrapolated as the pendency of the linear part of the resulting plot; initial velocity of polymerization (V_i) was calculated as the maximal variation of mass *versus* time ($\delta A/\delta t$); MT assembly was deduced from the extent of absorbance variation (ΔA) at the steady-state. The x-intercept of the linear dependence of ΔA from the initial tubulin concentration represents the tubulin critical concentration. To evaluate MT length and number, 2.7 μM rhodamine-labelled tubulin (Cytoskeleton, Denver, CO) was included in the polymerization solutions and the reaction was stopped by addition of 0.5% glutaraldehyde. MTs were laid on slides and their length was measured using a digital image processing software (Axiovision, Carl Zeiss, Oberkochen, Germany) to analyse the images acquired with the Axiovert 200 M microscope (Carl Zeiss). To assess the ultrastructure of assembled MTs, samples were fixed with 0.5% glutaraldehyde and then placed on Formvar-coated nickel grids, negative stained with uranyl acetate and observed with a Philips CM10 transmission electron microscope at 80 kV, equipped with a Morada Olympus digital camera.

Co-sedimentation assay. MTs were polymerized (from tubulin 40 μM) 20 min at 37 °C, stabilized 10 min with paclitaxel (Sigma-Aldrich) and then diluted to 4 μM. Syn (0.5–32 μM) was incubated 20 min at 37 °C in the absence or in the presence of MTs and then centrifuged at 70000× *g* for 15 min at 25 °C. Supernatant and pellet were loaded on SDS-PAGE, proteins were transferred onto PVDF membranes and immunostained with anti-Syn rabbit IgG (Sigma-Aldrich) HRP goat anti-rabbit IgG (Sigma-Aldrich). Immunostaining was revealed by enhanced chemiluminescence (Super-Signal West Pico Chemiluminescent, Pierce). Quantification was performed by Image J software (NIH) subtracting the background around bands. According to Ackmann *et al.*[12], $[Syn]_{bound}$ was plotted *versus* $[Syn]_{free}$ and the data fitted by nonlinear regression to a standard binding equation (Equation 1) using SigmaPlot (Jandel, CA):

$$[Syn]_{bound} = \frac{B_{max}\ [Syn]_{free}}{K_d\ +\ [Syn]_{free}} \quad (1)$$

Mass spectrometry. Nano-ESI-MS was performed on a hybrid quadrupole-time-of-flight instrument (QSTAR Elite, Applied Biosystems, Foster City, CA) with minor modifications to previously reported conditions[49]. Purified proteins were thawed and buffer exchanged by two cycles of desalting on Micro Bio-Spin™ P-6 Gel columns (Bio-Rad laboratories, Hercules, CA), immediately before use. All spectra were acquired in 10 mM ammonium acetate after incubation at room temperature for at least 10 min and no longer than 1 h.

Circular dichroism. Circular dichroism spectra were acquired using a Jasco J810 spectropolarimeter. Secondary structure of Syn (0.2 mg/ml) and RB3-SLD (0.1 mg/ml), either alone or in the presence of tubulin (1.4 mg/ml), was investigated by recording far-UV circular dichroism spectra in 0.1 cm quartz cuvettes. All proteins were dissolved in BRB buffer. Spectra of pure Syn and RB3-SLD were baseline-corrected by subtracting a buffer spectrum, while difference spectra of the Syn/tubulin and RB3-SLD/tubulin mixtures were "tubulin-corrected" by subtracting the spectrum of the pure tubulin from those of the mixtures. Syn spectra were normalized in terms of mean residual ellipticity by using a mean residue weight of 103 Da. Since BRB buffer does not allow to record spectra below 215 nm, the α-helical content was estimated from the mean residual ellipticity at 222 nm according to Chen and Yang[50].

NMR spectroscopy. The NMR spectra were recorded on a Bruker AV600 spectrometer (Bruker Spectrospin AG, Rheinstetten, Germany), operating at 600.10 MHz for the ^1H nucleus and equipped with a standard triple-resonance probe with z-axis gradients. Temperature control was achieved through the spectrometer BVT3000 temperature control unit, using nitrogen gas (flow 270 l/h) pre-cooled with a Bruker BCU20 refrigeration unit. ^1H-NMR chemical shifts (δ) were measured in ppm, using as reference external sodium 4,4-dimethyl-2-silapentane-1-sulfonate (DSS) set at 0.00 ppm. DOSY (Diffusion Oriented Spectroscopy) measurements were performed at 25 °C on a freshly prepared 27 μM solution of tubulin, dissolved in 0.6 ml H_2O:D_2O 9:1 (v/v), pH 6.8 50 mM phosphate buffer, in the presence of various amounts of Syn (Syn/tubulin molar ratios varied between 0 and 10) after at least 0.5 h incubation. DSS, deuterium oxide (99.8% purity) and 5 mm O.D. NMR

tubes (Wilmad 535-PP type) were purchased from Sigma-Aldrich. Solvent suppression was achieved by including in the DOSY pulse-sequence a WATERGATE pulse-scheme[51]. A gradient-based stimulated echo bipolar pulse sequence was utilized[52], with a 0.3 s diffusion delay ("big delta") and a 1.5 ms gradient pulse length ("little delta"). 32 one-dimensional spectra were collected with a gradient strength varying between 0.67 and 33.4 Gauss/cm. Values for "little delta" and "big delta" parameters were chosen by taking into account also the expected short transverse relaxation rates due to the formation of high molecular weight aggregates. Other relevant acquisition parameters: time-domain: 2 K; number of scans: 196; relaxation delay: 2 s. Raw data were Fourier-transformed after apodization with a 90°-shifted sine-bell-squared function and baseline corrected. Log(D) values were derived by a two-components non-linear fitting and displayed as pseudo-2D spectra.

Limiting values for the molar fraction of free Syn (α) were estimated from the experimental diffusion coefficients (D, Equation 2) as:

$$\frac{(D_{exp} - D_{tub:syn})}{(D_{syn} - D_{tub:syn})} < a < \frac{(D_{exp} - D_{tub2:syn})}{(D_{syn} - D_{tub2:syn})} \tag{2}$$

where D_{syn} is the experimental value determined for free Syn. $D_{tub:syn}$ and $D_{tub2:syn}$ are the D values expected for complexes formed by Syn with $\alpha\beta$ tubulin dimer and $\alpha_2\beta_2$ tubulin tetramer, respectively. These last values were estimated by applying the following correction factors to D_{tub}:

$$\log(D_{tub:syn}) = \log(D_{tub}) - \frac{1}{3}\log\left(\frac{MW_{tub:syn}}{MW_{tub}}\right) = -10.44 \tag{3}$$

$$\log(D_{tub_2:syn}) = \log(D_{tub}) - \frac{1}{3}\log\left(\frac{MW_{tub_2:syn}}{MW_{tub}}\right) = -10.54 \tag{4}$$

The dissociation constant K_d of Syn-tubulin complex was derived by applying the following equation 5:

$$K_d = [TUB]_0 \frac{D_{bound} - D_{exp}}{D_{exp} - D_{syn}} + [Syn]_0 \frac{D_{exp} - D_{bound}}{D_{bound} - D_{syn}} \tag{5}$$

where D_{bound} can be either $D_{tub:syn}$ or $D_{tub2:syn}$ as derived from equation 3 and 4.

Video-microscopy and data analysis. MTs were assembled from purified axonemes with tubulin (10–15 μM) and increasing concentrations of preincubated Syn (5–15 μM). Samples were prepared in perfusion chambers, previously saturated with 50 μM Syn, and observed at 37 °C with an Olympus BX-51 microscope equipped with DIC prisms and a video camera coupled to an Argus 20 image processor (Hamamatsu, Hamamatsu City, Japan), as previously described[53]. Images were recorded every 2 s over periods of 5 min. The total recording time did not exceed 60 min for each chamber. Measurements of MT dynamics and data analysis were carried out using Image J (NIH, Bethesda, MD) and Kaleidagraph (Synergy Software Systems, Dubai, UAE), as previously described[53].

Immunoblotting and live cell imaging. PC12 cells were maintained in cultures and differentiated as previously described[39]. PC12 cells were transiently transfected using Lipofectamine 2000 (Invitrogen), with C-terminal GFP-fused human WT Syn or with GFP-containing control vector (eGFP-N1). Whole cell extracts were loaded on SDS-PAGE, transferred onto PVDF membranes and immunostained with anti-Syn rabbit IgG and anti-GAPDH as loading control. For live cell imaging experiments, GFP-WT Syn and GFP-containing vectors were co-transfected with EB3-mCherry construct[24] (kindly provided by Dr Galjart, Medical Genetic Center, Erasmus University, Rotterdam, The Netherlands). As previously described[39], cultures were transferred to a live cell imaging workstation; images were collected every 6 s with a cooled camera (Axiocam HRM Rev. 2; Zeiss) for periods of 3-4 min, and the total recording time did not exceed 60 min for each dish. MT growth dynamics was automatically analysed using plusTipTracker software[54]. The area of the analysed neurites was estimated by ImageJ software (Supplementary Fig. S6).

Protein alignment. Pairwise alignments between Syn and stathmin sequences were made using Pam250 or Bl50 matrix, whereas multiple protein alignment was performed with ClustalW software.

Statistical analyses. For multiple comparisons, the statistical significance of treatment was assessed by one-way ANOVA with Dunnett 2-sided or Fischer LSD *post-hoc* testing, whereas differences between WT Syn and controls were assessed using Student's t-test. All analyses were performed using STATISTICA (StatSoft Inc., Tulsa, OK).

References

1. Conde, C. & Cáceres, A. Microtubule assembly, organization and dynamics in axons and dendrites. *Nat. Rev. Neurosci.* **10,** 319–332 (2009).
2. Stiess, M. *et al.* Axon extension occurs independently of centrosomal microtubule nucleation. *Science* **327,** 704–707 (2010).
3. Lashuel, H. A., Overk, C. R., Oueslati, A. & Masliah, E. The many faces of α-synuclein: from structure and toxicity to therapeutic target. *Nat. Rev. Neurosci.* **14,** 38–48 (2013).
4. Winner, B. *et al. In vivo* demonstration that alpha-synuclein oligomers are toxic. *Proc Natl Acad Sci USA* **108,** 4194–4199 (2001).
5. Prots, I. *et al.* α-Synuclein oligomers impair neuronal microtubule-kinesin interplay. *J. Biol. Chem.* **288,** 21742–21754 (2013).
6. Alim, M. A. *et al.* Tubulin seeds alpha-synuclein fibril formation. *J. Biol. Chem.* **277,** 2112–2117 (2002).

7. Esteves, A. R., Arduíno, D. M., Swerdlow, R. H., Oliveira, C. R. & Cardoso, S. M. Microtubule depolymerization potentiates alpha-synuclein oligomerization. *Front. Aging Neurosci*. **1,** 5 (2010).
8. Nakayama, K., Suzuki, Y. & Yazawa, I. Microtubule depolymerization suppresses alpha-synuclein accumulation in a mouse model of multiple system atrophy. *Am. J. Pathol*. **174,** 1471–1480 (2009).
9. Alim, M. A. *et al.* Demonstration of a role for alpha-synuclein as a functional microtubule-associated protein. *J. Alzheimers Dis*. **6,** 435–442 discussion 443–449 (2004).
10. Chen, L. *et al.* Oligomeric alpha-synuclein inhibits tubulin polymerization. *Biochem. Biophys. Res. Commun*. **356,** 548–553 (2007).
11. Payton, J. E., Perrin, R. J., Clayton, D. F. & George, J. M. Protein-protein interactions of alpha-synuclein in brain homogenates and transfected cells. *Brain Res. Mol. Brain Res*. **95,** 138–145 (2001).
12. Ackmann, M., Wiech, H. & Mandelkow, E. Nonsaturable Binding Indicates Clustering of Tau on the Microtubule Surface in a Paired Helical Filament-like Conformation. *J. Biol. Chem*. **275,** 30335–30343 (2000).
13. Castoldi, M. & Popov, A. V. Purification of brain tubulin through two cycles of polymerization-depolymerization in a high-molarity buffer. *Protein Expr. Purif.* **32,** 83–88 (2003).
14. Testa, L. *et al.* Electrospray ionization-mass spectrometry conformational analysis of isolated domains of an intrinsically disordered protein. *Biotechnol. J*. **6,** 96–100 (2011).
15. Weinreb, P. H., Zhen, W., Poon, A. W., Conway, K. A. & Lansbury, P. T. Jr. NACP, a protein implicated in Alzheimer's disease and learning, is natively unfolded. *Biochemistry* **35,** 13709–13715 (1996).
16. Burré, J. *et al.* Properties of native brain α-synuclein. *Nature* **498,** E4–6 discussion E6-7 (2013).
17. Eliezer, D., Kutluay, E., Bussell, R. Jr & Browne, G. Conformational properties of alpha-synuclein in its free and lipid-associated states. *J. Mol. Biol*. **307,** 1061–1073 (2001).
18. Steinmetz, M. O. Structure and thermodynamics of the tubulin-stathmin interaction. *J. Struct. Biol.* **158,** 137–147 (2007).
19. Uversky, V. N., Li, J. & Fink, A. L. Evidence for Partially Folded Intermediate in α-Synuclein Fibril Formation. *J. Biol. Chem*. **276,** 10737–10744 (2001).
20. Bonfils, C., Bec, N., Lacroix, B., Harricane, M. C. & Larroque, C. Kinetic analysis of tubulin assembly in the presence of the microtubule-associated protein TOGp. *J. Biol. Chem*. **282,** 5570–5581 (2007).
21. Hiller, G. & Weber, K. Radioimmunoassay for tubulin: a quantitative comparison of the tubulin content of different established tissue culture cells and tissues. *Cell* **14,** 795–804 (1978).
22. Kamp, F. *et al.* Inhibition of mitochondrial fusion by α-synuclein is rescued by PINK1, Parkin and DJ-1. *EMBO J.* **29,** 3571–3589 (2010).
23. Stefanis, L., Kholodilov, N., Rideout, H. J., Burke, R. E. & Greene, L. A. Synuclein-1 is selectively up-regulated in response to nerve growth factor treatment in PC12 cells. *J. Neurochem*. **76,** 1165–1176 (2001).
24. Komarova, Y. *et al.* Mammalian end binding proteins control persistent microtubule growth. *J. Cell Biol*. **184,** 691–706 (2009).
25. Uversky, V. N. Neuropathology, biochemistry, and biophysics of alpha-synuclein aggregation. *J. Neurochem*. **103,** 17–37 (2007).
26. Zhou, R. M. *et al.* Molecular interaction of α-synuclein with tubulin influences on the polymerization of microtubule *in vitro* and structure of microtubule in cells. *Mol. Biol. Rep*. **37,** 3183–3192 (2010).
27. Kara, E. *et al.* α-Synuclein mutations cluster around a putative protein loop. *Neurosci. Lett*. **546,** 67–70 (2013).
28. Honnappa, S., Cutting, B., Jahnke, W., Seelig, J. & Steinmetz, M. O. Thermodynamics of Op18/stathmin-tubulin interaction. *J. Biol. Chem*. **278,** 38926–38934 (2003).
29. Feng, Y. & Walsh, C. A. Protein-protein interactions, cytoskeletal regulation and neuronal migration. *Nat. Rev. Neurosci*. **2,** 408–416 (2001).
30. Erent, M., Drummond, D. R. & Cross, R. A. S. pombe kinesins-8 promote both nucleation and catastrophe of microtubules. *PLoS One*. **7,** e30738 (2012).
31. Gardner, M. K., Zanic, M., Gell, C., Bormuth, V. & Howard, J. Depolymerizing kinesins Kip3 and MCAK shape cellular microtubule architecture by differential control of catastrophe. *Cell* **147,** 1092–1103 (2011).
32. Mozziconacci, J., Sandblad, L., Wachsmuth, M., Brunner, D. & Karsenti, E. Tubulin dimers oligomerize before their incorporation into microtubules. *PLoS One* **3,** e3821 (2008).
33. Schek, H. T. 3rd, Gardner, M. K., Cheng, J., Odde, D. J. & Hunt, A. J. Microtubule assembly dynamics at the nanoscale. *Curr. Biol*. **17,** 1445–1455 (2007).
34. Slep, K. C. & Vale, R. D. Structural basis of microtubule plus end tracking by XMAP215, CLIP-170, and EB1. *Mol. Cell*. **27,** 976–991 (2007).
35. Manna, T., Thrower, D. A., Honnappa, S., Steinmetz, M. O. & Wilson, L. Regulation of microtubule dynamic instability *in vitro* by differentially phosphorylated stathmin. *J. Biol. Chem.* **284,** 15640–15649 (2009).
36. Gasser, T., Hardy, J. & Mizuno, Y. Milestones in PD genetics. *Mov. Disord*. **26,** 1042–1048 (2011).
37. Salinas, S., Carazo-Salas, R. E., Proukakis, C., Schiavo, G. & Warner, T. T. Spastin and microtubules: Functions in health and disease. *J. Neurosci. Res*. **85,** 2778–2782 (2007).
38. Morfini, G. A. *et al.* Axonal transport defects in neurodegenerative diseases. *J. Neurosci*. **29,** 12776–12786 (2009).
39. Cartelli, D. *et al.* Microtubule dysfunction precedes transport impairment and mitochondria damage in MPP+-induced neurodegeneration. *J. Neurochem*. **115,** 247–258 (2010).
40. Cartelli, D. *et al.* Microtubule alterations occur early in experimental parkinsonism and the microtubule stabilizer epothilone D is neuroprotective. *Sci. Rep.* **3,** 1837 (2013).
41. Fleming, S. M. *et al.* A pilot trial of the microtubule-interacting peptide (NAP) in mice overexpressing alpha-synuclein shows improvement in motor function and reduction of alpha-synuclein inclusions. *Mol. Cell Neurosci*. **46,** 597–606 (2011).
42. Cartelli, D., Goldwurm, S., Casagrande, F., Pezzoli, G. & Cappelletti, G. Microtubule destabilization is shared by genetic and idiopathic Parkinson's disease patient fibroblasts. *PLoS One* **7,** e37467 (2012).
43. Esteves, A. R., Gozes, I. & Cardoso, S. M. The rescue of microtubule-dependent traffic recovers mitochondrial function in Parkinson's disease. *Biochim. Biophys. Acta*. **1842,** 7–21 (2014).
44. Ren, Y. *et al.* Parkin Mutations Reduce the Complexity of Neuronal Processes in iPSC-derived Human Neurons. *Stem Cells* **33,** 68–78 (2015).
45. Bartels, T., Choi, J. G. & Selkoe, D. J. α-Synuclein occurs physiologically as a helically folded tetramer that resists aggregation. *Nature* **477,** 107–110 (2011).
46. Martinez, J., Moeller, I., Erdjument-Bromage, H., Tempst, P. & Lauring, B. Parkinson's disease-associated alpha-synuclein is a calmodulin substrate. *J. Biol. Chem*. **278,** 17379–17387 (2003).
47. Charbaut, E. *et al.* Stathmin family proteins display specific molecular and tubulin binding properties. *J. Biol. Chem*. **276,** 16146–16154 (2001).
48. Contini, A., Cappelletti, G., Cartelli, D., Fontana, G. & Gelmi, M. L. Molecular dynamics and tubulin polymerization kinetics study on 1,14-heterofused taxanes: evidences of stabilization of the tubulin head-to-tail dimer-dimer interaction. *Mol. Biosyst*. **8,** 3254–3261 (2012).
49. Santambrogio, C. *et al.* DE-loop mutations affect beta2 microglobulin stability, oligomerization, and the low-pH unfolded form. *Protein Sci*. **19,** 1386–1397 (2010).
50. Chen, Y. H. & Yang, J. T. A new approach of the calculation of secondary structures of globular proteins by optical rotatory disoersion and circular dichroism. *Biochem. Biophys. Res. Commun.* **44,** 1285–1291 (1971).

51. Piotto, M., Saudek, V. & Sklenar, V. Gradient-tailored excitatiojn for single-quantum NMR spectroscopy of aqueous solutions. *J. Biomol. NMR* **2,** 661–665 (1992).
52. Wu, D., Chen, A. & Johnson, C. S. Jr. An Improved Diffusion-Ordered Spectroscopy Experiment Incorporating Bipolar-Gradient Pulses. *J. Magn. Reson. Series A* **108,** 255–258 (1995).
53. Vitre, B. *et al.* EB1 regulates microtubule dynamics and tubulin sheet closure *in vitro*. *Nat. Cell Biol.* **10,** 415–421 (2008).
54. Applegate, K. T. *et al.* plusTipTracker: Quantitative image analysis software for the measurement of microtubule dynamics. *J. Struct. Biol.* **176,** 168–184 (2011).
55. Walker, R. A. *et al.* Dynamic instability of individual microtubules analysed by video light microscopy: rate constants and transition frequencies. *J. Cell Biol.* **107,** 1437–1448 (1988).

Acknowledgements

The authors are grateful to Dr. Croci (Università degli Studi di Milano) for support with bioinformatics tools and to Dr. Pavesi (Università degli Studi di Milano) for helpful discussion on bioinformatics data. We thank Dr. Galjart (Erasmus University) for the pEB3-mCherry. The authors are thankful to Dr. Francolini (Department of Medical Biotechnology and Translational Medicine, Università degli Studi di Milano, Milano, Italy) for the use of electron microscope. The authors are also grateful to Dr. Bonomi (Università degli Studi di Milano) for critical reading of the manuscript and Dr. Jennifer S. Hartwig for reading and editing the manuscript. Finally, the authors thank Dr. M. Gritti, Dr. M. Magri and the present members of the lab who contributed to the preparation of the manuscript and whose names are not included in the authors list, and we apologize for each possible involuntary paper omission. This work was supported by Fondazione Grigioni per il Morbo di Parkinson, Milan, Italy (to G.C.), and "Dote ricerca", FSE, Regione Lombardia (to D.C.).

Author Contributions

D.C. and G.C. conceived of the study and participated in its design and coordination. D.C., A.A., V.P., L.B. and A.B. carried out protein purification and circular dichroism assays. E.M.R. carried out N.M.R. spectrometry. C.S. and R.G. performed mass spectrometry analysis. D.C. performed *in vitro* assays. D.C. and F.C. performed electron microscopy analyses. D.C. and I.A. performed video microscopy assays. C.D.G. and M.E. set up cell cultures and performed immunofluorescence analyses. D.C. and S.B. performed western blotting. D.C. performed live cell imaging studies. F.V.M.C., S.H. and L.R. carried out analyses on human embryonic stem cells. S.P. and J.M. participated in the sequence alignment. D.C., G.P., E.C., L.B. and G.C. designed the analysis based on experimental data. D.C., I.A. and G.C. wrote the article. All authors read and approved the final manuscript.

Additional Information

Supplementary information accompanies this paper at http://www.nature.com/srep

Competing financial interests: The authors declare no competing financial interests.

How to cite this article: Cartelli, D. *et al.* α-Synuclein is a Novel Microtubule Dynamase. *Sci. Rep.* **6**, 33289; doi: 10.1038/srep33289 (2016).